Oxo-biodegradation of clay-based polyethylene nanocomposites

Maryam Rezaei

B.Sc. (Chemical Eng.), M.Sc. (Chemical Eng.)

A thesis submitted in fulfilment of the requirements for the degree of Doctor of Philosophy

School of Civil, Environment and Chemical Engineering

RMIT University

March 2012

Declaration

I certify that except where due acknowledgement has been made, the work is that of the author alone; the work has not been submitted previously, in whole or in part, to qualify for any other academic award; the content of the thesis is the result of work which has been carried out since the official commencement date of the approved research program; and, any editorial work, paid or unpaid, carried out by a third party is acknowledged.

Maryam Rezaei

March 2012

منت خدای را عز و جل که طاعتش موجب قربت است و به شکر اندرش مزید نعمت.هر نفسی که

فرو می رود ممد حیات است و چون برمیاید مفرح ذات.پس در هر نفسی دو نعمت

موجود است و بر هر نعمتی شکری واجب.

گلستان سعدی

"Teach us to care and not to care"

T. S. Eliot

Dedication

To My Parents;

The True Meanings

of

Love and Selflessness

Acknowledgments

The completion of this thesis would not have been possible without the support and help of several individuals who in one way or another contributed. I would hereby like to acknowledge their valuable contribution in the preparation and completion of this study.

First and foremost, my utmost gratitude to Dr Rajarathinam Parthasarathy, my senior supervisor, whose encouragement, guidance, support and patience from the initial to the final stage enabled me to complete this study. He always had tried to show me the way when I was lost and give me the guidance when I was needed. I am heartily thankful to him for making this journey of getting PhD a fruitful study time by training me to be a real researcher in my own life. He taught me how to work independently and never giving up until to reach the ultimate goal.

My special thanks goes to Associate Professor Margaret Jollands, my second supervisor, for all the moral supports, all the time we spent together, all the words of wisdom she gave me and all the lessons she tried to teach me during this 4 years. I am eternally thankful to her for showing me how important is each and every individual, for showing me how to live with having respect to myself and others and how to overcome the obstacles when they look impossible. And thanks to her for being there when no one was.

My grateful thanks also goes to Ms Sharon Taylor, who was always there to guide, support and assist all postgraduate students and tried to make this journey as easy as possible in administrative point of view. I also take this opportunity to thank the technical officers at RMIT University, especially Mr Mike Allan, Mr Cameron Crombie, Dr Sandro Logano, Dr Muthu

Pannirselvam, Mr Frank Antolasic, Mr Phillip Francis and Mr Peter Rummel for helping me with the laboratory work, equipment problems and technical advice.

I would also like to thank Associate Professor Enzo Palombo and Suchetana Chattopadhyay for giving me the opportunity to use their experimental set up at Swinburne University of Technology.

It is a pleasure to thank those who made this journey very special for me, my extended thanks goes to:

Professor Felicity Roddick who lightened my days with her beautiful smiles which I will never forget.

Ms Irina Palm, my lovely friend from the first day in Australia till now who was like a mother for me. Her lovely personality and dignity taught a lot of lessons to me and I will never forget our chatting time over the table or in the corridor. We always tried to solve the world's problem together!

My dearest friends, Firoozeh Jad, Kamyar Eyvaz, Sylwia Solarska, Nahid Jaffari, Saeed Joulaei, Kaveh Mozaffarian, Nikki Oshea and Minnie Bong for their memorable time we spent together and their love and support when it was most needed. I am so grateful for having them in my life.

My RMIT friends Torika Oshadie Kumanayaka, Raymond Guang, Dr Nicky Eshtiagi, Alex Ardila, Albert Yek, Jyoti Sharma, Balwinder Kaur, Alicia Anindya, Siew Cheng Low, Peggy Chang, Yong Tee Goh, Amita Bhatia, Subhendu Bhattacharya, Edwin Baez, Kullawadee

Sungsanit and Louise Cini for the time we shared together at RMIT. I will never forget the laughs, foods, coffees and stories we shared in four years.

My teachers and mentors who directly and indirectly helped me to reach to this point especially Dr Ali Vatani, Dr Saeid Mokhatab and Mr Ramyar Rashed.

I owe my deepest gratitude to my family, my sisters, Faem and Neda, my brothers, Mehdi and Mojtaba and my splendid parents whose unconditional love and support made it possible for me to end this journey. Equal credits of this work go to my beloved parents who taught me giving up is not an option. They have given me repeatedly the confidence and courage to go further and to reach more. They showed me how to live to the most, but not forgetting the others in my life. If I am here, in this place today, it is because of them. I am so proud of them and I am so thankful to God for having them.

Last but not the least I thank my lovely partner, my beautiful friend, Dr Reza Taghipour who came into my life in the last years of my study and turned it into a meaningful, loving journey by his endless love, kindness and support.

And at the end I would like to thank HIM for being by my side all the time and showed me the light when everything looked dark. I will promise him here that I would be a light in other people's life and I would be a hope when everything looks impossible.

Table of Contents

List of Tables

List of Figures

Summary

Polyethylene is one of the most popular polymers used in many applications in various industries ranging from automobile to agriculture. One of its main applications is in the packaging industry due to its excellent mechanical, chemical and biological properties. Polyethylene is easy to process and has lower cost compared to other polymers. However, the widespread use of polyethylene has led to a problem called 'plastic pollution'. In addition to pollution, polyethylene discarded in the environment accumulates and causes the deaths of millions sea birds and animals. Among the several strategies used to solve the problem of plastic pollution, the important ones are recycling and production of degradable plastics. Recycling is costly and not preferable from a hygiene point of view. Degradable plastics are made by blending polymer with additives which enhance the degradability of the material. Metal ions and naturally biodegradable polymers such as starch are commonly used as additives in the production of degradable polyethylene. Degradable polyethylene disintegrates into smaller fragments in the presence of heat, light and oxygen and disappears from sight. However, these small fragments remain in the environment for very long period and contaminate soil and water. To make polyethylene completely biodegradable, the smaller fragments must be made compatible to microorganisms which convert them into CO_2 and water during its metabolism. Current knowledge on the mechanisms of polyethylene biodegradation is far from complete and therefore needs more research. Enhanced understanding of biodegradation mechanism will help in finding the effective factors that are responsible for polyethylene biodegradability and producing environmentally-friendly polymers which will biodegrade rapidly in the environment and enter the carbon cycle of nature.

Previous studies on polyethylene degradability have shown that degradability is enhanced remarkably by incorporating metal ions called pro-oxidant into the polymer matrix. Metal ions were found to help in initiating the oxidation process by enhancing the rate of free radical formation but not to help much in the biotic stage of biodegradation. Recent studies on polyethylene nanocomposites, which are made by blending nanoclay with polymer for the purpose of enhancing the mechanical, thermal, and barrier properties of the composites, were found to have better biodegradability. Nanoclay was found to enhance the polyethylene biodegradability by maintaining the pH of the environment suitable for microorganism activity and providing more hydrophilic surface area to attract water and microorganisms. The role of clay, however, on the degradation of polyethylene is not completely understood yet.

The main objective of this work was to investigate the combined effects of manganese stearate as pro-oxidant and nanoclay on polyethylene biodegradation. It also aimed to develop a mathematical model for predicting the biodegradation rate of oxo-biodegradable polyethylene nanocomposites (nanocomposites with pro-oxidant) using the experimental data.

Films of polyethylene nanocomposites and oxo-biodegradable polyethylene nanocomposites were prepared using melt intercalation followed by film blowing. A biodegradation study was carried out in two stages: an abiotic stage and a biotic stage. Abiotic degradation was achieved by subjecting the film samples to heat at 70°C in an air circulated oven for a period of 14 days. Thermally degraded samples were then subjected to biodegradation in a closely monitored composting system according to AS-ISO 14855. Thermally degraded samples were subjected to TGA and FTIR analysis. Biodegradation was monitored by measuring the volume of CO_2

produced as a function of time. Biodegraded film samples were also subjected to ESEM (bio-film growth) and FTIR analysis.

Experimental results show that manganese stearate helps in different aspects of both abiotic and biotic stages of biodegradation. During thermal oxidation, manganese helps to initiate and propagate the free radical formation leading to the production of more oxidation products. However, the presence of clay itself has no significant effect on the thermal degradation of polyethylene nanocomposites. But nanoclay has been found to enhance the overall degradation by either catalysing the thermal oxidation or making the material suitable for the growth of microorganisms. It is clear that clay cannot initiate the degradation by itself and will lead to longer degradation period without pro-oxidant. Extensive degradation observed in oxo-biodegradable nanocomposites indicates that co-existence of manganese stearate and nanoclay in polyethylene structure is vital to achieve an effective biodegradation process.

CO_2 evolution data obtained in biodegradation studies were used to develop a mathematical model that describes the biodegradation behaviour. A modified logistic model and a first-order rate model similar to equations used for describing bacterial growth were fitted successfully to the experimental data. The kinetic parameters for models were obtained by least squares analysis using MATLAB 7.10.0 (R2010a). The proposed model can be used as a tool to analyse the kinetics of biodegradation and estimate the biodegradation potential of polyethylene-clay nanocomposites.

1 Introduction and objective

1.1 Introduction

Among all polymers, polyethylene has been used widely in many applications such as packaging, agriculture and automobile manufacturing. In the past few years, packaging polymers including polyethylene have received much criticism because of their very poor degradability. In a recent survey, it has been shown that North America and Western Europe accounts for nearly 80 percent of world`s plastic bag usage (Worldwatch Institute 2009). The Wall Street Journal reported that the U.S. uses 100 billion plastic shopping bags annually. According to Green Street website, the use of plastic bags in Australia accounts for about 6.9 billion each year, which equals to 326 plastic bags per person. According to Australia's Department of Environment, an estimated 49,600,000 plastic bags annually end up as litter in landfills or environment (Plastic Bag Facts 2010). It has been estimated that 500 billion plastic bags are produced annually (almost 1 million per minute) and only less than 1% of them are recycled. These plastic bags are used mostly for only 20 minutes but they persist in the environment for 100 to 1000 years (estimated). When they are not recycled, the plastic bags end up in the throats and stomach of wildlife, clogging gutters and sewers, and floating in waterways leading to the death of over a million seabirds, 100,000 sea turtles, and 100,000 marine mammals every year. Figure 1-1 shows a picture from bag monster website (http://www.bagmonster.com/). This website is dedicated to create public awareness on the consequences of production and usage of single-use plastic bags. The site outlines the facts regarding how plastic bag pollution threatens the earth and how the responsible use of them can make a difference.

Figure 1-1 The Bag Monster, http://www.bagmonster.com/

Environmentalists are concerned that the chemical inertness and stability of polyethylene is contributing to its undesirable solid waste disposal problems which consequently lead to serious non sustainability in eco-system. Thus, there is a pressing need for developing a new generation of degradable polymer that can replace polyethylene in various products and overcome the ecological problems caused by synthetic plastics.

It has been shown by many researchers that polyethylene can be made degradable by the use of additives such as transition metal ions and metal complexes. Harden *et al.* (1990) patented a degradable polyethylene by incorporating cerium (+3) stearate into polyethylene. They have found this composition is effective in promoting the environmental degradation of polyethylene by both thermal- and photo-oxidation to low molecular weight oxygenated products such as ketones, carboxylic acids, alcohols, esters and aldehydes. Orhan *et al*. (2004) reported metals act as good pro-oxidants in polyolefins making them susceptible to thermo-oxidative degradation. Upon activation by heat, in the presence of oxygen, pro-oxidants have been shown to produce free radicals on polyethylene chains which undergo further oxidation thus changing the physical properties of the polymer. Jakubowicz *et al.* (2003) claimed that the pro-oxidant catalyses the chain scission reaction in the polymer leading to the production of products containing low molecular mass oxidation products such as aldehydes, ketones and carboxylic acids. Zheng *et al*. (2005) proved by experiments that transition metals have accelerated the thermal oxidative processes of polyolefins by inducing hydroperoxide decomposition.

Recently, polymer-clay nanocomposites generated an interest due to their potential for exceptional improvements in properties at lower filler concentrations compared to conventional micro- and macro composites. As the research progressed in the field of polymer nanocomposites, they have been used in packaging applications and automotive industries due to their unique properties and biodegradability. But knowledge on their use as biodegradable polymer is not complete yet. Nanocomposites are multiphase materials containing two or more distinctly dissimilar components with at least one dimension in the nanometre scale. In the past decade, polymer layered silicate (clay) nanocomposites were one of the extensively studied

classes of materials for a variety of applications due to their improved mechanical properties, gas barrier performance, thermal properties and degradability (Vaia *et al*. 1996, Pinnavaia & Beall 2000). Numerous studies have been conducted to prepare and characterise layered silicate nanocomposites with different polymers. But many of them have focused on the preparation, mechanical properties and the stability of the nanocomposites. In a few recent studies, the presence of nanoclay has been found to improve the biodegradation of oxo-biodegradable polyethylene, which is just a mixture of polyethylene and a pro-oxidant (Ray and Okamoto 2003, Qin *et al.* 2003, and Reddy *et al*. 2008). The role of clay, however, on the degradation of polyethylene is not completely understood yet.

Abiotic oxidation of polyethylene is facilitated by the addition of transition metal ion complexes (pro-oxidants) as discussed above. The low molecular mass species generated in abiotic oxidation are metabolised by micro-organisms in the biotic stage. Effect of clay on biotic stages has been studied by many researchers recently. Kounty *et al*. (2006) reported that clay promotes the growth of microbes on polymer surface because the pH on the clay surface is conducive to their sustained growth. Recently Reddy *et al*. (2008) have studied the effect of nanoclay on oxo-biodegradation of polyethylene and concluded that the presence of clay in polymer matrix helps in biotic degradation stage.

From the above discussion, it can be seen that the roles of pro-oxidant in abiotic oxidation and clay in biotic degradation have been investigated but the interaction of these materials in both abiotic and biotic stages has not yet been fully understood.

Research just based on trial and error (experimental) approach has some problems. Experiments are costly and time consuming. Therefore a mathematical model that can predict the behaviour of polyethylene nanocomposite degradation process appears to be necessary. This model can provide a better understanding of the physical-chemical processes involved and help to find the solution for undegradability problem.

1.2 Main objectives of the research work

This research is aimed at benefiting the industries such as packaging industry by enhancing the fundamental knowledge on the thermal–oxidation and biodegradation of polyethylene nanocomposites and also by investigating the interaction between manganese stearate (a pro-oxidant) and nanoclay on the oxo-biodegradation of polyethylene systematically. Current methods of nanocomposites production will be carried out to achieve more environmentally friendly and economical polyethylene nanocomposites. This study will be beneficial to industry and community as it will help in the preparation of degradable polyethylene products that can be used in commercial applications. The specific objectives of the works in this research are as follows:

- identify suitable transition metal ion complexes that will enhance the thermal-oxidation of polyethylene nanocomposites,
- prepare polyethylene nanocomposites by melt intercalation,
- investigate the structure and morphology of polyethylene nanocomposite to find out the relationship between the amount of clay loadings and nanocomposte properties,

- prepare oxo-biodegradable polyethylene nanocomposites using optimal concentration of selected pro-oxidant (metal ions) and nanoclay by melt intercalation,
- investigate the morphology and chemical properties of oxo-polyethylene nanocomposites ,
- evaluate the effect of clay and pro-oxidant on thermal oxidation of polyethylene nanocomposite and oxo-biodegradable polyethylene nanocomposites,
- investigate the biodegradation of polyethylene nanocomposites and oxo-biodegradable polyethylene nanocomposites under controlled composting conditions and evaluate the effect of incorporating clay and pro-oxidants on biodegradation process,
- develop a model for the biodegradation process of polyethylene nanocomposites.

2 Literature review

2.1 Overview of polymer biodegradation

2.1.1 Polymer biodegradation

Plastics are synthetic materials introduced to the human usage just about more than one and half century ago. The first man-made plastic was demonstrated in public by Alexander Parkes at the 1862 Great International Exhibition in London. The material called "Parkesine" and it was an organic material derived from cellulose that once heated could be moulded but retained its shape when cooled. The inventor claimed it is versatile and cheaper than natural polymers such as rubber. However, the first truly synthetic plastic-Bakelite - was patented by Leo Baekeland in 1907. It was made from carboxylic acid and formaldehyde. Bakelite resin was normally reinforced with fillers such as fibres and wood flour. But it was not until World War II that the use of synthetic plastics increased significantly. The production of plastics such as polyethylene, polystyrene, polyester, PET and silicone in huge commercial amount started mainly during the wartime. Since then, synthetic plastics have been used in wide range of applications including packaging, building, agriculture, automobile and others.

Among the synthetic plastics, polyethylene has been used widely as a packaging material, particularly as blown films. This is mainly because of its light weight, excellent mechanical properties (tensile properties, tear resistance, and impact resistance), readily controllable and superior optical properties (clarity, gloss, and colour), chemical and biological inertness and lower cost. On the other hand, accumulation of plastic wastes in the environment is a major concern due to their poor or very slow degradation and threat to the life of plants, animals, birds and sea creatures. Several strategies have been

implemented to minimise plastic waste in environment such as source reduction, product reuse, primary/secondary recycling, incineration, and development of environmentally degradable polymeric materials. In practice, all of these approaches have failed to solve the issue completely. For example, recycling of wastes, which seems to be more promising than the others requires prior collection and segregation which adds to the final price of recycled products thus making them economically undesirable. Recycled plastics also show inferior quality which limits their applications. Also, contaminations found in the final products of recycled plastics prevent them from being used in food and hygiene packaging applications. According to the report by United States Environmental Production Agency (EPA) on 'Municipal solid waste (MSW) in the United States: 2009 facts and figures' (2010), plastics waste ranked 4th (behind paper, food scraps, and yard trimmings) at 29.8 million tons and accounted for 12.3% of MSW generation (Figure 2-1). Out of this, only 3% has been recovered for reuse (Figure 2-2).

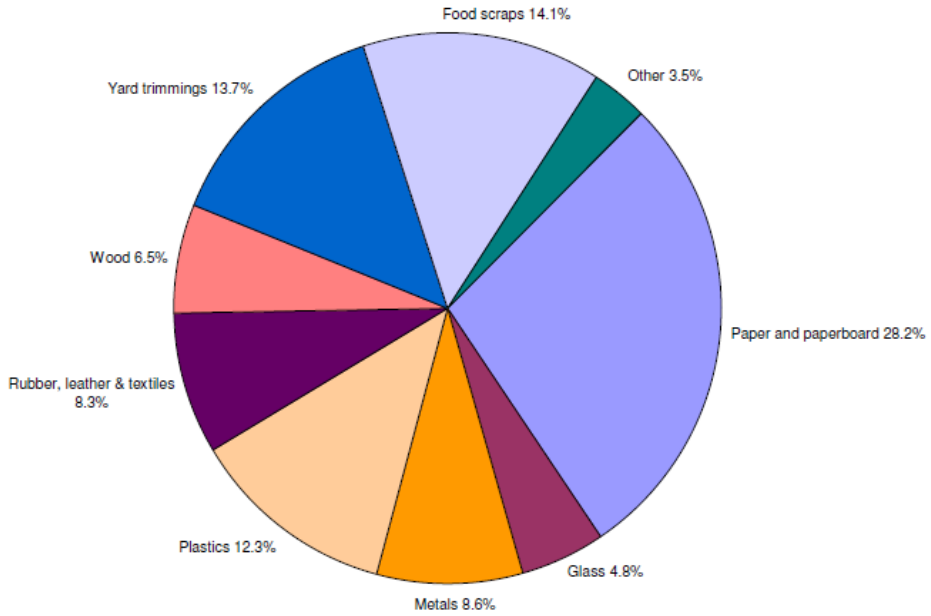

Figure 2-1 Material generation in Municipal Solid Wastes, 2009 (Total 243 million tons) (EPA 2010)

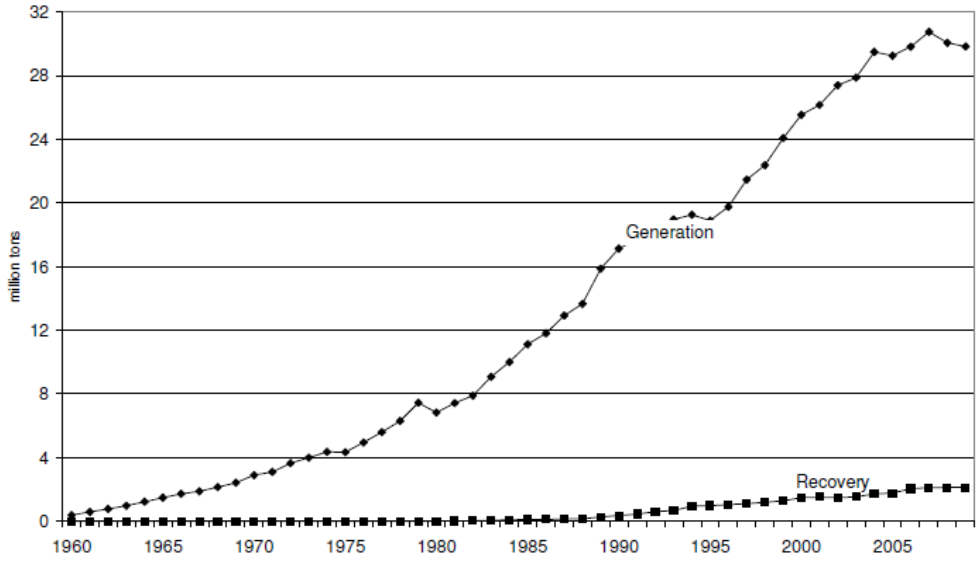

Figure 2-2 Plastic generation and recovery, 1960 to 2009 (EPA 2010)

Failure to reduce plastic waste and consequent increase in its accumulation have led to increased criticisms on plastic usage. This has led many research groups around the world to work on developing environmentally degradable polymeric materials which can degrade and return to their natural carbon cycle. Environmentally-degradable polymers can degrade via physical, chemical, mechanical or biological means or by a combination of these mechanisms and change into either CO_2 and H_2O or CH_4 and H_2O (Albertsson & Karlsson 1995). In other words, changes in polymer properties such as physical, chemical, mechanical or biological properties that lead to bond scission and conversion or transformation into other materials are called degradation (Pospisil *et al*. 1998). Okada (2002) defined biodegradable polymers as polymers which can degrade and catabolise to CO_2, H_2O, and minerals in the nature with the help of microorganisms.

Based on the definitions of degradability mentioned above, polymers can be divided into two main categories:

1. **Biodegradable polymers**: Polymers that belong to this category may either be natural (starch, cellulose, chitosan, natural rubber) or synthetic (PLA, PCL, poly hydroxy-butyrate). These naturally biodegradable polymers can degrade due to the actions of microorganisms or by purely hydrolytic mechanism and get converted naturally into CO_2 and H_2O (or) CH_4 and H_2O under aerobic or anaerobic conditions, respectively. They are also hydrophilic.

However, there is a trade-off for producing biodegradable polymers in commercial quantities. Although they are eco-friendly and minimise the waste in environment, their poor properties such as brittleness, high gas permeability, low thermal stability and high

costs make their applications limited and specific (Okada 2002 and Ray & Bousmina 2005).

2. **Oxo-biodegradable polymers**: The initial step in polymer degradation is oxidative degradation and it is followed by biological degradation. The initiation step, (oxidative degradation) might take place in two ways. If the chain scission starts as a consequence of light/UV effect, the degradation process is considered as photo-oxidative degradation. If the decomposition of polymer matrix is triggered by heat, it is known as thermal-oxidative degradation.

It is worth noting that the photochemical reactions occur only on the surface of polymer while thermal degradation takes place in the bulk (Taylor 2004).

2.1.2 Polymer biodegradation mechanism

A better understanding on the mechanisms involved in polymer degradation will lead to designing and developing new generation of environmentally biodegradable polymers that will have an optimum life. Without such knowledge, research in the field of biodegradable polymers will not proceed very far (Singh *et al*. 2008).

In the biodegradation process, long chains of polymer molecules undergo chain cleavage leading to the formation of low molecular weight fragments that can be assimilated easily by microorganisms. Microbes assimilate low molecular weight compounds and produce carbon dioxide and other metabolic products. It has been shown that micro-organisms can only consume fragments with molecular weight less than 500 and therefore long chains of hydrocarbon molecules in polymers need to be broken down into smaller fragments to facilitate microbial consumption (Albertsson & Karlsson 1995).

Scott (2005) has also confirmed that biodegradation of polymers takes place in two stages namely, primary degradation and ultimate biodegradation. The degradation and stabilisation mechanism observed in polymers is summarised in Figure 2-3 (Pandey *et al*. 2005).

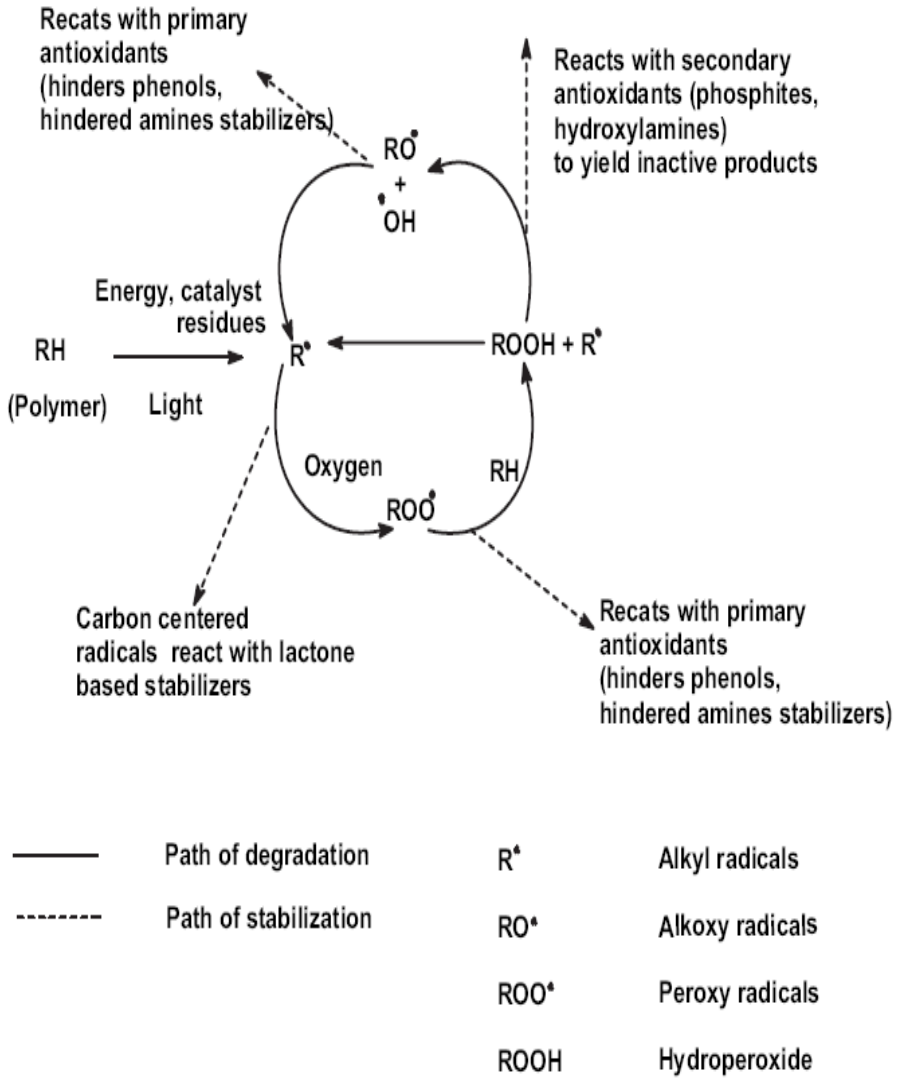

Figure 2-3 Different pathways of degradation and stabilization (Pandey *et al*. 2005)

2.1.3 Methods of evaluation of biodegradability of polymers

Considering the fact that polymer biodegradation process can be triggered and propagated by combination of factors such as heat, light, micro-organisms, humidity etc., techniques for evaluating biodegradability and its rate can vary. Several experimental techniques and instrumental analyses have been developed to measure and evaluate the biodegradability of different polymers and they have been summarised by Pandey *et al*. (2005) as shown in Figure 2-4.

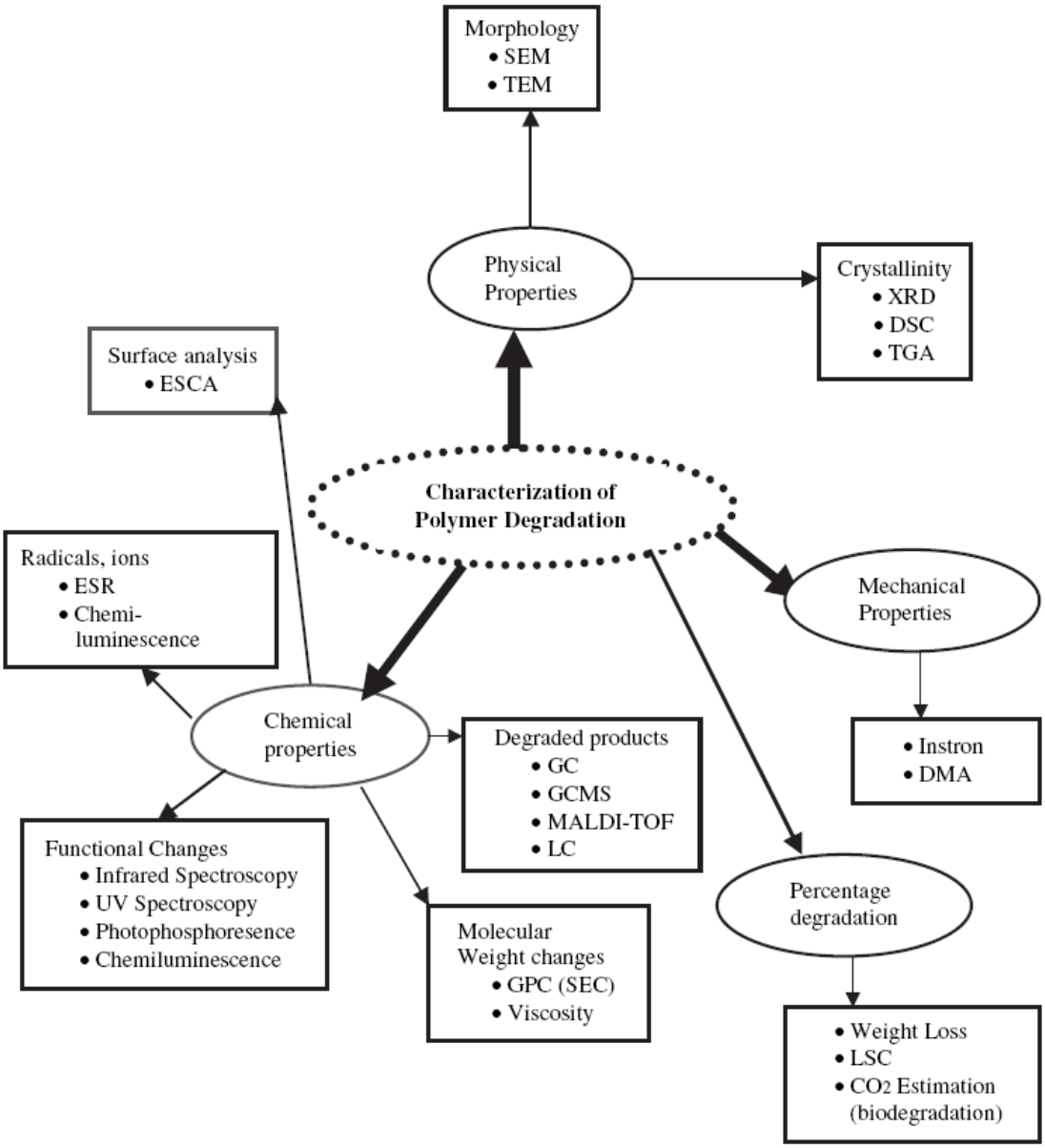

Figure 2-4 Different analytical techniques to evaluate polymer degradability (Pandey *et al*. 2005)

Choosing the most appropriate technique for testing polymer biodegradation is vital. A large number of biodegradation testing techniques have been reported in the literature. The selection of the test method should be based on the nature of the polymer and the

appropriate environmental condition the polymer is likely to be subjected (Yang *et al.* 2005).

Biodegradation tests can be classified into three categories:

1. **Aerobic tests**: In these tests, samples are exposed to microbial consortium in the presence of air. Microorganisms attack and assimilate the polymer and convert it to biomass and CO_2. Two types of quantitative data can be reported at the end of aerobic tests to indicate the percentage of biodegradation. They are: 1) consumption of oxygen by samples (BOD) and the ratio of oxygen consumed to theoretical oxygen demand (TOD); 2) quantity of evolved CO_2 expressed as a ratio of theoretical amount (Th_{CO2}).
2. **Anaerobic tests**: These tests are carried out in the absence of oxygen. The products of these tests are CH_4 and CO_2, and they can be used to quantify the percentage of biodegradation. However, the use of anaerobic tests for polymer wastes is questionable because plastics normally end up in landfills (not in sewage/water treatment plants) where they will be exposed to aerobic conditions rather than anaerobic conditions. Therefore, it is appropriate to use aerobic tests or composting systems for polymer wastes.
3. **Composting**: In this test, the material is exposed to a compost inoculum at a specific temperature or a temperature profile. The degree of biodegradation is determined by the amount of evolved CO_2, which is the end product of biodegradation. The most favourable and reliable test for the biodegradability of packaging materials and polymers is considered to be composting. However, it is worth noting that biodegradability and compostability are different (De Vlieger

2003). Biodegradation is a natural process after the service life of polymer when it is normally discarded into landfill where it begins without any further modification. On the other hand, a pre-treatment is necessary in composting. Removing the non-compostable materials such as metals and glass as well as controlling the particle size and moisture are very important in composting (Bhattacharya *et al*. 2007).

The most commonly used methods for assessing the biodegradability of polymers are reported by American Society for Testing and Materials (ASTM) and International Standard Organisation (ISO). According to these methods, biodegradability can be measured using the changes in chemical and physical properties, weight loss, the amount of carbon dioxide production, bacterial activities in soil, changes in shape and molecular weight distribution (Singh & Sharma 2007).

2.1.3.1 Assessment of biodegradability

Different methods can be used to assess the biodegradabilty of polymers. The most common assessment methods used by researchers are:

- Measurement of physico-mechanical change
- Chemical changes and formation of product
- Weight loss

2.1.3.1.1 Qualitative methods

- GPC

GPC or Gel Permeation Chromatography is a widely used technique to determine molecular weight and molecular size distribution. This technique works based on the

separation of molecules by size. Therefore, it is a suitable method to study the degradation of polymer as it can monitor the molecular size variation during the degradation period. It is well known that polymer macromolecules break down into fragments with much lower molecular weight during the degradation.

- Biofilm

Studying the biofilm on the surface of degraded polymer is a technique that is used to prove the presence and growth of micro-organisms. Consequently, it can be used to validate the biodegradability of polymer at a given condition. The final stage in the biodegradation of any material is considered to be the assimilation of the material by microorganisms leading to the generation of CO_2, H_2O and minerals. The existence and colonisation of bacteria or fungi on the polymer surface indicates their activity under a specific environment. It has been shown by Ojeda *et al*. (2009) that there is no sign of biofilm for pure polyethylene after its exposure to different environmental conditions.

2.1.3.1.2 Quantitative methods

- Fourier Transform Infrared Spectroscopy (FTIR)

Degradation of hydrocarbon chains leads to the formation of ketones, hydroxyl groups, and carbonyl groups which can be detected by FTIR spectra. Therefore, FTIR spectroscopy is used extensively to detect the degradation products of polymers. For instance, by studying the number and intensity of peaks in carbonyl region in FTIR spectra, the rate of degradation of polyethylene and therefore the rate of conversion of macromolecules into smaller fragments consisting of C=O band can be determined.

- CO_2 evolution

The degree of biodegradation can also be quantitatively determined by measuring the amount of CO_2 evolved, which is the ultimate product of biodegradation. This method has been chosen in this study to evaluate the biodegradation of polyethylene nanocomposites. The details of this technique will be discussed in Chapter 3.

2.2 Overview of polyethylene degradation

Although only around 12% of municipal solid wastes are plastics, they pose serious threat to the environment due to their longer degradation time. Among the plastic wastes, polyethylene is found in larger quantity because of its wider usage in packaging applications. Polyethylene has a simple structure because it consists of repeating CH_2-units and it can be produced by addition polymerisation of ethylene. It accounts for nearly 40% of the plastic usage in the world and it is the base polymer used in the production of plastic bags and packaging films. Synthetic polymer packaging film is one of the major sources of plastic wastes due to its non- biodegradability.

Polyethylene is normally not biodegradable because of its high molecular weight, long carbon chain, non-polar nature, lack of functional group and its hydrophobicity. It has to be degraded into low molecular mass species before they can be metabolised by micro-organisms (Albertsson *et al*. 1987 and Erlandsson *et al*. 1997). The physical degradation is the first step in the degradation process and is called oxidative or abiotic degradation. In the experimental study on degradation, the oxidative degradation should be carried out under conditions close to the real conditions for selected application. The rate of polymer degradation depends on several factors such as type of polymer, type and amount of

additives, temperature and so on (Sipinen & Rutherford 1993). Albertsson & Karlsson (1988) stated that it will take 100 years for polyethylene to mineralise to less than 0.5% without UV/heat exposure and the ultimate mineralisation after 100 years will reach 1% if it is exposed to sunlight regularly.

As mentioned above, polymer degradation takes place in two main stages: the first stage, which is defined as "the rate determining step", is the abiotic oxidation. It may be followed by the second stage, known as the biotic stage, in which bio-assimilation of oxidised products by microorganisms occurs (Albertsson *et al*. 1987). Abiotic oxidation may occur due to either thermal oxidation or photo-oxidation. The combination of abiotic oxidation and biodegradation is known as oxo-biodegradation. In the abiotic oxidation stage, large polyethylene molecules oxidise and break into lower molecular weight products such as aldehydes, ketones, carboxylic acids, alcohols, etc. The presence of OH, C=O and COOH groups in the products leads to further oxidation of polyethylene. Jakubowicz *et al.* (2006) have shown that the products of thermal oxidation such as carboxylic acids, alcohols, ketones, etc. can be easily consumed by micro-organisms as nutrients to produce cell biomass.

Several patents and articles have been published in the last few decades about making polyethylene degradable by adding very low concentration of primarily carboxylate of transition metal ions such as Fe, Co, Ni and Mn with or without fatty acids, esters, natural oils, unsaturated elastomers and corn starch (Wiles *et al*. 2006, Griffin US patents no. 4016117 (1977); 4021388 (1977); 4218350 (1980); 4983651 (1991) and Hudson US patent no. 5,393,831 (1995)). Harnden *et al*. (1990) patented a degradable polyethylene by incorporating cerium (+3) stearate into polyethylene. They have found that this

composition is effective in promoting the environmental degradation of polyethylene both by thermal-oxidation and photo-oxidation to produce low molecular weight oxygenated products such as ketones, carboxylic acids, alcohols, esters and aldehydes. Orhan *et al*. (2004) also reported that metals act as good pro-oxidants in polyolefins. For example, manganese (Mn) was shown to be a good pro-oxidant in the thermal degradation of polyethylene. It can lead to the production of free radicals on polymer chains when it is activated by heat in the presence of oxygen. Jakubowicz *et al*. (2003) claimed that, by adding metal ions, degradation starts with free radical chain reaction consuming oxygen from atmosphere. The pro-oxidant catalyses the chain scission in polymer leading to the production of low molecular mass oxidation products containing -COOH, -OH and C=O groups. They have also shown that the presence of pro-oxidants lowers the activation energy for the reaction. Zheng *et al.* (2005) proved by experiments that transition metals have accelerated thermal oxidative processes of polyolefins by inducing hydroperoxide decomposition. Sipinen & Rutherford (1993) suggested that the metal ions like Mn^{2+}/Mn^{3+}, which have two different oxidation numbers with one unit difference, are the most active ones in thermal degradation.

2.2.1 Abiotic oxidation of polyethylene (thermal oxidation)

Abiotic stage has the main role in entire degradation process as it controls the rate of oxidation because micro-organisms only can assimilate low molecular weight compounds. Heat (temperature) and sunlight are the two main factors that influence the abiotic oxidation. Therefore, oxidation process of polyethylene can be categorized into two categories: thermal oxidation and photo oxidation (Albertsson *et al.* 1987). Thermal

oxidation depends on various factors such as temperature, heating rate, pressure and environmental condition.

The mechanism of thermal degradation of polymers involves two reactions: random scission reaction and chain-end scission of C-C bonds. In random scission reaction, macromolecules of polymer cleave into shorter chain fragments leading to molecular weight reduction of original sample. Random scission chain can be initiated at any weak sites or imperfection point in the chain structure like carbon double bond, sites of oxygen, nitrogen or any other impurities. During the manufacture of polyolefins at high temperature, they get some impurities and therefore they are sensitive to thermal oxidation (Khabbaz *et al*. 1999 and Gowariker *et al*. 2000).

Chain-end reaction mainly takes place at the interface of gas-liquid phases and the products of this reaction are volatile molecules (Murata *et al*. 2002). Degradation starts at the chain end followed by the release of monomers from the polymer. Molecular weight of polymer decreases gradually due to the release of monomer units from the end of polymer chain. This type of reaction is also called depolymerisation. Mechanisms of chain-end degradation (unzipping route) and random scission route are shown below:

$$M_n^* \rightarrow M_{n-1}^* + M$$

$$M_{n-1}^* \rightarrow M_{n-2}^* + M$$

$$M_n \rightarrow M_x + M_y$$

In the case of polyethylene, degradation occurs mainly through random scission. Hydrogen atom migrates from one carbon to another and produces two other shorter molecules.

Aguado *et al*. (2007) and Rodriguez-Vazquez *et al*. (2006) studied thermal degradation of LDPE at 400°C and they have shown that the degradation route involves mainly intra-molecular hydrogen abstraction followed by β-scission. In Figure 2-5, the general route of degradation is presented. In the first step, degradation is initiated by either random or chain-end scission. In the second step (propagation step), monomers are formed. In the final step, the reactions terminate through radical coupling and radical disproportionation (Soto-Oviedo *et al*. 2003).

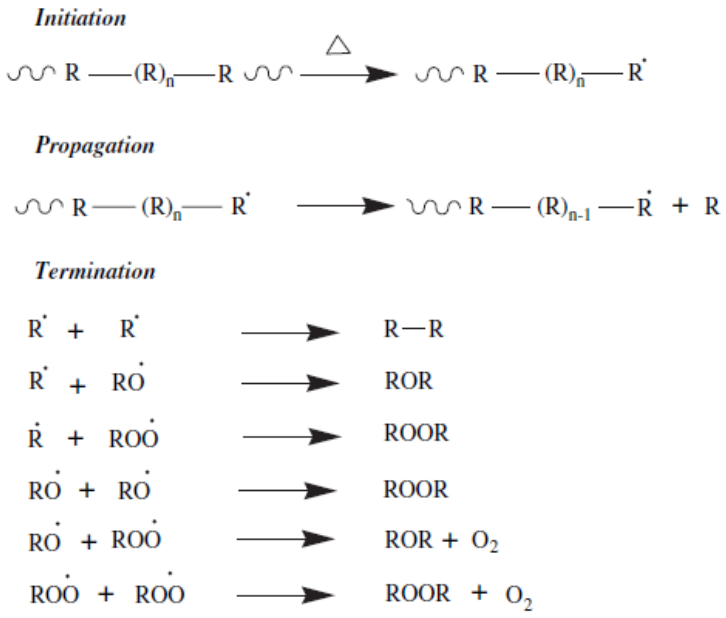

Figure 2-5 Thermal degradation mechanism (Soto-Oviedo *et al.* 2003)

Degradation in polyethylene, leads to the formation of hydro-peroxides which will undergo further oxidation to form carbonyl compounds (Karlsson & Albertson 1998). As a result of this reaction, chain scission occurs and the polymer loses its mechanical strength (Albertson *at al*. 1987). The role of pro-oxidant is important in this stage as it can produce free radicals, which can generate polyethylene macro radicals. These macro radicals react

with oxygen and form intermediate hydroperoxides which lead to the decomposition of polymer chain (Albertsson & Karlsson 1990 and Orhan 2000). The degradation proceeds further by auto-oxidation and chain cleavage of polyethylene (Scott 2001 and Chiellini *et al*. 2003). Metal ions produce free radicals that attack the polyethylene carbon chain, break it into smaller fragments with functional groups which will lead to auto-oxidation reactions (Hakkarainen *et al*. 1997, Khabbaz *et al*. 1998, 1999 and Albertsson *et al.* 1992).

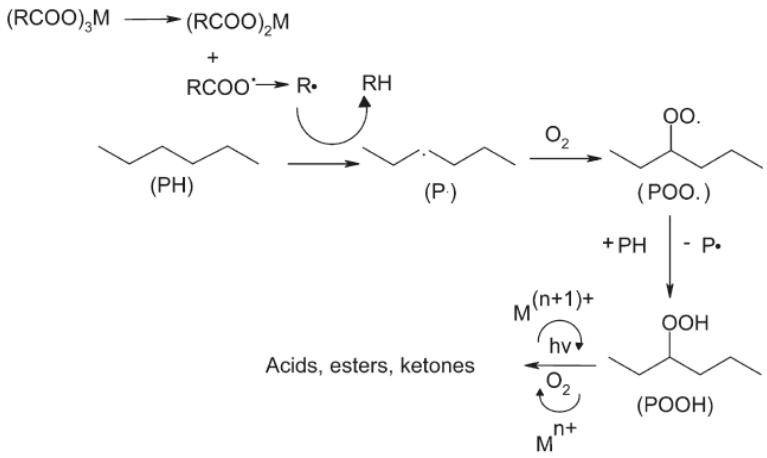

Figure 2-6 Abiotic degradation of polyethylene (Albertsson *et al*. 1987)

Albertson *et al.* (1987) presented a scheme showing the mechanism of polyethylene degradation (Figure 2-6). They also proposed a mechanism for the biodegradation of polyethylene after oxidative degradation (Figure 2-7). Their scheme shows that the products of oxidation of polyethylene such as carbonyl group fragments can be attacked by microorganisms leading to the production of the ultimate products of biodegradation: CO_2 and H_2O.

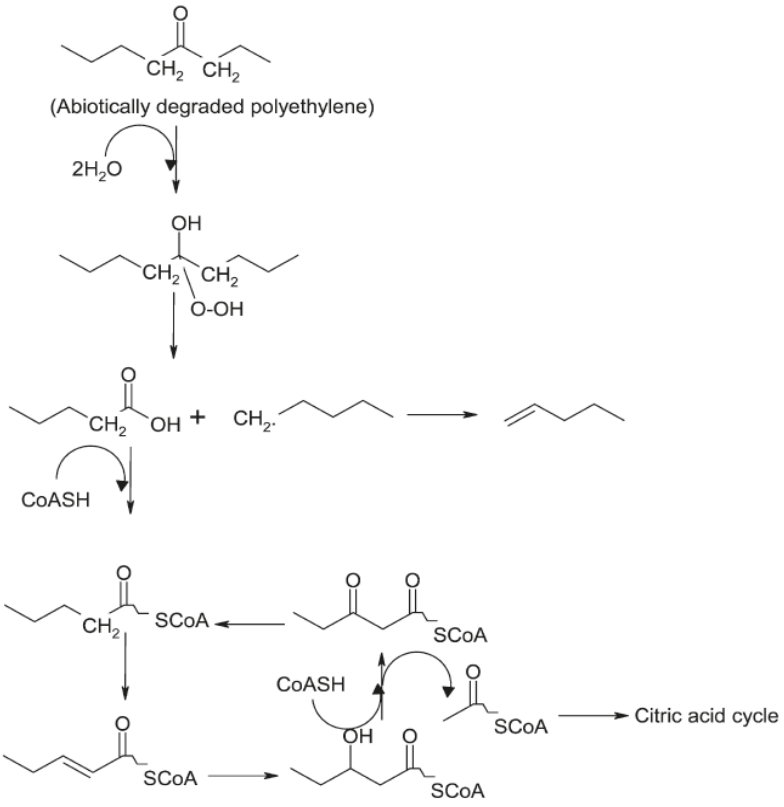

Figure 2-7 Proposed mechanism for the biodegradation of polyethylene (Albertsson *et al.* 1987)

As mentioned earlier in this chapter, pro-oxidants play a vital role in the abiotic stage of polymer degradation. Therefore, many researchers have attempted to study the role of pro-oxidant in polymer degradation. Jakubowicz (2003) conducted extensive experiments to evaluate the degradability of polyethylene films containing manganese and find a relationship between temperature, oxygen content and time needed for the degradation of polyethylene films. Two different films with different concentrations of Mn-stearate have been used in his study. The amount of manganese stearate in one film was twice that in the other film. However, the amount of pro-oxidant used was not mentioned in the paper. Thermal oxidation was performed at 50, 60 and 70°C. The oxygen content in the gas used

in his experiment was varied from 21% oxygen (using air) to 10% and 5% oxygen (by using a mixture of oxygen and nitrogen). It was concluded that the temperature is the most effective factor in degradation. However, the samples were found to degrade quickly at all temperatures used. Results showed that the molecular weight of both polymer samples decreased to less than 5000 after 2 and 8 weeks at 70 and 60°C, respectively. Figures 2-8 and 2-9 show clearly the effects of oxygen and temperature on oxidation time. It is evident that there is no significant difference in molecular weight reduction by changing the oxygen content. However, results of this study showed a dramatic decrease in degradation time with increase in pro-oxidant concentration. For instance, at 60°C, film with lower amount of Mn degraded to a molecular mass of 10000 in about 18 days, while the other sample which had twice the amount of Mn reached this point in 11 days. Jakubowicz studied the rate of biodegradability of samples oxidised in an oven at 70°C for 4 weeks using a mineralisation test which used an activated soil composed of 90% plant substrate of peat basis and 10% of mature compost at 60°C for 180 days. Jakubowicz reported that 60% biodegradation occurred without any lag phase. He also claimed that the samples would eventually biodegrade completely. However, considering the natural process of degradation of plastics in landfills, 4 weeks of heat exposure at 70°C appears to be a long time for pre-treatment. Therefore, the conditions which Jakubowicz used cannot be justified to compare with natural biodegradation of polyethylene.

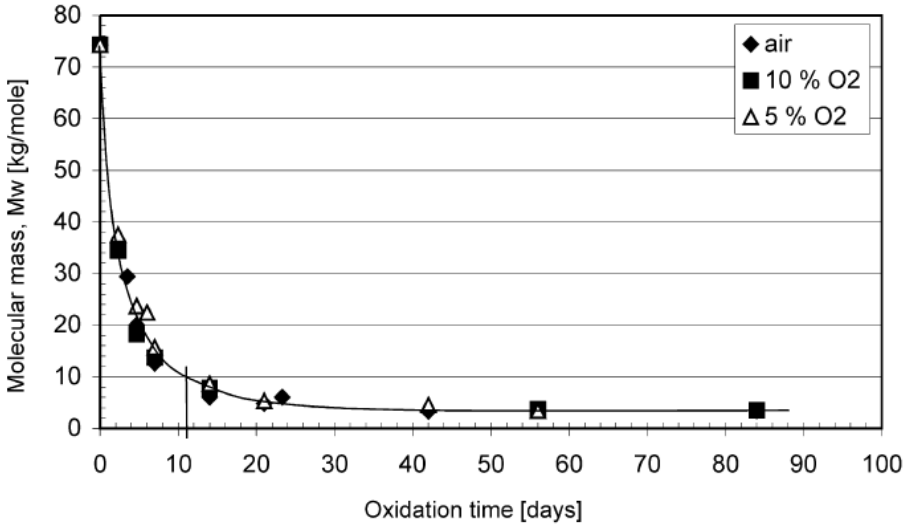

Figure 2-8 Effect of oxygen content on the rate of degradation of the AF 20 material. Superposition analysis by shifting data to 60˚C (Jakubowicz 2003)

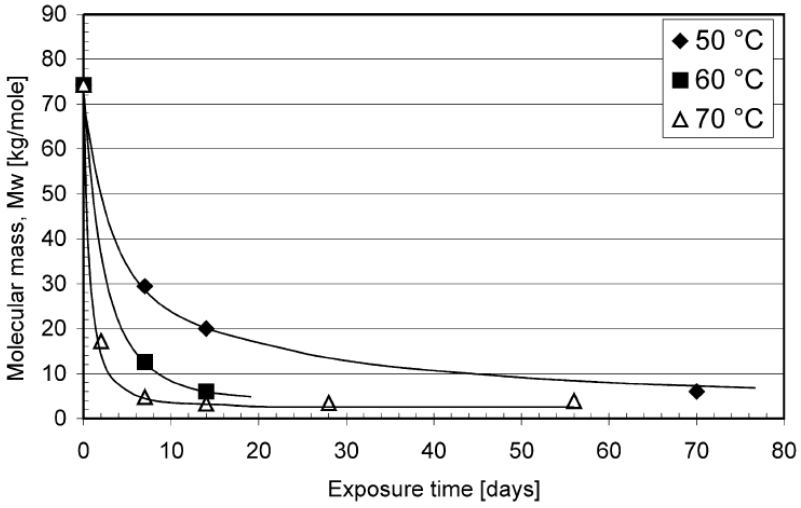

Figure 2-9 Change of molecular weight of sample with exposure time at various temperatures in air (Jakubowicz 2003)

Furthermore, Jakubowicz (2006) continued his study on the rate of abiotic degradation of biodegradable polyethylene under various environments to investigate the effect of humidity on degradation. In this study, degradation of polyethylene films containing

manganese ions has been investigated. This study has revealed that the degradation is faster under higher humidity. However, when the tests samples exposed to humid air and compost inoculum with the same moisture content, sample in the compost showed much slower degradation. Jakubowicz proposed that the generation of ammonia and/or hydrogen peroxide by microorganisms in the compost may have a deactivation effect.

In an earlier study, Sipinen & Rutherford (1993) conducted an extensive investigation on the effect of different metal ions on oxidation time. They incorporated several different transition metal salts into polypropylene and measured the time for embrittlement to study the effect of different metal ions on the degradation process. The results are shown in Figure 2-10. Manganese led to the shortest degradation time among all the transition metal ions used. Sipinen & Rutherford attributed this observation to the redox potential of manganese and the several oxidation states for this metal which make it more active.

Metal (150 ppm)	Time to embrittlement (h)	
	104 °C	70 °C
Mn(II)	41	541
Co(II)	41	720
Cu(II)	41	723
Ce(III)	85	1610
V(III)	172	2114
Fe(II)	750	>3000
Mo(IV)	1050	>3000
Zr(IV)	1400	>3000
Ni(II)	>2500	>3000
Ti(II)	>2000	>2000
Pd(II)	>2000	>2000
Pt(II)	>2000	>2000

Figure 2-10 Time to Embrittlement for Various Transition Metal Salts Mixed into Polypropylene at a Concentration of 150-ppm Metal Ion (Sipinen & Rutherford 1993)

2.2.2 Biodegradation of polyethylene

Microorganisms produce extra cellular enzymes which disintegrate the polymer macromolecules and break them down into smaller fragments. Smaller molecules can cross the cell wall and cytoplasmic membranes. Polyethylene is non-polar and it contains only C-C and C-H bonds and therefore cannot provide centres for nucleophilic of electrophilic attack. Therefore, radical reaction is one of the options that can break down the neutral polyethylene molecule to molecules with functional groups. For example, Scott (1997) showed pre-oxidation modifies surface of a polymer to hydrophilic, thus makes it favourable for micro-organism growth. Also, addition of some materials to polyolefins can create a suitable environment for growth of microorganism. Different approaches to produce biodegradable polymers include using naturally biodegradable fillers in the synthesis of polymer, modification of polymer back bone with hetero-groups such as oxygen, and having unsaturated bond in the carbon chain (Gowariker *et al*. 2000).

In majority of published studies on biodegradation of polyethylene, biodegradability has been demonstrated by the formation of biofilm on the surface of polyethylene, physical brittleness, and weight loss. None of these involves any quantitative measure that can prove the actual conversion of polymer into the end products of biodegradation (CO_2 and H_2O). Moreover, there is a doubt about the suitability of these methods for evaluating the extent of biodegradation. For example, weight loss can happen due to additive leaching or fragmentation, and it does not necessarily show the amount of biodegradability in polymer. The fragments could be so small that they cannot be collected for weighing (Roy *et al*. 2011). In this thesis, the focus is on the studies which have reported quantitative results for composting and soil burial conditions. It has been accepted by many researchers that the

biodegradation of polyethylene needs extremely long period. A ten year study on the biodegradation of polyethylene by Albertsson *et al*. (1990) showed that biodegradation in soil for UV irradiated PE samples is less than 0.5 wt% and also it was even lower for samples not irradiated (0.2 wt%). Similar results were reported later by other researchers who confirmed that pre-treatment is necessary for polyethylene before biotic stage.

In a later study, Chiellini *et al*. (2003) investigated the biodegradation of commercially available polyethylene films containing pro-oxidant (LDPE-TDPA). Polyethylene samples were thermally degraded in an oven for 44 days at 55°C, then mineralised in soil and mature composts diluted with perlite and supplemented with 25 ml of 0.1% $(NH_4)_2HPO_4$ solution. They reported significant degree of biodegradation (50- 60 %) over a period of 18 months. By looking at the trend and the effective factors responsible for biodegradation, Chiellini *et al*. noted that mineralisation process starts without apparent lag phase and the polymer continually degrades. But their results showed that the degradation process tends to a plateau at about 4% mineralisation after 30 days of incubation (Figure 2-11). On day 40, their samples were agitated in their inoculum. It can be seen from Figure 2-11 that a slight increase in mineralisation occurred after agitation. However, the rate of biodegradation stayed very low. After 5 weeks of incubation, more modifications and culture treatment were carried out by Chiellini *et al*. to study the effectiveness of these factors. Samples were agitated and water was added to the first set of samples (Q-LDPE run Q1) while the other set was modified with water and fresh forest soil (Q-LDPE run Q2). It is clearly evident from Figure 2-11 that this modification had a substantial influence on the biodegradation rate leading to an exponential increase in the mineralisation profile after that the modification. Furthermore, it is also clear that, even at the end of incubation time, a positive degradation profile is still apparent.

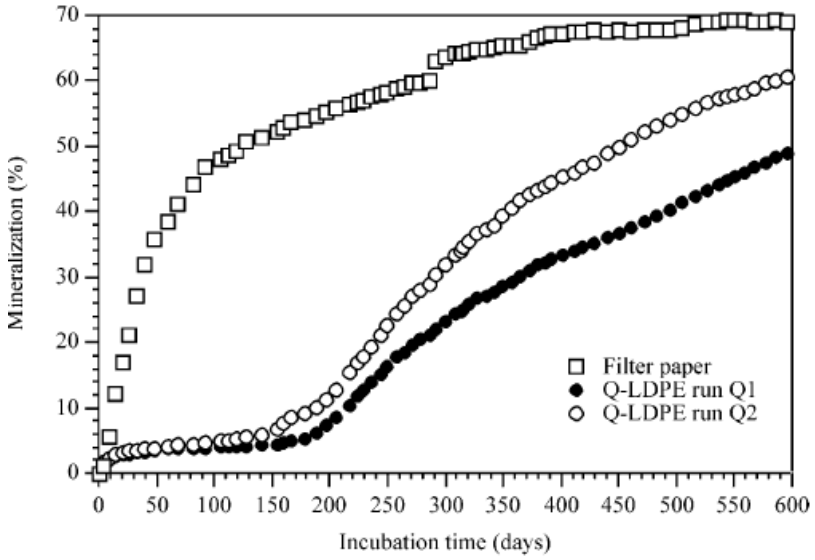

Figure 2-11 Mineralisation profiles of thermally fragmented Q-LDPE samples and filter paper in soil burial test (Chiellini *et al*. 2003)

Chiellini *et al*. (2006), in a following study, investigated the effects of temperature and relative humidity on the degradation/biodegradation behaviour of their LDPE-TDPA samples. As was expected, the induction time (lag phase) was significantly shorter at higher temperature compared to lower temperature. However, the overall degradation rates of both samples were comparable. Although samples under the environment with 75% relative humidity had a slower start of oxidation compared to the one under dry air, there was no big difference in the final oxidation level. A substantial drop in molecular weight was also reported by the authors in thermally treated samples. They noted that by analysing the molecular weight decrease versus carbonyl index graph, the degradation trend is in agreement with the statistical chain scission mechanism proposed by other researchers for photo- and thermal degradation of polyolefins.

In another study, Chiellini *et al*. (2007) questioned the suitability of the media used for biodegradability tests. As all the plastic waste do not end up in landfill, they questioned the fate of oxidised fragments of oxo-biodegradable polyethylene in natural environments other than soil and compost. They were particularly interested in the polymer biodegradation in aqueous media (river, lake, brackish and marine waters) where a relatively high percentage of plastic wastes might end up endangering lives of millions of birds and sea animals. They conducted their degradation experiments in a water medium using thermally pre-oxidised LDPE-TDPA samples and monitored the amount of CO_2 evolved over a period of time. After 100 days of incubation, they reported up to 10% biodegradation for tested samples. This work confirmed their pervious results on biodegradability of commercially available LDPE-TDPA plastics supplied by EPI (Environmental Plastics Inc.) in solid incubation media.

An interesting research was conducted by Ojeda *et al*. (2009) on biodegradability of LDPE samples containing a commercially available pro-oxidant in the form of plastic bags (currently used in supermarkets in Brazil). They exposed their samples to natural weathering condition for one year. Test samples were analysed at various time intervals to monitor the degradation stages by visual inspection, Size Exclusion Chromatography (SEC) and Fourier Transform Infrared Spectroscopy (FTIR). After a year, residues of samples were incubated in compost and perlite substrate. Their biodegradation tests were carried out following the method used by Chiellini *et al*. (2003). They observed cracking and fragmentation in samples containing pro-oxidant after 13 weeks of testing under weathering condition. They reported the formation of biofilm on the surface of the film samples after one year. They have attributed it to the development of fungi of genera *Aspergillus* and *Penicillin* which use degradation products such as carbon as energy

source. No microbial colonisation was reported in LDPE without pro-oxidant. Using the CO_2 evolution for aged films over a period of 3 months incubation, Ojeda *et al.* showed 12.4 % mineralisation which was less than what were reported earlier by Chiellini *et al*. (2003, 2006 & 2007) and Jackubowicz (2003). However, Ojeda *et al.* conducted their experiments under conditions most suitable for the biodegradation process. Samples without pre-oxidation have shown significantly lower mineralisation (2.1%).

Ojeda *et al*. (2009) also estimated the maximum potential mineralisation of samples (C_{max}) and the mineralization rate coefficient k by using the curve fitting program Sigmastat to simple exponential equation $C_m = C_{max}[1 - \exp(-kt)]$. The maximum potential mineralisation calculated from later formula was 23.2%. Another worthwhile observation made by Ojeda *et al*. in this study was the dramatic changes in sample degradation after 3 – 4 months of exposure to sunlight. They compared the degree of mineralisation of test samples as a function of the exposure time. They showed, when samples with pro-oxidant exposed to weathering condition for 30 days, mineralisation halved compared to the same samples exposed to the same conditions for a year (12.5% in the first case compared to 6.3% for the second one). Figure 2-12 shows a dramatic reduction in mineralisation when the exposure time was only 7 days (about 2.2% mineralisation). Ojeda *et al.* concluded that prior pre-oxidation is an essential pre-requisite to the biodegradation of polyethylene. In other words, polymer must first go through a stage of pre-treatment, such as solar radiation or heating in the presence of oxygen, to be susceptible for the next stage of microbial attack.

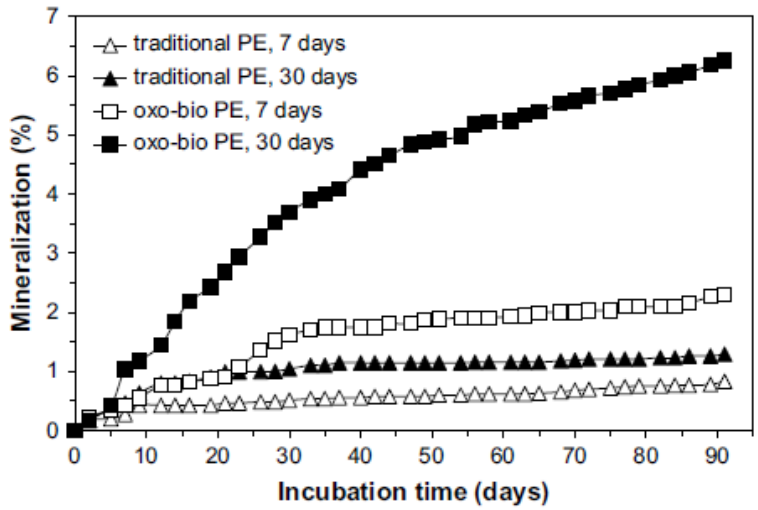

Figure 2-12 The biodegradation of oxo-biodegradable and conventional PE films exposed to a natural environment for 7 and 30 sunny days (Ojeda *et al*. 2009)

Feuilloley *et al*. (2005) examined the biodegradability of so-called "biodegradable" PE, which is commercial mulch film containing pro-oxidant, using 10 standardised methods. Results from a respiratory test in natural soil did not show more than 15% degradation after a year. It can be seen from Figure 2-13 that biodegradation reached a plateau after 200 days of incubation.

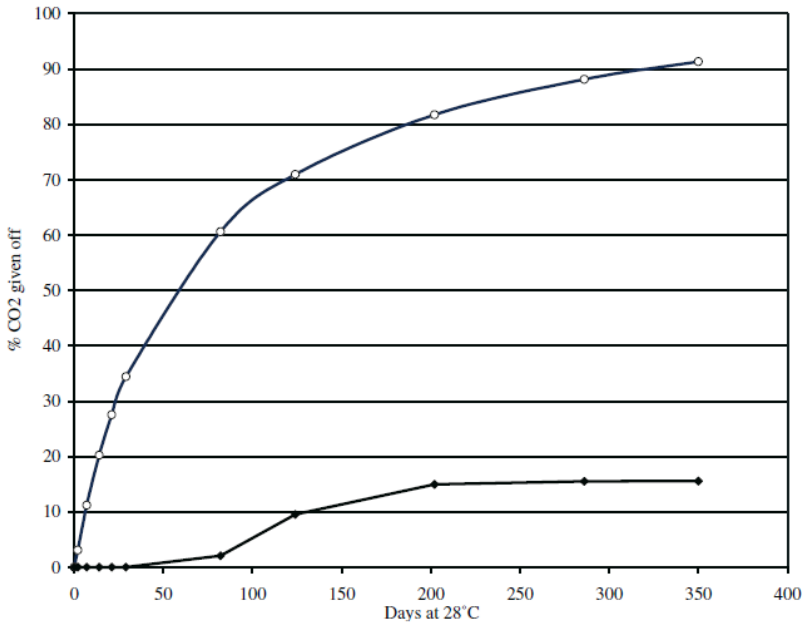

Figure 2-13 Respirometric test on real soil (ASTM D5988-96 modified). The percentage of CO_2 released as a function of time for the reference paper and PE with additives. ○ represents reference paper and • represents PE with pro-oxidant (Feuilloley *et al*. 2005)

Feuilloley *et al*. (2005) compared the biodegradability of a mulch film with that of two other commercially available biodegradable mulch films (Figure 2-14). They observed irrespective of the method used, Material A and B exhibited significant biodegradation (up to 95% for material A and 75% for material B), while PE based film failed to show noticeable biodegradability in all tests performed. It showed around 1.1% biodegradation in composting tests after 50 days. It is interesting to see that for the tests carried out in agriculture soil; biodegradation based on the visual assessment was 90%. In fact, 90% of the film was not distinguishable from other soil constituents after one year of field exposure. Feuilloley *et al*. also claimed that total fragmentation of samples occurs after 11 months. However, no quantitative data on the proportion of fragment remaining in soil was

reported in this paper. Feuilloley *et al*. have also questioned the relevance of pre-treatment of the films in biodegradation tests because in their view these films are mostly buried in the soil where the presence of UV/ high temperature is not possible.

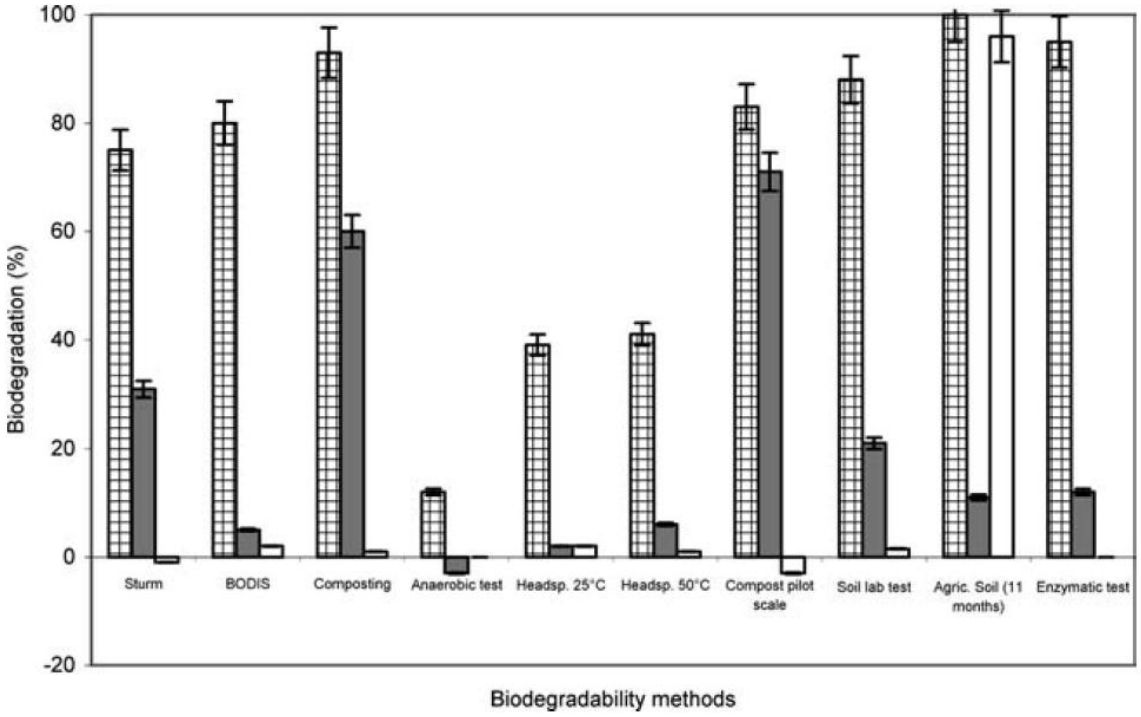

Figure 2-14 Comparison of the percentage of biodegradation for material A, B and C according to the nature of the test used. The first bar from left represents polymer A (starch based); 2*nd*, represents polymer B (aliphatic/aromatic polyester) and 3rd, represents polymer C (PE with pro-oxidant) (Feuilloley *et al*. 2005)

Relatively a new technique has been used by several researchers (Arnaud *et al*. 1994, Koutny *et al*. 2006, Reddy *et al*. 2009 and Kumanayaka *et al*. 2010) to evaluate the biodegradability of polyethylene based films. After pre-treatment by either UV or heat, test samples were subsequently exposed to well-defined one or more strains of bacteria and fungi. Microorganism growth and biodegradation were evaluated afterwards. However, it

would be far unrealistic to cite them here for the evaluation of biodegradability of PE as it is rather impossible to cultivate selected strains of microorganisms on polymer in real composting and soil burial conditions.

Recently Mohee *et al*. (2008) have conducted biodegradation experiments under both aerobic and anaerobic conditions using polyethylene with pro-oxidants. They observed that, in the absence of pre-oxidation, the amount of CO_2 and CH_4 evolved from vessels containing film samples was similar to that from blank vessels containing no sample. In other words, Mohee showed even samples containing pro-oxidant did not show any significant biodegradation without pre-oxidation or pre-treatment.

In an earlier study conducted by Yabannavar & Bartha (1994), two different "photo-degradable" samples were incubated in soil after exposure to sunlight for 6 and 12 weeks. Interestingly, samples with less exposure time exhibited higher CO_2 evolution. For those samples with 6 weeks of exposure, the conversion of polymer to CO_2 was 3.5 and 4.5% while the others subjected to longer period the conversion was 2.9 and 1.5%, respectively. This behaviour may be attributed to possible cross-linking in polymer, which makes it less amendable for microbial consumption (Feuilloley *et al*. 2005).

2.3 Overview on polymer-layered silicate nanocomposites

2.3.1 Introduction

Polymers are filled with synthetic or natural inorganic materials to

- improve their properties
- lower the cost (Pavlidoua & Papaspyrides 2008)

It has been more than 50 years since scientists started incorporating layered silicates into polymer matrices (Cho & Paul 2001). But the most significant achievement on polymer-layered silicate nanocomposite was the introduction of nylon 6/montmorillonite nanocomposites by TOYOTA in early 1990s. Today, almost all kinds of polymer matrices are used to produce nanocomposites (thermoplastics as well as thermosets with different polarities) (LeBaron *et al*. 1999, Fornes *et al*. 2001, Cho & Paul 2001, Manias *et al*. 2001, Shelley *et al*. 2002, Chin *et al*. 2001). But most of these materials are prepared in the laboratories in small scales to study the morphology and properties of the resulting nanocomposites. The nanocomposites have entirely different properties compared to conventional composites and pristine polymer due to the high surface area of dispersed materials in nano dimension (Alexandre & Dubois 2000 and Giannelis 1996).

Thus, nanocomposites can be defined as multiphase materials that contain two or more distinctly dissimilar components with at least one dimension in the nanometre scale. Nanocomposites based on naturally biodegradable polymers such as starch show outstanding biodegradation behaviours but the lack of structural and mechanical strength and also their poor barrier properties make them unpopular for applications in industry (Schmidt 2002).

The amount of exfoliation obtained in nanocomposites depends on the following:

1. the processing conditions
    a. temperature
    b. feeding rate
    c. extruder
    d. the screw configuration

2. compatibiliser
3. clay chemical treatment
4. type of organoclay

In addition, sufficient residence time in the extruder and appropriate shear history are the other factors that influence the morphology and properties of nanocomposites (Cho & Paul 2001).

According to the mechanism proposed by Dennis *et al*. (2001), three scenarios might exist based on the level of dispersion of clay particles into the polymer matrix (Figure 2-15). First one occurs when chemically-treated clay and polymer are compatible with each other to form exfoliated nanocomposites under any sets of processing conditions. This case is called chemistry-dependent process. In the second case, which is called chemistry/processing dependent, clay needs chemical treatment and the process conditions should be optimized. In this case, polymer and treated clay are marginally compatible, and they need optimum conditions to form exfoliated or intercalated morphology. The third case occurs when there is no compatibility between chemically-treated clay and polymer. The most desired result is obviously a relatively good dispersion of clay in the polymer matrix which can happen under optimum processing conditions. However, forming a complete exfoliated structure is not possible due to various constraints. (Figure 2-15)

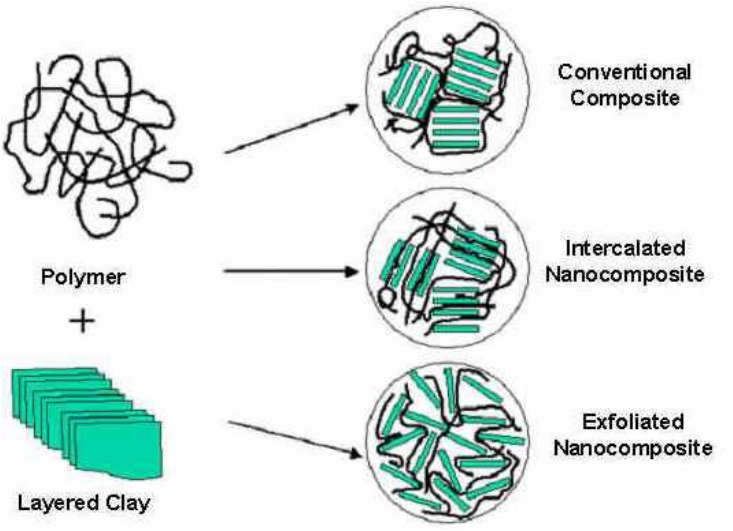

Figure 2-15 Schematic of different dispersions of polymer and layered silicate (Denault & Labrecque 2004)

Nanocomposites produced should meet many requirements. Especially their oxidation characteristics should be such that they should be durable during their service life but they should undergo rapid disintegration and biodegradation after they are discarded in the environment.

2.3.2 Preparation of polyethylene nanocomposites

2.3.2.1 Materials

- **Layered silicate (clay)**

Montmorillonite, hectonite and saponite are the most commonly used layered silicates in the preparation of nanocomposites due to their high aspect ratio and unique intercalation-exfoliation characteristics (Cho & Paul 2001). These layered silicates belong to 2:1 clay family known as 2:1 phyllosilicates, meaning that 2 tetrahedral sheets sandwiching a central octahedral sheet. The particles are plate-shaped and their average diameter varies

from 30 nm to several microns (Giannelis 1998 and Alexandre & Dubois 2000). Chemical formula for montmorillonite is given as follows:

(Na,Ca)0.33(Al,Mg)2(Si4O10)(OH)2·nH2O

and its structure is shown in Figure 2-16.

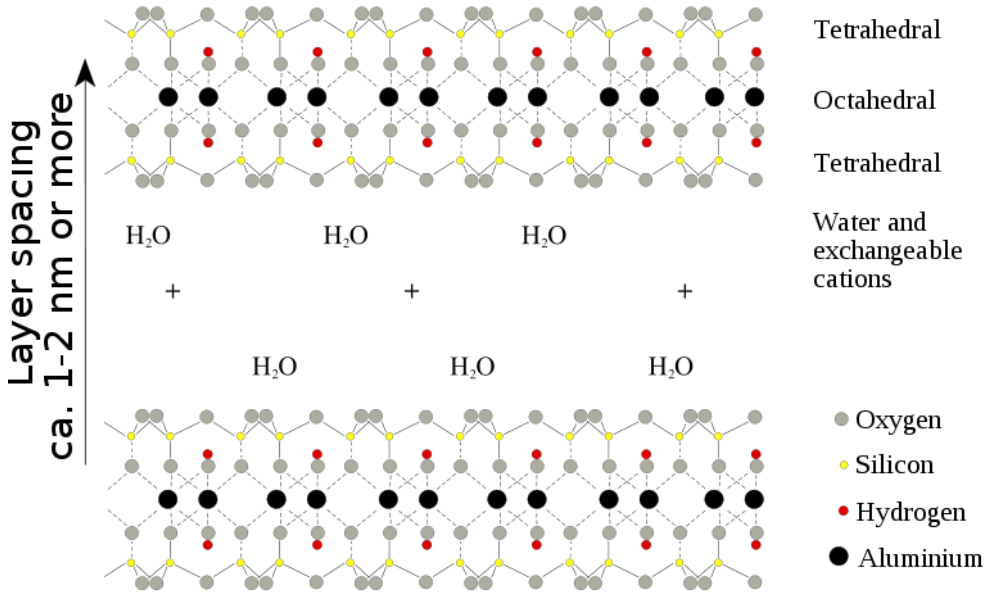

Figure 2-16 Montmorillonite structure

The concentration of clay used in the preparation of nanocomposites plays vital role on the morphology of nanocomposites. It has been reported that exfoliation of nanoclay occurs only in low concentration of clay. Higher amount of clay (less than 10%) results in intercalated structure. By incorporating high percentage of clay into polymer matrix, conventional micro-composites will result. The reason behind these results might be the percolation phenomena explained by Fischer (2003) and Liu *et al*. (1999).

- **Compatibiliser**

Under ideal conditions, polymer chain enters the space between the layers of layered silicates leading to complete and uniform dispersion of layered silicates in polymer matrix. Polyethylene is a non-polar, highly hydrophobic polymer but layered silicates are miscible only with hydrophilic polymers (Wang *et al*. 2001, Hotta & Paul 2004, Zanetti & Costa 2004, Preston *et al*. 2004, Zhai *et al*. 2004). In order to make layered silicate miscible with polyethylene, clay surface has to be modified to make it organophilic. It can be done through ion exchange reactions (Kornmann *et al*. 2001); where alkali counter-ions are exchanged with a cationic-organic surfactant such as alkyl-ammonium or any other onium salt (Alexandre & Dubois 2000, Manias *et al*. 2001, Zanetti *et al*. 2000). The nature of organic modifier and the resulting modified organoclay should be considered for each individual polymer to ensure the best possible compatibility between them so that they will lead to promising intercalated-exfoliated structure (Xie *et al*. 2001 and Vaia *et al*. 1997). Since the surface of layered silicates has the negative charge, the positively charged alkyl ammonium molecules, organise themselves in a position that their cationic head would reside at the surface of the silicate and the organic tail of the modifier will be away from the surface (Alexandre & Dubois 2000, Zanetti *et al*. 2000).

The most commonly used compatibiliser for polyolefins is reported to be maleic anhydride grafted polyolefins (Wang *et al*. 2001, Hotta & Paul 2004, Lu *et al*. 2005, Morawiec *et al*. 2005 and Zhang & Wilkie 2003). Durmus *et al*. (2007) have investigated the effects of concentration and type of compatibiliser in polyethylene nanocomposites. Their results showed that in producing polyethylene-clay nanocomposites, adding OxPE or maleic anhydride as compatibiliser to polymer matrix improved the miscibility between clay and

polyethylene. They have also found that the nanocomposites with maleic anhydride exhibits better structure compared to that with OxPE indicating nanoclay can be dispersed better into the polymer phase in the presence of maleic anhydride. They have also concluded from their experimental study involving polymer nanocomposites with OxPE in the concentration range of 1 to 10% that the level of clay dispersion and the nanocomposite microstructure do not change much if the compatibiliser/organoclay weight ratio remains constant.

2.3.2.2 Nanocomposite preparation methods

Different approaches have been used to incorporate the organoclay into polymer matrix. They are:

- In situ polymerization (sol-gel technology)
- Solution intercalation
- Melt intercalation (Alexandre & Dubois 2000, Fornes *et al*. 2001, Beyer 2002, Kim *et al*. 2001, Dennis *et al*. 2001)

- **Melt intercalation**

This method consists of blending directly layered silicate with polymer in a molten status. By appropriate choice of polymer and layered silicate, polymer matrix enters between the layers leading to the formation of either the intercalated or exfoliated nanocomposite structure. Melt intercalation is the most widely used method to prepare nanocomposites. Factors that make this method favourable can be listed as below.

- More versatile

- Environmentally friendly because there is no solution required (Giannelis 1996, Liu & Wu 2002)
- More economical (minimize the capital cost as there is no need to change the existing process)
- Simpler (extruders or mixers can be used directly)

2.3.3 Characterization of polyethylene nanocomposite

XRD (X-Ray Diffraction) and TEM (Transmission Electron Microscopy) are the most commonly used techniques to study the morphological structure of nanocomposite (Alexandre & Dubois 2000, Beyer 2002, Ray & Okamoto 2003 and Porter *et al*. 2000).

2.3.3.1 XRD

2.3.3.2 Using this technique, the space between structural layers of the silicate can be determined using Bragg's law.

Bragg's law: $\sin\theta = n\lambda / 2d$ 2-1

where λ is the wavelength of the x-ray radiation used in the diffractional experiment, d is the spacing between diffractional lattice places and θ is the measured diffraction angle (Alexandre & Dubois 2000 and Porter *et al*. 2000). The structure of nanocomposite can be studied by the basal angle reflections from the distributed silicate layers which are displayed in the form of peaks in the XRD plots. Structure and morphology can be identified by the shape, intensity and position of peaks (Ray & Okamoto 2003).

2.3.3.3 TEM

TEM is a microscopy technique in which a beam of electrons is transmitted through an ultra-thin specimen. The electron beam interacts with the specimen as it passes through. The result is a magnified image which shows the morphology of polymer, thus interaction of clay and polymer matrix can be seen directly (Morgan & Gilman 2003).

2.3.3.4 TGA

TGA or Thermal Gravimetric Analysis, is a test which determines the changes in the weight of the material with increase in temperature. It is a useful technique to study the thermal stability and also structure of polymers. In nanocomposites, changes in thermal stability as a function of concentration of clay can be studied by TGA. For example, Zhao *et al*. (2005) reported that the rate of degradation in nanocomposites will increase with an increase in organoclay loading, and this was attributed to the Hoffmann elimination reaction and the clay-catalysed degradation. Also, the nanocomposites were found to be more stable at higher temperatures compared to pure polyethylene. However, their stability decreased with an increase in the clay concentration. Zheo *et al*. suggested that this is because clay is dispersed very well in the matrix when the clay concentration is low but it acts like a barrier in higher concentrations when clay particles can agglomerate and catalyse the degradation process.

2.3.4 Degradation of polyethylene nanocomposites

2.3.4.1 Thermal degradation

There are several publications on the effect of clay on the thermal stability of polymer nanocomposites. In general, introducing clay into the structure increases the thermal

stability and this is attributed to clay acting as a great insulator and mass transfer barrier. It prevents oxygen from entering into the polymer structure and hinders the escape of volatile products generated during the decomposition from the nanocomposite structure (Ray & Bousima 2005, Ray & Okamoto 2003, Becker *et al*. 2004, Zhu *et al*. 2001, Dabrowski *et al*. 2000). By measuring the thermal stability in pure base polymer and its nanocomposites with different concentration of clay, it has been reported that pure polymer undergoes decomposition faster, onset of its thermal degradation is higher and its initial thermal degradation temperature is lower than those with clay in their matrix (Bandyopadhyay *et al*. 1999, Alexandre & Dubois 2000, Vyazovkin *et al*. 2004, Zanetti *et al*. 2004, Thellen *et al*. 2005, Lepoittevin *et al*. 2002). Zenetti *et al*. (2004) compared thermal stability of PE/EVA to those of its nanocomposites with different concentration of MMT under oxidative conditions. They concluded that nanoclay acts like a shield for polymer from oxygen, thus increasing its thermal stability in nanocomposites. Dabrowski *et al.* (2000) attributed the slower degradation rate in polyamide 6/clay nanocomposite to the barrier property of clay which slows down the diffusion of volatiles from the matrix to the surface of nanocomposites. Qin *et al*. (2004) mentioned that the physico-chemical adsorption of the volatile products on the surface of silicate is responsible for increasing the decomposition temperature.

On the contrary to the above findings, other papers in the literature reported that nanocomposites exhibit lower thermal stability than neat polymer. For example, Cho & Paul (2001) found PA6 is less stable than neat nylon 6. They attributed this behaviour to the presence of quaternary alkylammonium on the organically modified montmorillonite. Alkylammonium cations decompose easily following Hoffmann elimination reaction forming products which can catalyse the degradation process of nanocomposites. Another

explanation for the higher degradation rate in some nanocomposites was suggested by Ray & Okamato (2003). They suggested that, because of the layered nature of the clay, it has the ability to hold heat between its stacks of layers when heat is transferred from an external source to the nanocomposite; so the heat accumulated between the layers will act as a heat source and accelerate the rate of degradation by supplying more heat. Moreover, Xie *et al*. (2001) and Davis *et al*. (2003) reported that, by nature, the organoclay has the catalytic effect in thermal degradation. The complex crystallographic structure and nature of clay minerals form catalytically active site in the structure. The presence of weakly acidic SiOH and strongly acidic bridging hydroxyl groups at the edges act as Bronsted acidic sites; in addition to the transition metal ions in the layer and the complex crystallographic structure form those active sites. Qin *et al*. (2004) used this theory to describe the higher initial decomposition of PP nanocomposites compared to pure PP.

Based on the above discussions, it can be summarised that nanoclay has two contradictory effects on thermal stability in nanocomposites: 1) the barrier effect of clay which improves the thermal stability and 2) catalytic effect on degradation. Zhao *et al*. (2005) investigated the effect of nanoclay on thermal stability in PE based nanocomposites in nitrogen atmosphere using TGA and DTGA. They reported faster degradation of nanocomposites compared to neat PE at the first stage of degradation (below 400°C). They explained their results using Hoffmann elimination reaction and the catalytic effect of clay. However, above the 400°C, nanocomposites have shown to have better stability than PE.

Based on their study carried out for PP/clay nanocomposites, Qin *et al*. (2004) reported higher decomposition temperature in the presence of clay which they attributed to the hindrance of diffusion for volatile products when clay is well dispersed into the matrix.

They suggested that the better dispersion most likely occurs due to the surface modification of clay. They have also observed that weight loss in PP nanocomposites occurred at a lower temperature compared to pure PP, and they attributed it to the catalytic effect of clay in the initial decomposition of nanocomposites under oxygen environment.

2.3.4.2 Biodegradation

Effect of clay on biotic degradation has been studied by many authors. Kounty *et al*. (2006) reported that clay promotes the growth of microbes on polymer surface by keeping the pH of the environment at levels conducive to their sustained growth. Qin *et al*. (2003) investigated the effect of clay on the biodegradation of polyethylene. They exposed their PE/MMT nanocomposite samples to UV irradiation under atmospheric oxygen. After 200 hr of exposure, it was observed that the rate of production of carbonyl groups is significantly higher in polyethylene nanocomposites compared to that in neat polyethylene which indicates the clay has a strong impact on the photo-oxidation of polyethylene nanocomposites. This result was confirmed later by Kumanayaka *et al*. (2010), who showed that clay not only helps in photo degradation but also plays a vital role in the final biodegradation stage.

Reddy *et al*. (2008) have studied the effect of nanoclay on the oxo-biodegradation of polyethylene and they concluded that the presence of clay in polymer matrix helps in biotic degradation stage. They have reported that the microorganism *Pseudomonas aeruginosa* is able to access the polymer volume completely in the presence of clay and therefore can utilise the portions that remain after abiotic degradation stage.

From aforementioned review, it is obvious that the increase or the decrease in the rate of biodegradation in nanocomposites is not still understood clearly and no conclusion can be drawn about the biodegradation mechanisms on the basis of the current literature available.

2.4 Modeling

2.4.1 Introduction

Research based on trial and error (experimental) approach has some problems. Experiments are always costly in terms of time and money. For example, degradation of substances may take place over a period of several months or years. A better understanding of physio-chemical polymer degradation process is a key to understand the underlying problem in biodegradation and consequently to find a solution.

There are a wide range of factors that affect the biodegradability of polymers. They include chemical composition, molecular structure, morphology, process condition, environmental factors. In non-biodegradable polymers such as polyethylene, it also depends on the amount and nature of additives.

In modeling, the strategy is always to choose the simplest scheme but at the same time to make it consistent with the experimental data thereby making the models to predict the actual behaviour closely. It is better to avoid unnecessary simplification, assumption, and the unnecessarily details.

A rigorous and detailed mathematical model that considers all of the above factors is often impossible or, when possible, not properly usually validated by experimental data.

Fortunately, in many cases, simplified models can be developed and applied to get preliminary information.

A few researchers have attempted to model the biodegradation process or CO_2 evolution from different polymers. However, the difference between this study and those reported in the literature is that the polymers used in many of the studies were biodegradable polymers by nature while the polymer used in this study is oxo-biodegradable polyethylene with relatively low degradability. The best study on the biodegradation was published by Larson *et al*. (1996). Larson *et al*., conducted experiments to investigate the rate and extent of ultimate biodegradation of polyethylene glycols and polyaspartate and developed models to predict the amount of CO_2 evolved from these polymers. They obtained the kinetics of CO_2 evolution during biodegradation of different compounds by fitting the experimental data to microbial growth rate equations.

In previous studies, either a first-order rate curve with a flat lag phase or a logistic function with an s-shape curve (sigmoidal) has been used by researchers to describe microbial growth and degradation kinetics in batch systems (Larson 1984). Larson *et al*. (1996) showed that the kinetics for CO_2 evolution as a fraction of time was represented by a first-order reaction and fitted their kinetics data to Equations 2-2 and 2-3. Experimental data then were analysed by non-linear regression method using Table Curve 2D Windows ~2.0 software (Jandel Scientific, San Rafael, CA) and the parameters of first order rate constants were estimated. Larson *et al.* used both equations to determine the rate constant for degradation (k_1) and the extent of degradation for several test compounds.

First-order rate equation is used when the biodegradation rate is proportional to the concentration of test material and it can be expressed as follows:

$$y = \begin{cases} 0 & for \quad x \le c \\ a(1 - e^{-k_1(t-c)} & for \quad x \ge c \end{cases} \qquad 2\text{-}2$$

where y = cumulative $\%TCO_2$, t = time (days), a = the asymptote of CO_2 evolution curve (maximum of biodegradation degree), k_1 = the rate constant (day^{-1}) and c = lag time before CO_2 production occurs (days).

If the change of biodegradation rate with time is represented by a s-shaped curve, then following equation is used to fit the experimental data:

$$y = a(1 - be^{-k_1 t})^{-1/n} \qquad 2\text{-}3$$

where y = cumulative $\%TCO_2$, t = time (days), a = asymptote of curve ($\%TCO_2$), k_1 = rate constant (day^{-1}), n = empirical constant and b = coordinate scaling factor (= 1 in single-dose batch systems).

After analysing their results, Larson *et al.* (1996) have stated that the non-linear regression method which they have used to fit their experimental data can describe a wide variety of biodegradation patterns of different materials. These biodegradation patterns could be varied between materials. Some materials have rapid and complete degradation and no lag phase, and some materials show both complete and incomplete degradation at variable rates with variable lag phases. If first order reaction is applicable, the biodegradation rate is proportional to the concentration of test material.

In another attempt to model the biodegradation process, Srinivasan & Viraraghavan (2000) used first order rate equation to assess the potential biodegradability of an oil stabilizer sample from an oil company in Canada. They used Equation 2-2 stated by Larson *et al.*

(1996) to fit their data. Constant parameters of equation were estimated based on trial and error. Another form of logistic model has been used by Rogers *et al*. (1997). They fitted their data to a form of logistic function to quantify the kinetics of strychnine degradation in non-sterile Booleroo and Bute soils. Their modified logistic model is as follows (Equation 2-4):

$$y = a + \frac{c}{1 + e^{-b(t-m)}} \qquad 2\text{-}4$$

where y = strychnine concentration, t = time (days), a = the lower asymptote (minimal strychnine concentration), c = the upper asymptote (maximum strychnine concentration), b = slope parameter, m = point of inflection of the curve. Recently, Reuschenbach *et al*. (2003) used Equation 2-2 and also a modified logistic function model (Equation 2-5) to compare the respirometric data for their biodegradation tests. They showed that both equations appropriately describe the biodegradation behaviour of their test materials (diethylene glycol and 2-ethylhexylacrylate). The modified logistic model can expressed as follows:

$$y = \frac{L}{1 + Ae^{-kt}} - \frac{L}{1 + A} \qquad 2\text{-}5$$

where y = the % theoretical COD or $ThCO_2$, t = time (days), and k = rate constant ($days^{-1}$), and L and A are the best fit variables. They need to be optimised to fit the best curve to the experimental data. It is also necessary that second term of the equation on the right hand side ($\frac{L}{1 + A}$) reaches the minimum biodegradation (zero) at time t = 0.

Although the nature of biodegradation process for oxo-biodegradable polyethylene employed in this study is different from those mentioned in the literature, it seems that first-order and logistic models can be used extensively to express the experimental data for microbial growth and biodegradation with microorganisms. In addition the above mentioned equations have the ability to be modified to be used in conditions different from original definitions. This ability to quantify and determine the kinetics of biodegradation process can be used for predicting the life time of polymer. It is a very useful tool to describe the biodegradation behavoiur of polymer and it also can be used for comparing the kinetics and biodegradation rates of nanocomposites with different clay loadings.

3 Material and Experiment

This chapter contains a detailed description of the material, equipment, experimental methods and techniques used in this work to prepare polyethylene nanocomposites and study oxo-biodegradation of polyethylene.

These items are discussed in the following order:

- Raw materials
- Preparation of polymer-layered silicate nanocomposites with different clay concentrations
- Characterisation of polyethylene nanocomposites (structural and mechanical)
- Thermal degradation of polyethylene nanocomposite samples
- Biodegradation of polyethylene nanocomposites in a composting system
- Analytical characterisation of test samples
- Analysis of test results

3.1 Material

3.1.1 Polyethylene

Excellent properties, lower price, and easy processability of polyethylene made this polymer the most widely used polymer in industry. Nowadays, polyethylene contributes to around 64% of the total plastic usage in packaging applications and bottles. The general structure of polyethylene is $\mathbf{[-CH_2-CH_2-]_n}$ and it is synthesized by polymerization of ethane monomers. Polyethylene is classified into several different categories based on the

extent and type of branching, the crystal structure and the molecular weight. However, the most commonly used polyethylene grades are HDPE, LLDPE and LDPE.

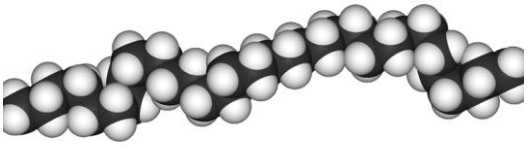

Figure 3-1 Space-filling model of a polyethylene chain

Polyethylene used in this study was film grade low density polyethylene supplied by Qenos, Australia. Physical properties of LDPE grade used in this study are shown in Table 3-1.

Table 3-1 Physical properties of polyethylene used in this study

PROPERTIES	POLYETHYLENE
Grade	LDJ225- Film extrusion
Appearance	Translucent pellets or powder
MW	220619 g/mol
Polydispersity	6.56
Melting point	100-130°C
Melt index @190°C	2.5 g/10 min
Density	0.922 g/cm

3.1.2 Organically modified montmorillonite clay

Among all the various kinds of layered silicates, montmorillonite (MMT) has more attractive properties as reinforcement for preparing polymer-clay nanocomposites. This can be attributed to the relatively weak bonding between the silicate layers and its large interfacial area (the specific surface area of MMT is about 750 m^2/g). Each layer of MMT is composed of an octahedral alumina sheet sandwiched between two tetrahedral silica sheets (Alexandre & Dubois 2000).

Organically modified montmorillonite clay, Cloisite® 15A, procured from Southern Clay Products, USA was used in this study. Cloisite® 15A is a commercially available organically modified MMT clay in which hydrophilic cations of Na+ in pristine clay are exchanged by a surface modifier (dimethyl dehydrogenated tallow quaternary ammonium chloride) to convert the hydrophilic silicate surface into organophilic surface so that it is compatible with non-polar, hydrophobic polymers such as polyethylene. The role of this modifier is to enhance polymer–clay interaction by lowering the surface energy of the inorganic layered silicate and improve the wetting characteristics with respect to the polymer. In addition, it has been mentioned by Esma *et al*. (2008) that Cloisite® 15A shows higher hydrophobicity than the other members of Cloisite family and therefore is expected to lead to better dispersion of clay into hydrophobic polymer.

X-ray diffraction of resulting organo-clay in Cloisite® 15A showed that d-Spacing (001) is 31.5 Angstroms. Figure 3-2 shows the structure of the organic modifier in which HT represents the hydrogenated tallow (65% C18, 30% C16, and 5% C14).

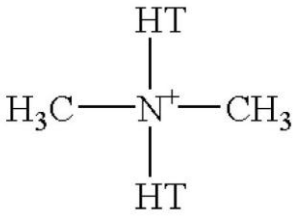

Figure 3-2 Molecular structure of the organic modifier

3.1.3 Maleic anhydride grafted polyethylene

To achieve the excellent mechanical and physical properties in polymer-clay nanocomposites, especially those with non-polar polymers such as polyethylene, it is necessary to have a good dispersion of nanoclay in the polymer matrix (exfoliation or intercalation) along with good interaction between the two mixing phases. This can be achieved by using a polymeric compatibiliser which creates the loops and tails on the clay surface so that it can interact with the thermoplastic melt (Tjong 2006).

The most commonly used compatibiliser (surfactant) for the preparation of polyethylene nanocomposite is alkylammonium salts/compounds which typically should have more than 8 carbon atoms. It has been found that maleic anhydride (Figure 3-3), an organic compound with the formula of $C_2H_2(CO)_2O$, promotes strong interactions between polyethylene and montmorillonite leading to homogeneous dispersion of clay layers (Reddy *et al*, 2007).

A commercial grade of alkylammonium compounds, maleic anhydride-grafted polyethylene (PE-g-MA) with the trade name of Fusabond 226D supplied by Dupont, USA

was used in this study. Fusabond resins are polyolefins and copolymers grafted with maleic anhydride.

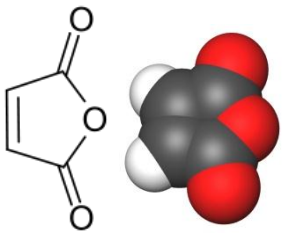

Figure 3-3 Molecular structure of maleic anhydride

3.1.4 Pro-oxidant

Albertsson *et al*. (1987) showed that the first stage of polyethylene degradation, which is disintegration of macromolecules of polymer into smaller fragments, determines the entire rate of degradation process. Therefore, it is very important to find a suitable pro-oxidant for obtaining optimum result in the biodegradability of polyethyelene. In other words, making the first step shorter and quicker will lead to more food for microorganisms in the second stage. It has been also shown that the degradation mechanisms would follow different pathways depending on the type of pro-oxidant used in PE (Burman *et al*. 2005).

In this study, manganese stearate supplied by Alcan International Network, USA was used as the pro-oxidant. Manganese stearate has been chosen as the pro-oxidant based on the research carried out by Sipinen & Rutherford (1993). After testing different metal ions as pro-oxidant, they found that the metal ions like Mn^{2+}/Mn^{3+}, which have two different oxidation numbers with one unit difference, are the most active ones. Also, manganese is known as an important element in biological systems as it is used by microbial organisms, plants and animals as nutrition and a source of energy (Jakubowicz *et al*. 2006). Enzymatic

and non-enzymatic oxidations of Mn by bacteria and fungi are described in detail by Ehrlich (1990).

3.2 Experiments

3.2.1 Preparation of polyethylene nanocomposites films

3.2.1.1 Preparation of masterbatch

A masterbatch of Fusabond and organoclay (Cloisite® 15A) in a weight ratio of 4 to 1 was prepared using a Brabender twin screw extruder (Figure 3-4). It has been reported by Treece & Oberhauser (2007), Shah & Paul (2004), and Lee *et al*. (2005) that using masterbatch to prepare nanocomposites results in better mixing and homogenous structure of products. The organoclay was dried in a vacuum oven at 40°C for 24 hours and then mixed with Fusabond beads in Brabender twin screw extruder with a temperature profile from 135°C in the hopper to 185°C in the die section. The screw speed was set at 80 or 90 rpm. Masterbatch prepared by the extruder was pelletised and stored in plastic bags for further usage.

Figure 3-4 Brabender twin screw extruder

3.2.1.2 Preparation of nanocomposites

Polymer nanocomposites were prepared by diluting the masterbatch with low density polyethylene using Brabender twin screw extruder. Oxo-degradable polyethylene nanocomposite was prepared by adding manganese stearate as pro-oxidant to the mixture in the form of a powder. Temperature profile in the extruder was maintained between 125 and 160°C from hopper to die section. Tables 3-1 and 3-2 show the composition of polyethylene nanocomposites used in this work. All the samples were processed three times to ensure homogeneously dispersed organoclay particles in the polymer matrix. Virgin LDPE was also processed three times in the extruder using the same procedure so that it can be a reliable and comparable reference.

Table 3-2 Compositions of polyethylene nanocomposites with and without pro-oxidant; PE – Polyethylene, LDPE – Low density polyethylene, F – Fusabond, C – Clay, OPE – Oxo-biodegradable polyethylene.

Sample name	PE (wt%)	PE-g-MA (wt%)	MMT (wt%)	Pro-oxidant (wt%)
PEF (PE+F)	92	8	-	-
LDPE + Pro-oxidant (OPE)	91	8	-	1
LDPE + 2% Clay + Pro-oxidant (OPE 2C)	89	8	2	1
LDPE + 3% Clay + Pro-oxidant (OPE 3C)	84	12	3	1
LDPE + 5% Clay + Pro-oxidant (OPE 5C)	74	20	5	1
LDPE + 2% Clay (PE 2C)	90	8	2	-
LDPE + 3% Clay (PE 3C)	85	12	3	-
LDPE + 5% Clay (PE 5C)	75	20	5	-

3.2.1.3 Blown film process

Polymer films were prepared from polymer beads using advanced blown film assembly unit made by Strand Palst Maskiner, Sweden (Figure 3-5). The temperature profile in the unit varied from 150°C in section 1 to 180°C in zone 5. The extruder screw speed was maintained at 35 rpm while the die gap was 0.3 mm, nip roll speed was 15 rpm and the lay flat was 160 mm. Motor AMPS was set about 3.5 during the processing. The film thickness

was found to vary between 55 and 65 µm. All the prepared samples were processed under identical condition.

Figure 3-5 Blown film assembly unit

3.2.2 Morphological characterization of polyethylene nanocomposites

3.2.2.1 Wide Angle X-ray Scattering

Wide angle X-ray Scattering (WAXS) is a technique used to study the morphological structure of polymer nanocomposites and evaluate the degree of intercalation between organo-clay and polymer matrix. This technique works based on the reflected or scattered x-ray beam and its intensity. An X-ray tube produces the radiation which hits the composite at an angle of θ (Figure 3-6). Thus the diffraction angle from the composite is

equal to twice of the incident angle (= 2θ). The interlayer d-spacing can be calculated using Bragg's law:

$$n\lambda = 2d\sin\theta \qquad 3\text{-}1$$

where n is an integer (n = 1), λ is the wave length of the incident X-ray beam (λ = 1.5406 Aº), θ is the angle of incidence of the X-ray beam and d is the interlayer distance between the silicate layers.

The d-spacing is the distance between the structural layers (basal layers) of the silicate and it can be used as a tool to determine the degree of swelling of silicate layers caused by the entry of the polymer chains between them. According to Bragg's law, as the d-spacing of layer silicate (clay) increases, the representative peak for clay in the WAXS results will shift to the left side or to lower angles.

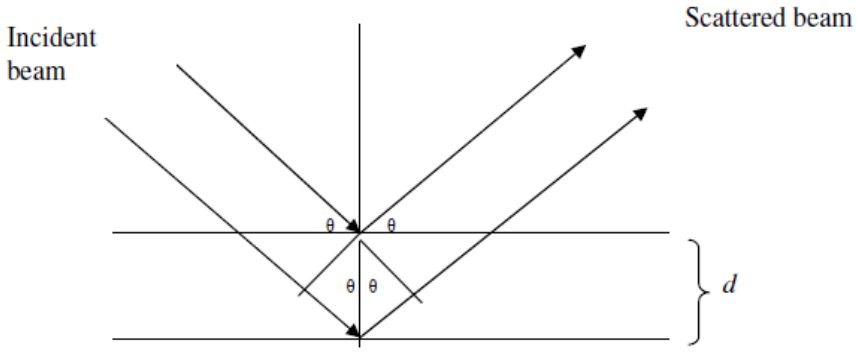

Figure 3-6 schematic representation of the XRD process

In this study, a Bruker AXS D8 X-ray diffractometer with Cu-Kα radiation (λ = 0.154 nm) operating at 40 kV with 35 mA current was used to study the degree of intercalation/ exfoliation of polyethylene nanocomposite films (Figure 3-7). Scans were taken between 2

and 20º at a speed of 1º/min, with a step size of 0.02 and step time of 1 s. The degree of exfoliation/intercalation can be determined using the changes in the representative peaks of clay in WAXS results. In general, in an exfoliated structure, no apparent peak can be observed in the graph, as it indicates that polymer chains have penetrated into the layers and separated the silicate layers in a way that d-spacing is too large to be detected by WAXS. In an intercalated morphology, although polymer chains penetrate into the layer and increase the spacing, they do not manage to separate the layers completely and hence, the clay peak can be observed but at lower angles. For immiscible morphologies, the observed peak is almost identical to that of the original clay, showing a poor penetration of polymer chain into the layers of clay.

Figure 3-7 Wide angle X-Ray Scattering unit

3.2.3 Thermal characterisation of polyethylene nanocomposites

3.2.3.1 Thermo Gravimetric Analysis (TGA)

Thermo gravimetric analysis is a testing method to determine the changes in the weight of polymer sample due to the changes in temperature. TGA can be used for the following: compositional analysis – quantitative content analysis, decomposition temperatures, engine oil volatility measurements (TGA Noack test), filler content, flammability studies, lifetime predictions (via TGA kinetics software), measurement of volatiles (e.g., water, oil), oxidative stabilities, thermal stabilities, catalyst and coking studies, hyphenation to identify out-gassing products.

As mentioned above, one of the TGA applications is testing the thermal stability of materials. Thermal stability can be monitored by recording the changes in the weight of a sample as it is heated, cooled or held at a constant temperature. In this study, TGA has been used to evaluate the thermal stability of different polymer nanocomposite samples with different clay loadings. The effect of introducing pro-oxidant into the nanocomposites was also studied by TGA.

Thermal degradation of samples was performed using STA 6000 (Simultaneous Thermal Analyzer) - a PerkinElmer Pyris 1 TGA instrument. The temperature reproducibility of the instrument is < ±0.5 °C. The STA 6000 was calibrated and verified using calcium oxalate. Calcium oxalate is a well characterized material that has three distinct weight loss events that occur during heating. These three weight losses are due to H_2O, CO and CO_2. The samples of 15 mg of calcium oxalate were subjected to thermal degradation using a heating rate of 20 °C/minute with nitrogen as a purge gas. As can be seen from Figure 3-8, the

weight loss events recorded by the STA 6000 in our laboratory were comparable with the theoretical values.

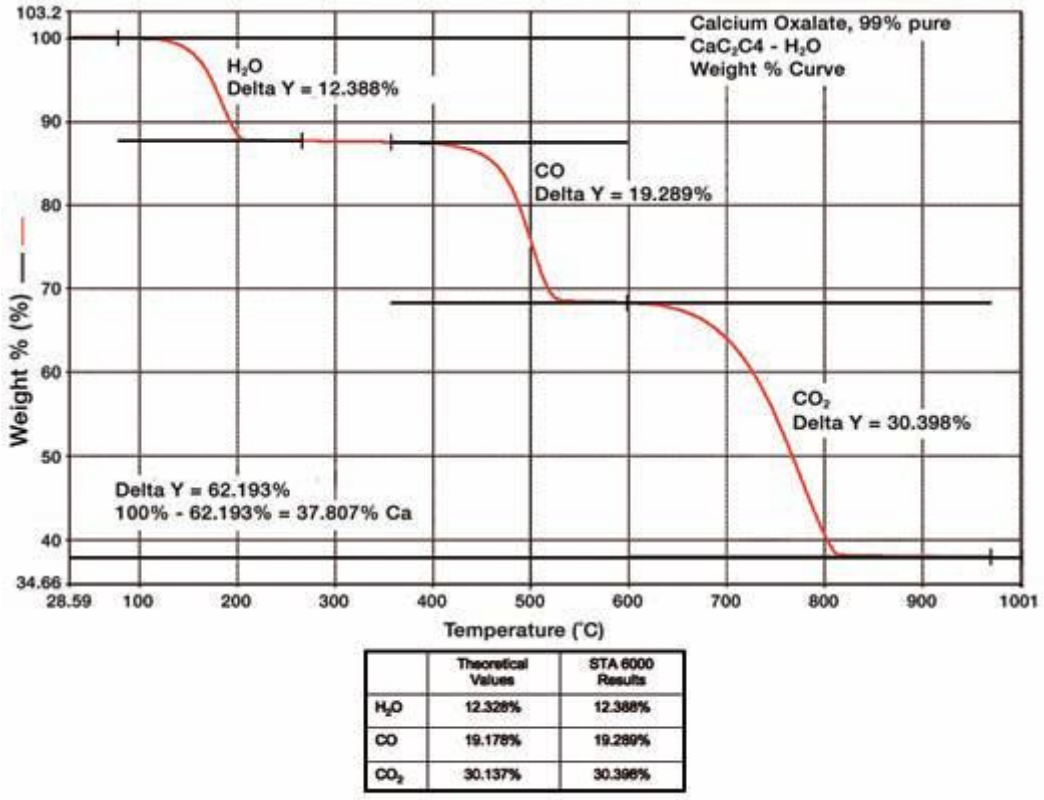

	Theoretical Values	STA 6000 Results
H_2O	12.328%	12.388%
CO	19.178%	19.289%
CO_2	30.137%	30.398%

Figure 3-8 Calibration curve for calcium oxalate

Polymer samples of 3 to 12 mg were placed in a sample holder mounted on a platinum pan and heated at a heating rate of 20°C/min under nitrogen flow rate of 20 ml/min from 40 to 650°C. Weight loss from the start to the end point of the test was plotted by the software. Also the derivative weight loss curve for each sample was obtained to identify the point where weight loss is most apparent. For each sample, all the tests were repeated to check the reproducibility of the results.

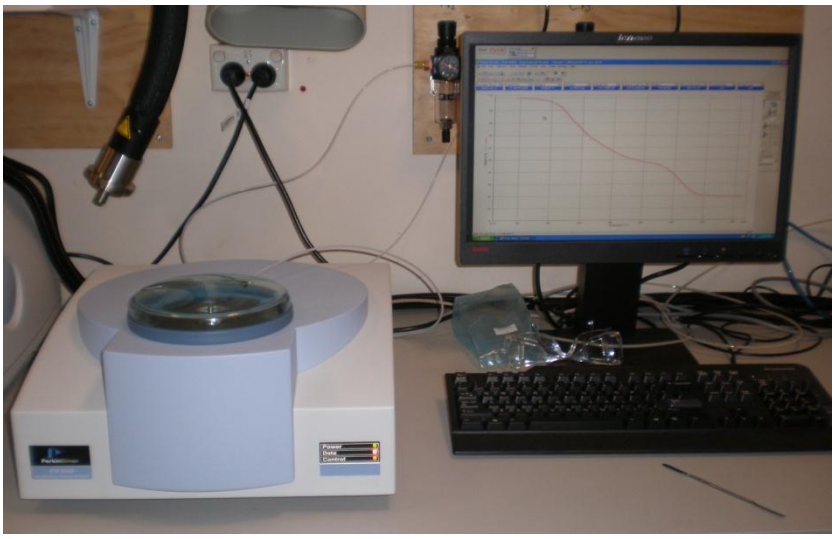

Figure 3-9 Thermo Gravimetric Analysis (TGA) unit

3.3 Oxo-biodegradation experiment

3.3.1 Abiotic oxidation procedure

Thermal oxidation was carried out in an air circulated oven according to ASTM D5247. Polymer films were cut into 150 × 50 mm strips and placed in an aluminium pan which was then subjected to thermal oxidation in an oven at 70°C for 14 days. Samples were taken out daily to monitor the progress of thermal degradation closely. The thermally degraded film samples were sealed and stored at -4°C to prevent from further oxidation before performing FTIR and ESEM tests.

3.3.2 Biodegradation procedure

Biodegradation can be monitored by:

- carbon conversion which is conversion of organic carbon to inorganic CO_2
- physical disintegration

- weight loss

To monitor the biodegradation of test samples, a composting test system was chosen and it was conducted according to AS-ISO 14855. The test period was 45 days for each run. These tests were carried out under optimum temperature and well aerated condition so that it provides optimum oxygen and moisture to simulate the real composting condition. To validate the data obtained in sample vessels, a blank vessel and a reference (control) was used in parallel as instructed in AS-ISO 14855. Also, each sample was used in triplicate to check the reproducibility of the results (Figure 3-10).

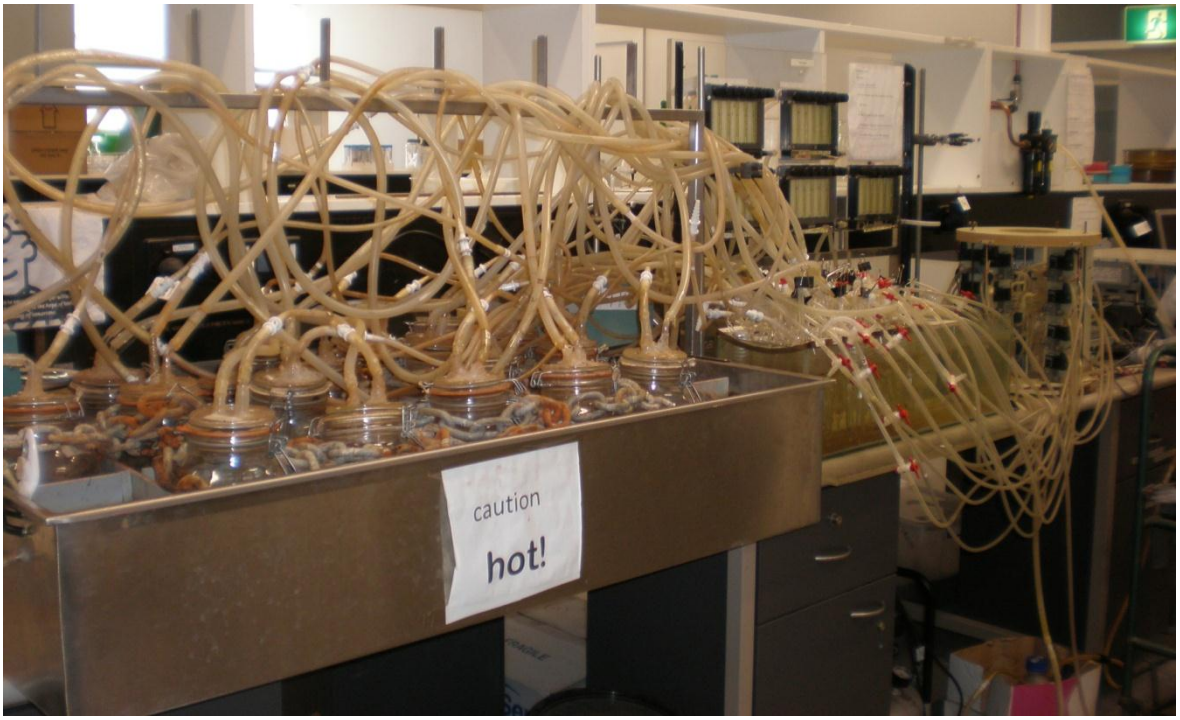

Figure 3-10 Biodegradation setup

3.3.2.1 Preparation of the inoculum

Well aerated, 3 to 4 months old compost was supplied by Natural Recovery Systems (Australia). All the large inert objects like glass, metal pieces, and stones were removed

from the compost before it was sieved on a 5 mm mesh. Total and volatile solid contents were measured and they were found to meet the requirements for using them as inoculum.

For the preparation of inoculum and samples, first total dry solid content of the compost inoculum was determined according to AS-ISO 14855 using equation 3-2. About 10 grams of compost was placed in the oven at 105° C and dried for 2 hours before it was weighed. The dish with samples was returned to oven for 30 minutes, and then it was cooled before it was weighed again. The whole process was repeated again until the weigh difference was minimal. Using the Equation (3-2), it was found that total dry solid was 52% which is within the range recommended by standards (between 50- 55% of the wet solids).

$$\text{Total solid},\% = \frac{(\text{A-B})}{(\text{D-B})} \times 100\% \qquad 3\text{-}2$$

where

A = weight of dish + dry sample, (g)

B = weight of dish, (g)

D = weight of dish + wet sample, (g)

The measurement of volatile solids of the compost inoculum was carried out in next step as follows:

Dish with the residue after drying in the oven (residue after total solid analysis) was placed in a furnace at 550° C for 30 minutes. It was then cooled, placed in a desiccator and weighed. This process was repeated until the measured weight showed little difference.

Weight was recorded, and then the following formula was used to calculate the volatile total solids:

$$\text{Volatile total solids, \%} = \frac{(A-C)}{(A-B)} \times 100 \qquad 3\text{-}3$$

where

A = weight of dish + dry sample, (g)

B = weight of dish, (g)

C = weight of dish + sample after ashing or ignition, (g)

The volatile solids should be greater than 30% according to AS-ISO 14855 and in this case, it was calculated to be 39%.

pH of the inoculum was determined by preparing a mixture of inoculum and deionised water with the mass ratio of 1 to 5 and measuring its pH value. The pH found to be 7.5, which is in the acceptable range of 7 to 9 recommended by AS- ISO 14855.

3.3.2.2 Preparation of samples

All the test samples are required to be in the form of granule, film or powder with a surface area not more than 2 cm × 2 cm for each individual piece of test materials. Eight samples based on polyethylene (Table 3-2) and positive control (or reference material) were prepared and used in the test. Reference material was TCL (thin-layer chromatography) grade cellulose supplied by Sigma-Aldrich, Germany.

3.3.2.3 Start-up procedure

Mixtures of nanocomposite films and inoculum were placed in 3 litre flasks, large enough to have an even flow of gas purge in an upward direction. Test was carried out according to AS-ISO 14855. The experimental arrangement consisted of:

- three blank vessels
- three vessels containing reference material as test control
- three vessels containing the test material

Each test vessel contained a mixture of inoculum and the test material. The amount of inoculum and the test material depended on the type of inoculum and the test material. The ratio of the dry mass of inoculum to the dry mass of test material was 6:1 according to ISO 14855. Similar amounts of inoculum were placed in blank vessels, too. But blank vessels contained only the compost. To maintain a homogenous mixture and well respirated system, and also to be able to shake the vessels manually, sufficient headspace in vessels was provided in the experimental arrangement. It was recommended by AS-ISO 14855 that not more than $3/4^{th}$ of the vessel volume may be filled with the test mixture. All the vessels were placed in a water bath to maintain a homogeneous, constant temperature in test vessels. The water bath temperature was maintained at 58±2 °C during the test. The reproducibility of the results was checked by using three replicate of each samples in each run. A schematic of the biodegradation unit is shown in Figure 3-11.

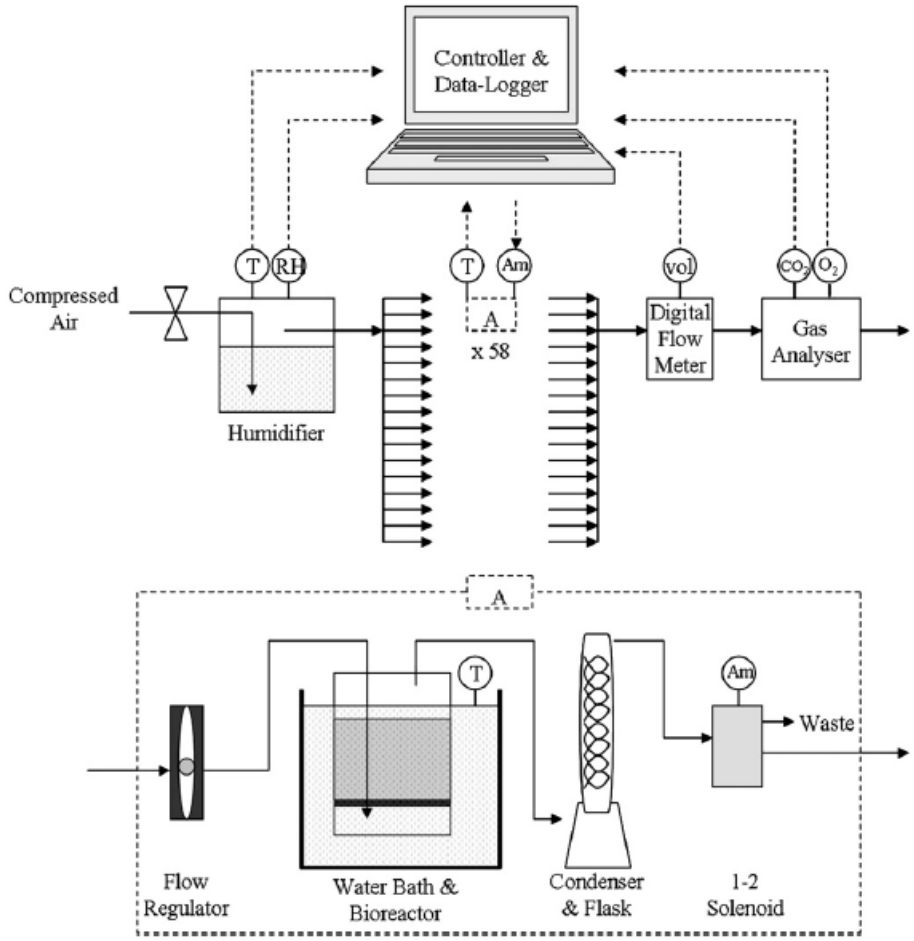

Figure 3-11 Schematic of biodegradation unit

3.3.2.4 Operating procedure

The gas produced by the compost inoculum and polymer samples was sent to an infrared analyser to measure the amount of CO_2 evolved. The infrared analyser was connected to the vessels by gas-tight tubes. There was a 6 hour time interval between successive readings for each vessel. Each reading was recorded using a PC and stored for further analysis.

According to AS-ISO 14855, the measurement frequency of CO_2 evolved depends on the measurement method used and the biodegradability of samples. If direct measurement

methods such as a gas chromatograph, TOC or infrared analyser are used the CO_2 evolved could be measured twice a day during the biodegradation phase and once a day in the plateau phase. In the indirect measurement method, cumulative CO_2 evolved can be measured by determining the dissolved inorganic carbon (DIC) using the absorption of CO_2 in a basic solution such as NaOH or BaOH on a daily basis during the biodegradation phase and twice a week in the plateau phase.

It is recommended by AS-ISO 14855 to shake the vessels manually each week to maintain a homogenous composting environment in terms of aeration, humidity and microbial attack.

Moisture content of the test mixtures was checked regularly by visual observation. The vessels were moisturised by spraying water when needed. The moisture content of test mixture should be kept at about 50% and it should not appear dry nor should it have standing water.

Biodegradation test period is normally 45 days according to AS-ISO 14855 but it can be extended if needed. In this study, due to time constraints, the test was terminated after 45 days.

The plastic fragments recovered from the compost were subjected to further analysis by FTIR and ESEM to study the changes in the structure and microbial growth after composting.

3.3.2.5 Calculations

Theoretical amount of CO_2 was calculated for each vessel. Using the CO_2 evolution data and the theoretical amount of CO_2, the %biodegradation ($\%D_{t)}$ of each material were determined and plotted as a function of incubation time.

3.3.3 Analysis of oxo-biodegradation of polyethylene nanocomposites

3.3.3.1 Fourier Transform Infrared Spectroscopy (FTIR)

Fourier transform infrared spectroscopy (FTIR) is one of the most widely used techniques to determine the chemical changes or the formation of functional groups on the polymer surface during or after the degradation process. In this technique, an infrared spectrum of absorption or emission of a solid, liquid or gas sample is obtained in a wide spectral range. This method is based on the principle that each molecule, vibrates or rotates at specific frequencies; so that it can absorb or emit certain amount of energies at a specific wave number corresponding to its discrete energy levels. When a beam containing many different frequencies of light, hits the sample, depending on the type of chemical functional groups in the sample, beam will be absorbed to different extent by the sample. This is measured and recorded as an interferogram; then using a mathematical algorithm called the Fourier transform, according to the Equation 3-4, computer converts the interferogram into the desired result (light absorption for each wavelength) and produces an infrared spectrum versus wave number for each sample.

$$A = -\log 10\ T \qquad 3\text{-}4$$

where T is transmittance and A is the absorbance.

As mentioned above, the frequency of the emitted or absorbed radiation is a characteristic of chemical groups. Hamid *et al*. (1992) categorised three main regions of the IR spectrum as follows:

- The O-H stretching (3200 – 3600 cm^{-1}): The broad band peaking consists of the O-H, stretching group of hydroperoxides, alcohols and carboxylic acids.
- Vinyl groups (1641 cm^{-1})
- Carbonyl stretching (C=O) (1700 – 1800 cm^{-1}): This broad band is particularly important in the study of polymer oxidation as it can be used to calculate the 'carbonyl index', which is a useful tool to quantify the degree of degradation in polymer. Carbonyl region is composed of carboxylic acids (1712 cm^{-1}), ketones (1723 cm^{-1}), aldehydes (1730 cm^{-1}), and lactones (1780 cm^{-1}).

In this study, FTIR measurements were carried out using Perkin-Elmer 2000 infrared spectrum analyser in the spectra region of 400 - 4000 cm^{-1}. Film samples were placed in contact with a Zn-Se crystal with a 45° angle of incidence. Interferograms were obtained from 32 scans. Before running the samples, background spectra was obtained without samples in the chamber and it was recorded in order to minimise the noises in analysis of the results. Thermally degraded samples as well as composted samples were analysed by FTIR and their corresponding spectra were recorded.

Also, the changes in carbonyl index (CI) as a function of exposure time were studied as a measurement of the degree of degradation. Carbonyl index (CI) is defined as the ratio of absorbance of carbonyl groups (absorption at 1713 cm^{-1}) to that of methylene groups (absorption at 1465 cm^{-1}) (Albertsson & Karlsson 1987).

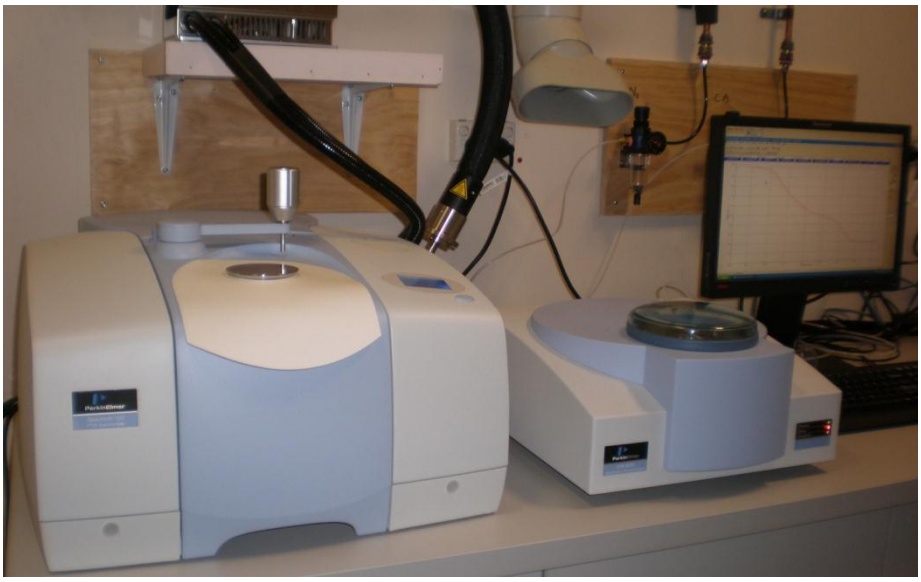

Figure 3-12 Fourier Transform Infrared Spectroscopy (FTIR)

3.3.3.2 Environmental Scanning Electron Microscopy (ESEM)

Scanning Electron Microscope (SEM) is a widely used technique for scanning the surface of a specimen with a finely focused electron beam to produce an image of the surface. A scanning electron microscope consists of an electron optical column, a vacuum system and electronics. Using conventional SEM is problematic for samples containing volatile components, uncoated or so called wet samples. The samples used in conventional SEM generally have to be clean, dry, vacuum compatible and electrically conductive. To solve the addressed issue, the Environmental Scanning Electron Microscope (ESEM) has been introduced to provide a unique solution by placing the sample in an environmental chamber isolated from the main column by one or more differential pumping apertures. The Gaseous Secondary Electron Detector (GSED detector) uses cascade amplification to enhance the secondary electron signal as well as to produce positive ions which are

attracted by negative charge on the insulated specimen surface, and effectively suppress charging artefacts. Figure 3-13 shows a schematic of ESEM.

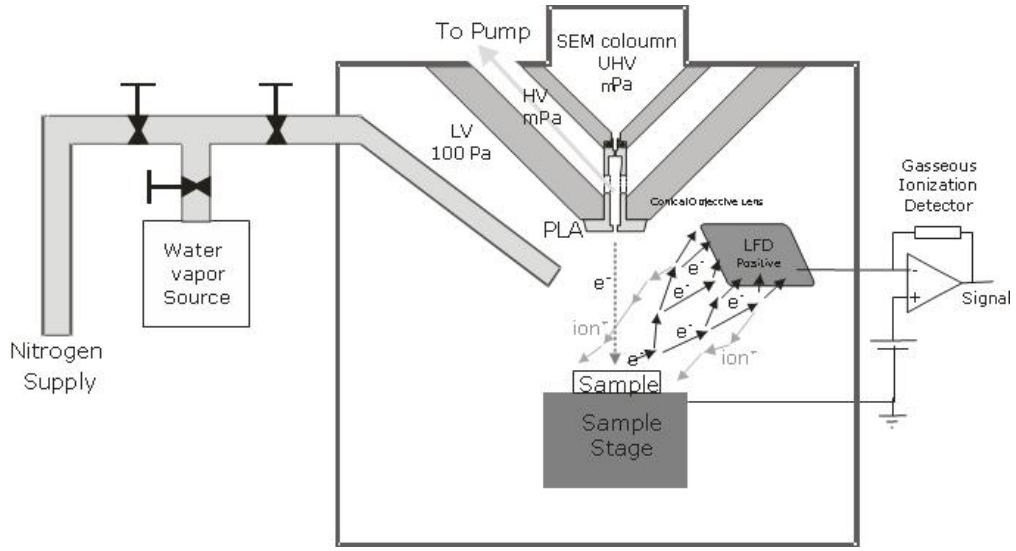

Figure 3-13 Schematic of Environmental Scanning Electron Microscopy (ESEM)

ESEM analysis was performed in this study using FEI Quanta 200 Environmental Scanning Electron Microscopy to study the growth of biofilm on the surface of polyethylene samples with different clay and pro-oxidant loadings after composting. The existence of micro-organisms on the surface of polymer after composting and also the opportunity to compare biofilm for different samples under similar testing conditions can help to find and understand the factors affecting biodegradation in polyethylene nanocomposites. This technique will lead to determining optimising factors which have positive effects on biodegradation and minimising the negative ones. Samples were run in ESEM or wet mode using GSED detector, the accelerating voltage was between 15-20 kV and the spot size was 4. It has been found the best working distance for the samples used in this study is around 6.4 mm.

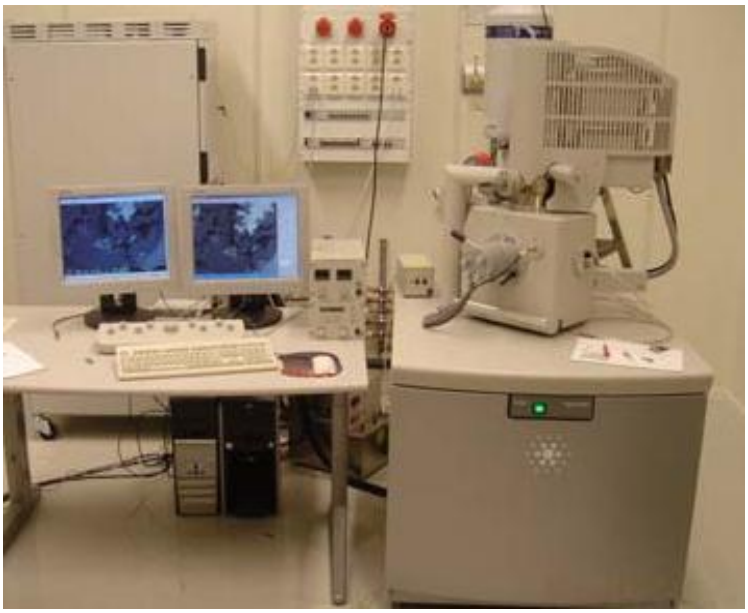

Figure 3-14 ESEM microscopy

4 Biodegradation of Oxo-biodegradable polyethylene

4.1 Introduction

The main objective of this work is to improve the degree of ultimate biodegradation of polyethylene by blending it with carefully chosen additives with an optimum concentration so that it can oxo-biodegrade in the environment after its service life. As it has been described in Chapter 3, oxo-biodegradable polyethylene films were prepared by adding 1% of manganese stearate to pure polyethylene. Virgin polyethylene pellets were processed under the same processing condition as a reference material to identify the effect of processing condition on degradation. Polymer film samples prepared from the pellets were then subjected to heat in an air circulated oven at 70°C (ASTM D6954) for a period of two weeks (14 days). After thermal treatment, film samples were analysed to obtain a clear understanding of the thermal oxidation process and also to identify the products of thermal degradation. Biodegradation tests were then carried out in a closely monitored composting system according to AS-ISO 14855.

In this chapter, the results of oxo-biodegradation of PE and OPE will be presented in two sections:

1. Abiotic stage (thermal degradation) of PE and OPE
2. Biotic stage (biodegradation) of PE and OPE

Results will illuminate how introducing manganese stearate as a pro-oxidant to polyethylene matrix can influence both abiotic and biotic stages of degradation.

4.2 Results and discussion

4.2.1 Abiotic stage

4.2.1.1 Thermogravimetric Analysis (TGA)

TGA traces of pure polyethylene, polyethylene with Fusabond (PE+F), and polyethylene with pro-oxidant (OPE) under nitrogen atmosphere are depicted in Figure 4-1 and the corresponding data are listed in Table 4-1. As can be seen from this Figure, initial decomposition temperature (IDT) of OPE is higher than that of pure polyethylene, but it is comparable with that of (PE+F). These results indicate that OPE and (PE+F) are more thermal stable than pure polyethylene. This can be attributed to the mixing of polyethylene with Fusabond which improves the thermal stability of polymer considerably leading to higher decomposition temperature compared to that of pure polyethylene. As can be seen from Table 4-1, the temperature for the onset of thermal degradation (which has been defined as the temperature at 10% degradation) $T_{0.1}$, for OPE and (PE+F) is approximately 9 and 14˚C, respectively higher than that of PE. On the other hand, at mid-point temperature, $T_{0.5}$, (which has been defined as the temperature at 50% degradation), thermogravimetric traces of OPE and PE come very close, while that for (PE+F) is removed from that for PE by about 7˚C.

These results indicate that the increase in the thermal stability of (PE+F) and OPE samples observed is mainly due to the addition of Fusabond to polyethylene matrix. At lower temperature, the presence of Fusabond in OPE hinders the influence of pro-oxidant and therefore deters the degradation. Therefore, the initial degradation for OPE is about 10˚C higher than that of pure polyethylene. However, at higher temperatures (at mid-point), the action of pro-oxidant becomes dominant which overrides the obstructing role of Fusabond thereby leading to a faster degradation rate. In general, OPE was more thermally stable compared to polyethylene under non-oxidative environment such as nitrogen atmosphere.

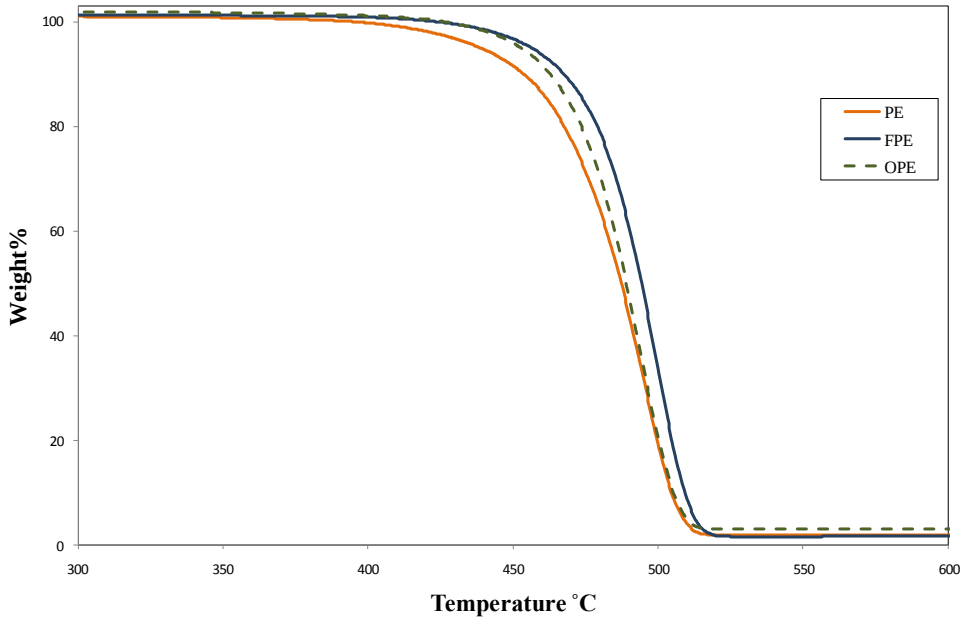

Figure 4-1 TGA traces for polyethylene, polyethylene with Fusabond (PE+F) and polyethylene with pro-oxidant (OPE) (under nitrogen environment).

Table 4-1 TGA data for polyethylene, (PE+F) and OPE samples (under nitrogen environment)

PE, wt%	Fusabond, wt%	Clay, wt%	Pro-oxidant, wt%	$T_{0.1}$, ˚C	$T_{0.5}$, ˚C
100	.	.	.	453.8	487.3
92	8	.	.	467.5	494.4
91	8	.	1	462.8	489.1

4.2.1.2 Fourier Transform Infrared Spectroscopy (FTIR) analysis of thermally oxidised PE and OPE

As mentioned in Chapter 3, polymer samples were subjected to thermal oxidation by placing them in an air circulated oven at 70°C for 14 days. After this period, all samples were subjected to FTIR analysis to study the thermal degradation behaviour of tested samples and determine the degradation products. Fourier Transform Infrared Spectroscopy (FTIR) has been used extensively for the study of degradation of polyethylene by many researchers. FTIR results can be used to determine the changes in the structure of macromolecules and the presence of functional groups such as carbonyl and hydroxyl groups generated during the thermal oxidation process.

FTIR spectra of unaged and abiotically oxidised PE, (PE+F), and OPE samples are shown in Figures 4-2 to 4-4. A specific spectra range has been chosen for Figure 4-4 to clearly show the spectra in which all the changes happened during thermal oxidation.

Mechanism of thermal degradation involves the formation of free radicals which subsequently leads to the formation of intermediates in the presence of oxygen (Figure 4-5). These, intermediates then undergo chain scission leading to the breakdown of polymer into smaller fragments with lower molecular weight. These new products normally have functional groups at the end of or along their chains, which make them susceptible to participate in reactions with microorganisms.

Roy *et al*. (2008) suggested the mechanism for the degradation of polyethylene containing manganese stearate. They suggested that, firstly, the electron in the third sub-shell of manganese gets promoted to a higher level by absorbing energy from a heat/light source thereby leading to the formation of intermediate carboxylate groups. These intermediate

products are then decarboxylated to form radicals which attack the hydrogen in polyethylene backbone and initiate the degradation process. Roy *et al*. suggested that pro-oxidant is responsible for the initiation of radical formation as well as propagation of it. Figure 4-5 and 4-6 represents two simplified schemes for the thermal degradation of polyethylene containing pro-oxidant proposed by Dintcheva *et al*. (2009) and Koutny *et al*. (2006), respectively.

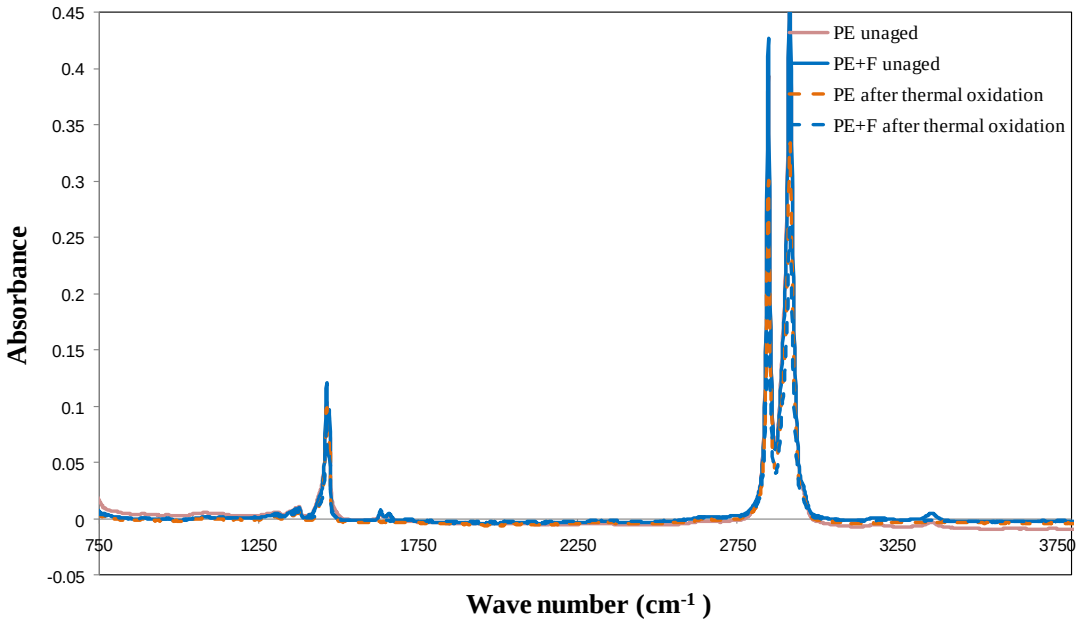

Figure 4-2 FTIR spectra of PE and (PE+F) before and after 14 days of thermal degradation

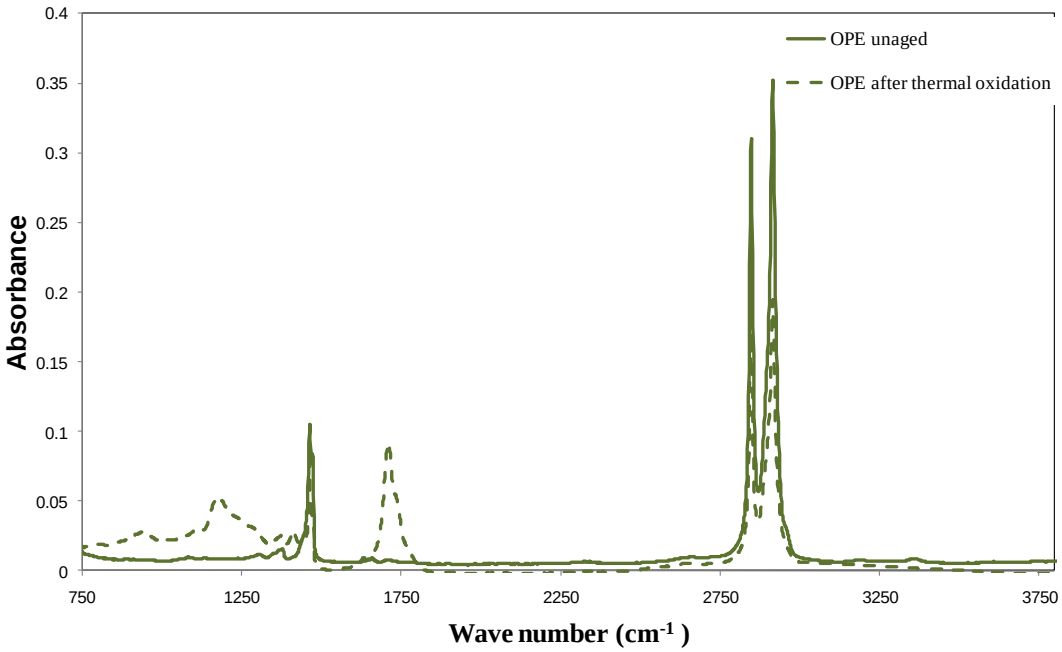

Figure 4-3 FTIR spectra of OPE before and after 14 days of thermal degradation

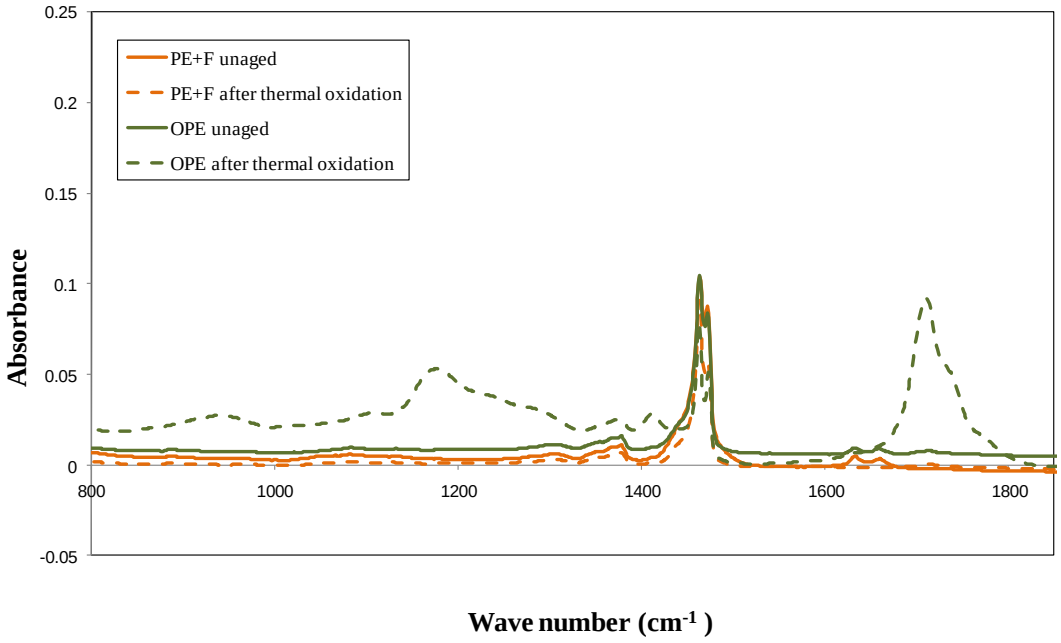

Figure 4-4 FTIR spectra of PE and (PE+F) before and after 14 days of thermal degradation

As can be seen clearly in Figure 4-2, there is no significant change in spectra before and after 14 days of thermal degradation in PE and (PE+F) samples. Other researchers have also

reported similar results which showed that polyethylene without additives does not show any changes during thermal degradation in a short period of time (Hinksen *et al*. 1991, Khabbaz & Albertsson 2000 and Reddy *et al*. 2008). In contrast to PE and (PE+F) results, the effect of adding manganese stearate to PE (OPE) can be clearly seen in Figure 4-3

A broad curve with a sharp peak can be observed at about 1713 cm^{-1}, which is assigned to C=O groups (1690-1870 cm^{-1}) and it is due to the formation of different carbonyl compounds in thermal degradation. The carbonyl groups band represents a combination of several absorption bands like those for aldehydes and/or esters (1733 cm^{-1}), carboxylic acid groups (1700 cm^{-1}), and γ lactones (1780 cm^{-1}) which all contain C=O functional group (Khabbaz *et al*. 1998).

The other significant observation in the spectra can be made between 750 to 1300 cm^{-1} with peaks at 930 and 1180 $cm^{-1.}$ The first peak between 880 and 995 cm^{-1}, which can be assigned to bending vibration of alkanes (=C-H and =CH2), indicates the presence of alkanes in the degradation products. The weak peaks between 1350 and 1470 cm^{-1}, which are assigned to deformation bending vibrations of alkanes, also confirm the presence of alkanes in the degradation products. The band between 995 and 1350 cm^{-1} represents the presence of O-C functional group (2-bands) which could be due to either stretching vibrations of alcohols and phenols (1000-1300 cm^{-1}) and/or carboxylic acids and derivatives (970-1250 cm^{-1}).

These results indicate that addition of manganese stearate as pro-oxidant has helped in initiating the degradation process. During the degradation, polyethylene macromolecules break down and form alkyl radicals. It has been reported by Peterson *et al*. (2001) that if the initial or final stage of degradation changes due to the changing of a factor, then the kinetics of degradation changes and it leads to variation in the activation energy. Based on this fact,

Roy *et al.* (2008) showed that manganese stearate can provide an alternative route for the degradation of polyethylene and it will effectively catalyses the degradation process.

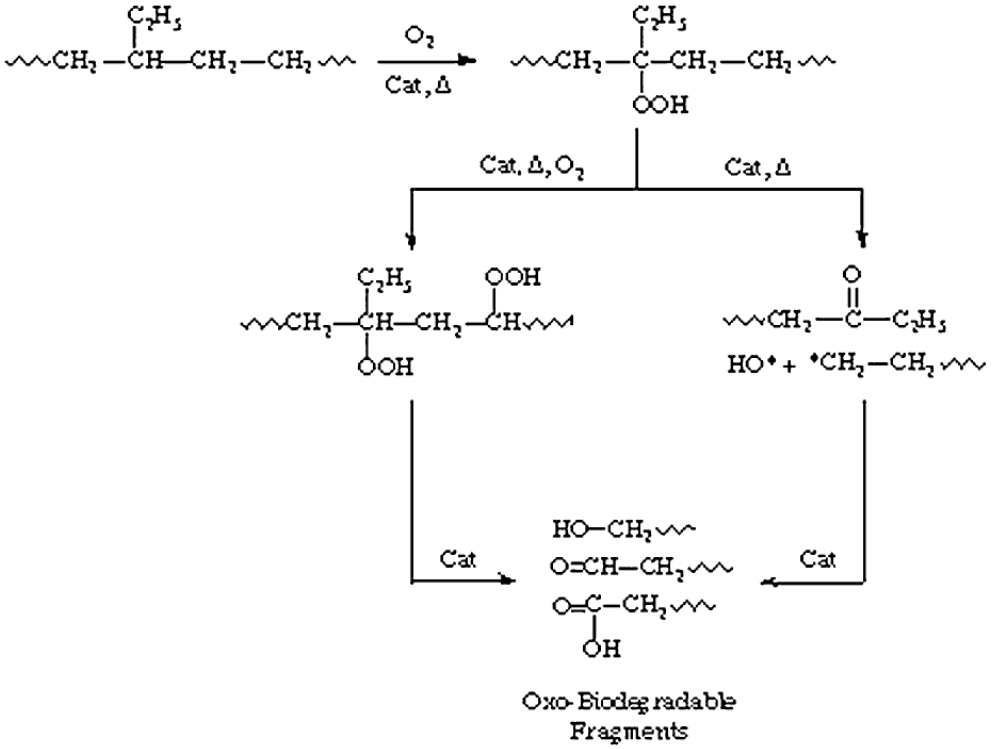

Figure 4-5 Mechanism of abiotic oxidation in polyethylene (Chiellini *et al*. 2006)

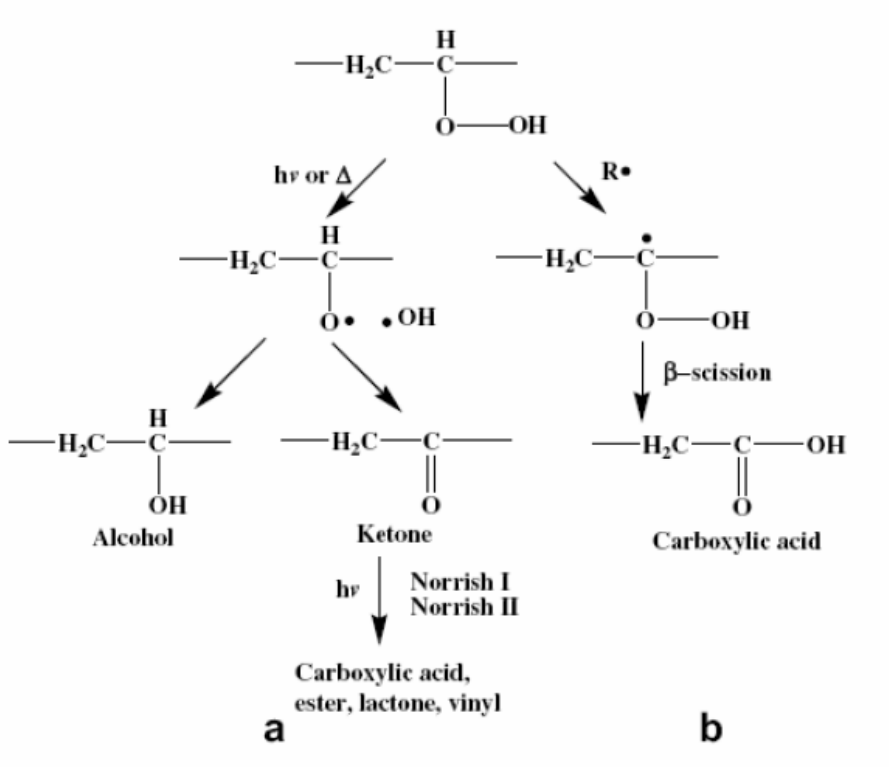

Figure 4-6 Reaction scheme for peroxide decomposition of hydroperoxide leading to oxidation products of polyethylene (Dintcheva *et al.* 2009)

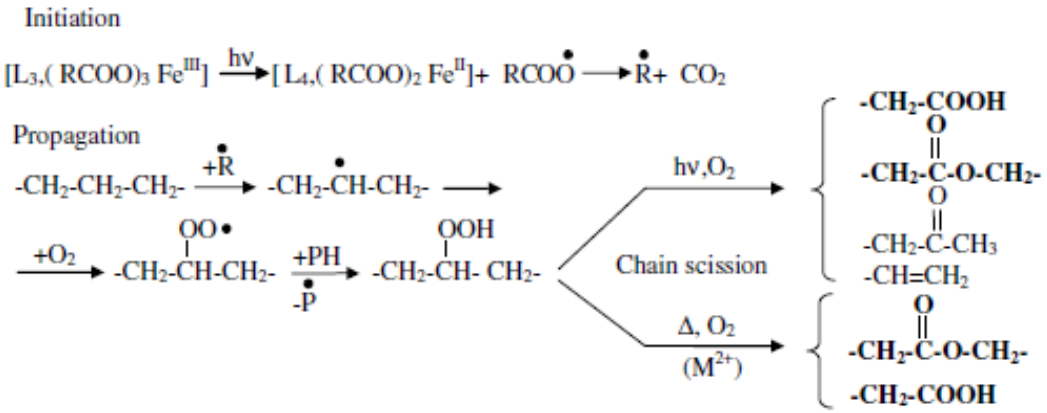

Figure 4-7 Simplified scheme of abiotic degradation of polyethylene contains pro-oxidant (Koutny *et al.* 2006)

Since the main products of abiotic degradation of polyethylene are in the category of carbonyl groups, carbonyl index (CI) has been used as a quantitative tool to measure the degradation rate. The definition of carbonyl index has been given in Equation 4-1.

$$\text{Carbonyl Index (CI)} = \frac{\text{Absorption at } 1713\,\text{cm}^{-1} \text{ (the maximum of carbonyl peak)}}{\text{Absorption at } 1464\,\text{cm}^{-1} \text{ (the maximum of methylene peak)}} \qquad 4\text{-}1$$

Figure 4-8 shows the changes in the carbonyl index values of (PE+F) and OPE during thermal oxidation process. Results for PE are excluded from this figure and the rest of the chapter since it has been proven by many researchers that the biodegradation of pure polyethylene takes place at a very slow rate which makes it impossible to study the process over a short period of time. Instead, (PE+F) is used as a reference material to study the effects of Fusabond and manganese stearate in thermal oxidation and biodegradation. CI result shows that degradation rate in OPE is remarkably higher than that of (PE+F). CI value of (PE+F) remains more or less constant over the period of 14 days whereas those for OPE increases continuously and reaches a value of 1.7 after 14 days. This result shows clearly the significant role of pro-oxidant in the degradation process. Presence of manganese stearate in polyethylene matrix changes the degradation behaviour completely and leads to the degradation of polymer to a good extent.

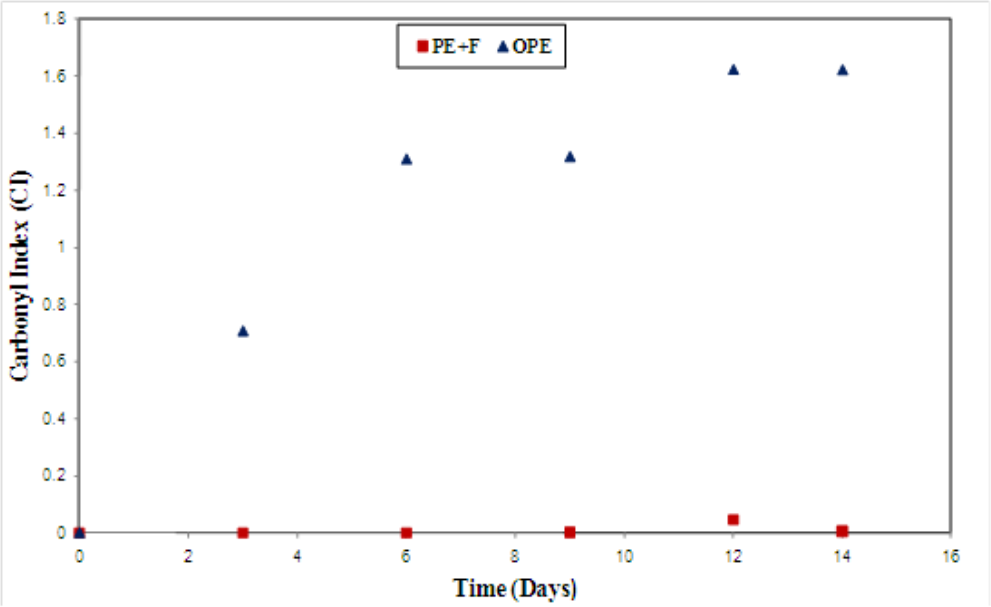

Figure 4-8 Changes in CI for (PE+F) and OPE samples in 14 days of thermal oxidation at 70°C

4.2.2 Biotic stage

4.2.2.1 Biodegradation analysis

As explained in Chapter 3, thermally-oxidised polymer films have been subjected to biodegradation in a controlled composting system. According to AS-ISO 14855, Equation (4-2) can be used to calculate the quantity of carbon dioxide evolved from each compost vessel. The data required to estimate the volume of CO_2 produced were collected using the infrared gas sensors.

$$\text{vol}(CO_2) = \Delta time \times \text{vol rate (air)} \times \text{concentration}[CO_2] \quad \text{4-2}$$

The cumulative amount of evolved CO_2 was then determined using Equation (4-3).

$$\text{Cumulative vol}(CO_2) = \int_0^t \text{vol}(CO_2) \cdot dt \quad \text{4-3}$$

Theoretical amount carbon dioxide ($ThCO_2$) that is generated by each test samples was then calculated using Equation (4-4):

$$ThCO_2 = M_t \times C_t \times \frac{44}{12} \quad \text{4-4}$$

where M_t = the total dry solids (g), C_t = the relative amount of total organic carbon in dry solids in each test vessel (-), 44 = the molar mass of carbon dioxide (g/mol), 12 = the atomic mass of carbon, (g/mol).

Table 4-2 shows the theoretical CO_2 calculated for each samples according to their formulation.

Table 4-2 Total carbon content% and $ThCO_2$ for all test samples

Sample name	Total Carbon %	$ThCO_2$ (g)
Cellulose	41.14	113.135
PE+F	85.70	235.675
OPE	84.84	233.310
OPE 2C	83.78	230.395
OPE 3C	83.24	228.910
OPE 5C	82.16	225.940
PE 2C	84.46	232.265
PE 3C	84.10	231.275
PE 5C	83.02	228.305

Then the degree of biodegradation of the test material (D_t) was calculated using Equation (4-5):

$$\%D_t = \frac{(CO_2)_t - (CO_2)_b}{ThCO_2} \times 100 \qquad 4\text{-}5$$

where $(CO_2)_t$ and $(CO_2)_b$ are the cumulative amount of carbon dioxide produced biologically in the test vessel and blank control vessel, respectively.

Since each sample was run in triplicates, the mean degradation was determined according to Equation (4-6):

$$\text{Mean degradation} = \frac{\text{degradation}_1 + \text{degradation}_2 + \text{degradation}_3}{3} \qquad 4\text{-}6$$

The degree of biodegradation of OPE and (PE+F) determined using the equations shown above are shown in Figure 4-9 as a function of incubation time. It is clear from the graph that biodegradation rate increases with time for both samples. However, there is a significant difference in the biodegradation behavior of OPE and (PE+F). After 45 days of incubation, the biodegradation rate of (PE+F) is 1% whereas that of OPE is about 7%. This result is remarkable especially for OPE because the biodegradation rate of pure PE is very slow. In the cases of both OPE and (PE+F), the biodegradation rate values are on an increasing trend as a function of time which suggests that it is possible for these samples to reach 100% biodegradation in an extended time. The validity of the biodegradation test results has been checked by using cellulose, which is a fully biodegradable material, as a positive control. It has been found that the biodegradation rate of cellulose reaches more than the required minimum of 60% at the end of test period.

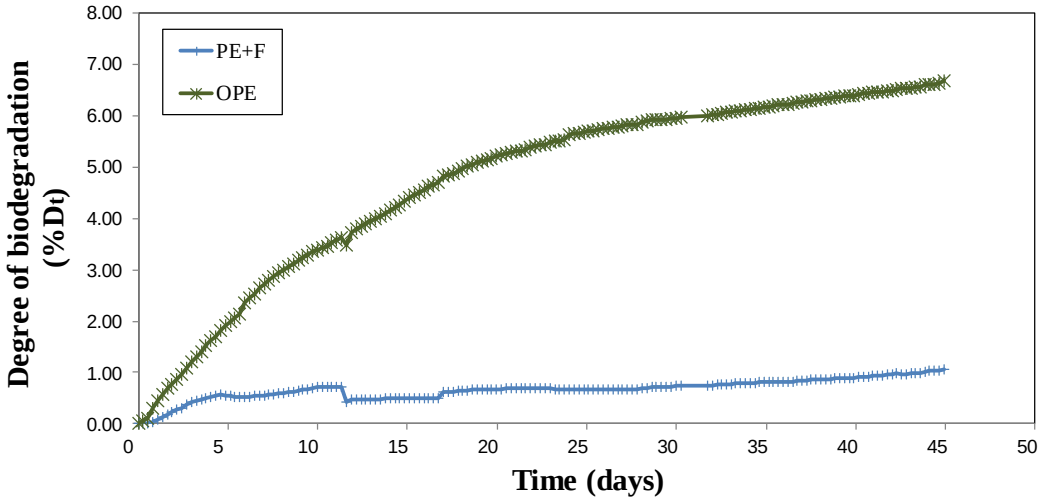

Figure 4-9 Biodegradation rate of (PE+F) and OPE over a period of 45 days

Cumulative CO_2 values collected from blank, (PE+F), OPE and cellulose samples during the 45 days incubation time are shown in Figure 4-10. It is evident from the figure that the cumulative CO_2 value increases continuously with time for all samples used. However, there is no significant difference between the cumulative CO_2 values for (PE+F) and blank samples over the entire 45 days test period. On the other hand, the cumulative CO_2 values for OPE are higher than those for blank and (PE+F) samples over the entire test period. The difference in cumulative CO_2 values for (PE+F) and OPE samples is small in the initial stages of the test but it becomes significant towards the end of the test period indicating the continual and accelerated rate of biodegradation of OPE. As expected, the cumulative CO_2 for cellulose is much greater than the other samples. Cumulative CO_2 for cellulose reaches about 98 g after 45 days of incubation, which is about 5 and 3 times greater than those for (PE+F) and OPE, respectively.

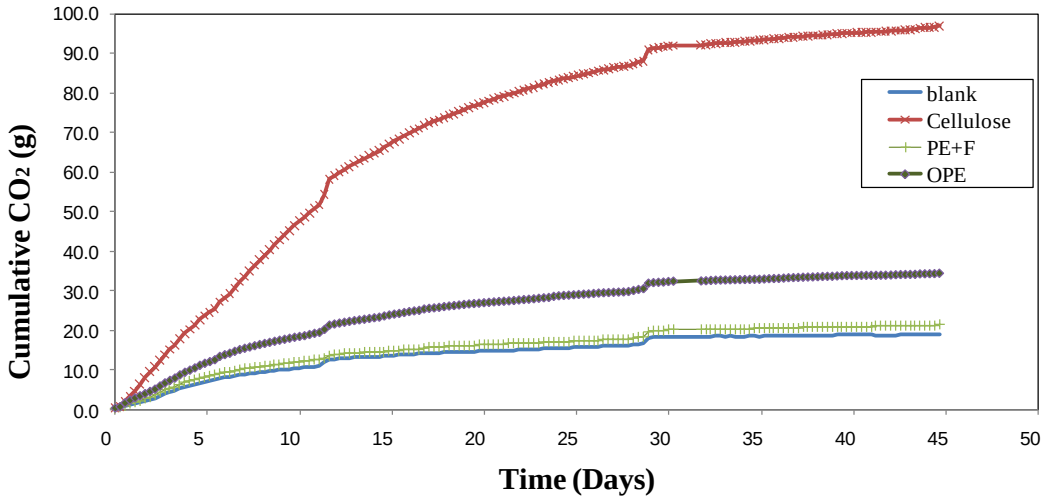

Figure 4-10 Cumulative CO_2 for blank, (PE+F), OPE and cellulose during incubation time (45 days)

4.2.2.2 Fourier Transform Infrared Spectroscopy (FTIR) analysis after composting

It is well known that low molecular weight products formed during abiotic degradation of polyethylene are consumed by microorganisms during the microbial stage of degradation. Biodegradation of low molecular weight groups can be monitored by subjecting the biodegraded samples from the compost to FTIR analysis. In this section, the effects of composting on thermally-oxidised polyethylene and OPE samples are discussed using FTIR spectra.

Changes in FTIR spectra of (PE+F) and OPE samples after thermal oxidation and biodegradation in composting are shown in Figures 4-11 to 4-13. FTIR spectra of aged (thermally oxidised) and unaged (PE+F) and OPE samples are shown in Figure 4-11 after their biodegradation in compost. The spectra for (PE+F) samples before and after thermal oxidation are nearly the same indicating that there is no significant thermal degradation and the generation of low molecular weight components for these samples. However, the spectra of biodegraded (PE+F) samples are different from those for non-biodegraded samples

indicating that some changes have occurred in the polymer molecules during composting. The spectra peak between 1000 and 1160 cm^{-1} indicate the presence of biofilm on the polymer film samples because this characteristic peak corresponds to polysaccharides. Polysaccharides are the common metabolites produced by microorganisms (Linos *et al.* 2000, Maquelin *et al*. 2002). The presence of weak peaks at about 1265, 1560 and 1590 cm^{-1} could be attributed to the presence of carboxylic acids, which indicates the beginning of the early stages of biodegradation process.

FTIR spectra for OPE samples in the wave number range of 800 – 3800 cm^{-1} are shown in Figure 4.12. However, to visualise the influence of biodegradation on the spectra clearly, a spectra in a narrower wave number range of 800 – 2000 cm^{-1} are shown in Figure 4-13. All the peaks for the biodegraded samples are higher than those for the thermally oxidised samples indicating OPE samples have undergone higher level of degradation during composting. In addition, there are significant difference in the amount of hydroxyl groups formed (shown by the peaks in 3200-3600 cm^{-1} range) between those for biodegraded and thermally oxidised OPE samples (Figure 4-11). In addition to the changes in the peaks, there are changes in the shapes of curves for carbonyl groups (Figure 4-12) which suggests possible consumption of some degradation products and production of others during the incubation time.

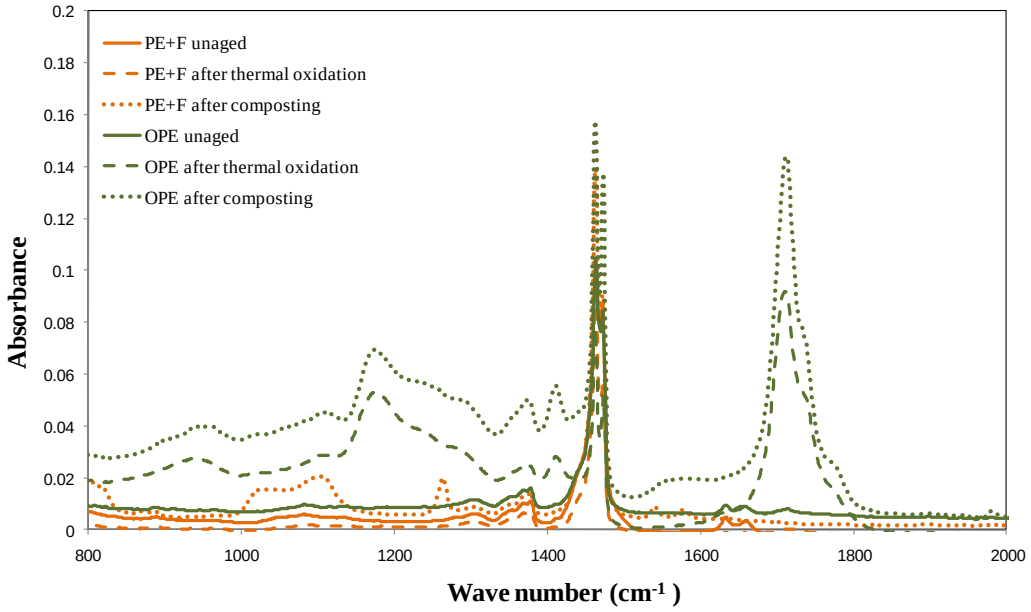

Figure 4-11 FTIR spectra of (PE+F) and OPE after thermal oxidation and composting

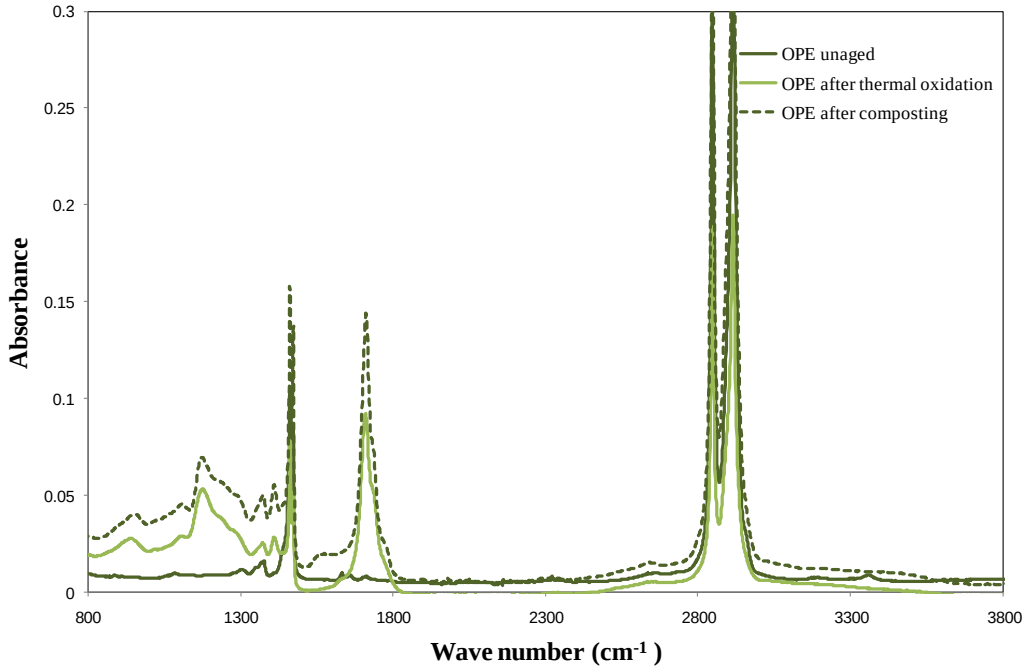

Figure 4-12 FTIR spectra of OPE after thermal oxidation and composting

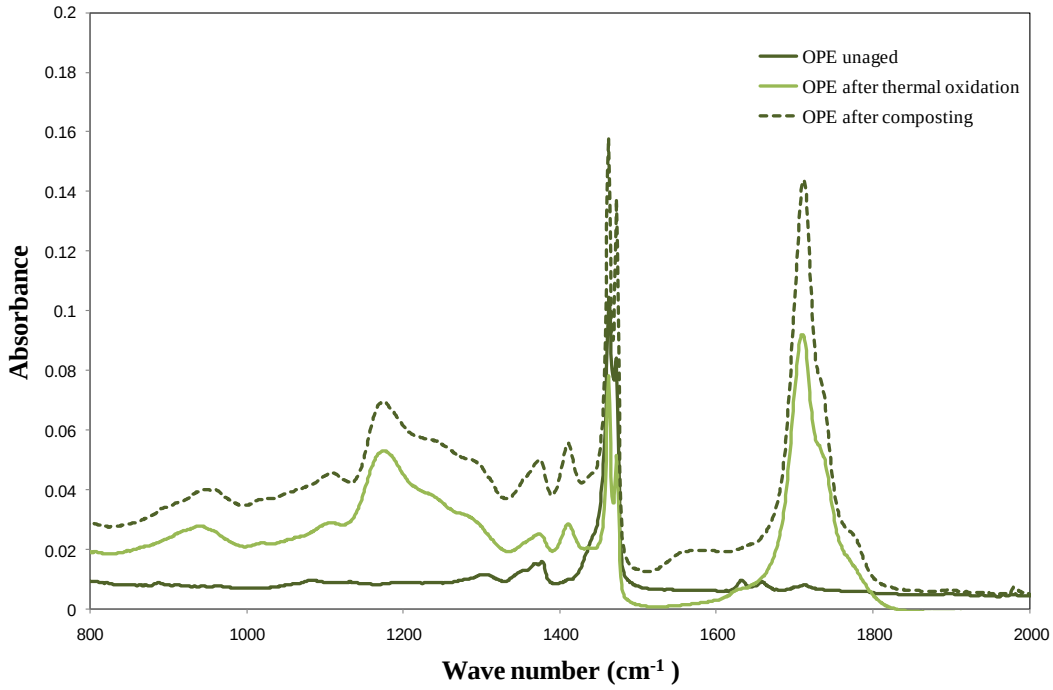

Figure 4-13 FTIR spectra of OPE after thermal oxidation and composting

The results from the spectra shown in Figures 4-11 and 4-12 indicate clearly that the degradation of OPE did not stop after 14 days of thermal oxidation and OPE samples degraded continuously to lower molecular weight products even during the composting period. The presence of sharper as well as broader peaks at carbonyl region (1690-1870 cm^{-1}) and unsaturated region (1300-1420 cm^{-1}) plus the presence of new peaks at hydroxyl region (3200-3600 cm^{-1}) confirm the observations made from cumulative CO_2 data shown above.

As explained above, the biodegradation rate of OPE and (PE+F) samples shows an upward trend throughout the composting period. The slopes of the degree of biodegradation curves (Figure 4-9) increases continuously with composting time and it can be postulated that it will continue further than 45 days if the composting had been continued. It can be further suggested that degree of degradation will continue with time and reach 100% eventually.

There have been many studies in the literature which state that the continuation of this biodegradation process is due to the action of microorganisms in soil and compost media. In

their study on biodegradation of PE wax, Kawai *et al*. (2004) showed that even the molecules with molecular weight greater than 1000 Da could be consumed by soil microorganisms in addition to the lower molecular weight (MW) products of thermal (abiotic) oxidation. Chiellini *et al.* (2003) showed that soil microorganisms could consume molecules with molecular weight (MW) of up to 1500 Da in their study on the biodegradation of thermally oxidised polyethylene.

It has been shown by Albertsson & Banhidi (1980), Kawai *et al*. (2002) and Kawai *et al*. (2004) that longer alkanes go under different pathway of biodegradation which consists of intercellular beta oxidation by the help microorganisms. Koutny *et al*. (2006) suggested a possible scheme for the mechanism of biodegradation of PE by microorganisms (Figure 4-14). According to this mechanism, if a molecule (1) is still bigger than it could pass the cell wall (2); soluble extracellular enzymes (3); or cell wall associated enzymes (4); can help to further oxidation. These enzymes may produce diffusible radicals (5); or they help to mobilise the insoluble PE fragments by the help of biosurfactants present on the cell wall (6); and pass them through the cell wall (7). Then they can be transformed by enzymes (8) in cytoplasmic membrane (9); and/or in the periplasmic space (10). Finally they will be assimilated in the beta oxidation pathway (11).

In conclusion, microorganisms not only just assimilate the lower molecular weight products of abiotic degradation, they also help in polyethylene oxidation by producing extracellular lingolytic enzymes and various peroxides that can help in chain cleavage of long chain-carbon molecules like polyethylene (Pometto *et al*. 1992, Kirk *et al*. 1984, Koutny *et al*. 2006).

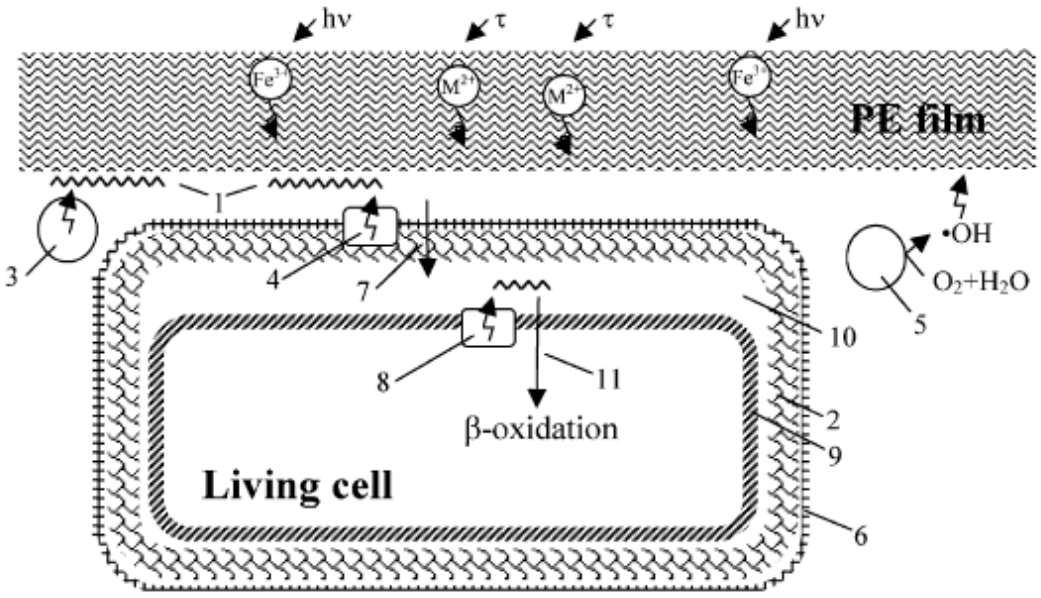

Figure 4-14 Scheme of possible biodegradation mechanism of PE by the help of microorganisms suggested by Koutny *et al*. (2006)

4.2.2.3 Biofilm formation

The ultimate biodegradation of polymer means conversion of it into CO_2 and H_2O, which are ultimate products of mineralization. This process cannot be accomplished without microorganisms. When microorganisms consume and assimilate the products of degradation during the biodegradation process, they lead to the formation of biofilm on the polymer sample. Therefore, the presence of biofilm on the surface of polymer film is a good evidence for the progress of biodegradation. ESEM micrographs were used to show the presence of biofilm on polymer samples in this study.

ESEM micrographs are shown in Figures 4-15 and 4-16 for biodegraded OPE and (PE+F) samples respectively. It can be seen that there is minimal biofilm growth on ((PE+F) sample while a significant amount microorganism is visible on OPE sample. This shows that OPE film provides a more suitable environment for bacteria to live and grow compared to (PE+F) film. Lower molecular weight fragments produced in abiotic stage act as a source of nutrients

for microorganisms (Albertsson *et al*. 1998, Bonhomme *et al*. 2003, Koutny *et al*. 2006). Moreover, the functional groups of these lower molecular weight products such as carboxylic acid and alcohols are hydrophilic which make the polymer surface a favourable environment for microorganism activities (Jakubowicz *et al*. 2006).

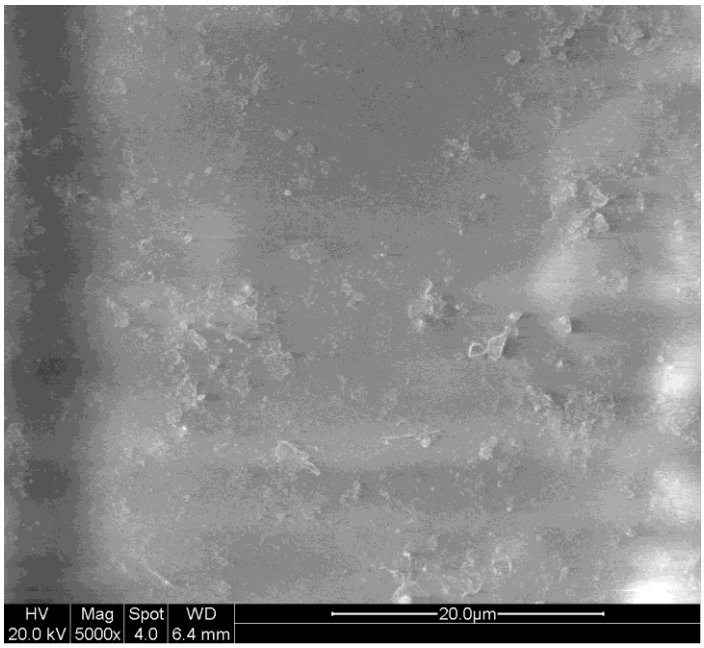

Figure 4-15 ESEM micrographs of biofilm on (PE+F) surface after composting

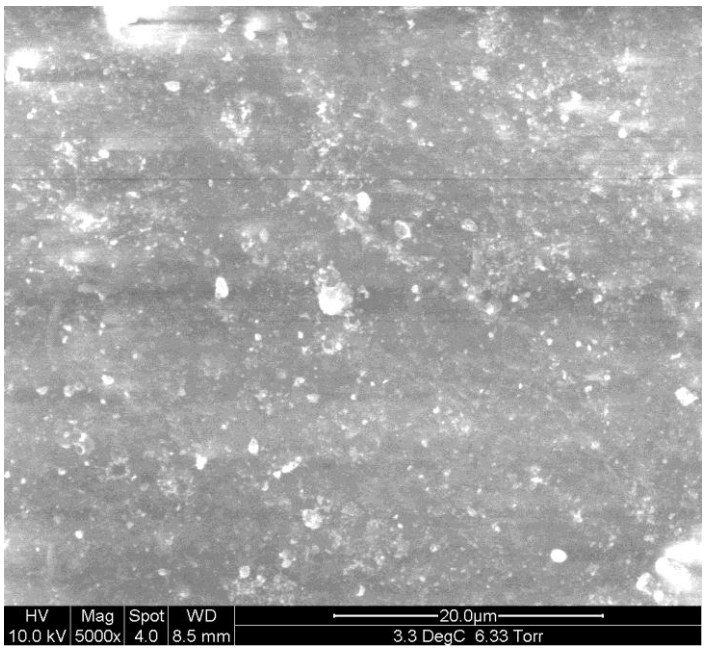

Figure 4-16 ESEM micrographs of biofilm on OPE surface after composting

4.3 Conclusions

It can be concluded from the results obtained in this study that the addition of manganese stearate as a pro-oxidant helps in different aspects of both abiotic and biotic stages of biodegradation process. In abiotic stage, manganese stearate helps to initiate and propagate the radical formation leading to the production of more oxidation products in a shorter oxidation period. These products are normally within the molecular weight range of products that can be consumed by microorganisms. These products also contain functional groups which make the polymer film hydrophilic which increases the attraction of microorganisms to the film surface. As a consequence, the biodegradation and ultimate mineralization takes place at a faster rate on the polymer film. It has also been observed, from FTIR spectra of degraded samples, that OPE samples continue to degrade and break down to smaller fragments even during the incubation (biodegradation) period.

5 Polyethylene nanocomposites

5.1 Introduction

Polyethylene nanocomposites were prepared by adding commercially available clay (Cloisite 15A) and Fusabond to polyethylene. The process of making polyethylene nanocomposite films was explained in Chapter 3. The compositions of polyethylene nanocomposites and their abbreviations are presented in Table 5-1. These nanocomposites were also subjected to thermal oxidation and biodegradation tests similar to those for PE and OPE samples explained in Chapters 3 and 4.

Widespread usage of clay in producing nanocomposites with enhanced physical and mechanical properties compared to pure polymers and conventional composites has led scientists to investigate their biological degradation behaviour after their service life. Since clay is mineral material, its presence in synthetic polymer structure alters the degradation pathway of polymer. It was reported that, in most cases, the nanocomposites show different biodegradation trends.

The main focus of this study is to understand the mechanism involved in the biodegradation of polyethylene and determine the factors that improve its biodegradability. To achieve a comprehensive understanding on the degradation mechanism, the effect of clay on abiotic and biotic stages of polyethylene degradation was examined in this work. Analytical technique and methods that were described in Chapter 4 for evaluating the biodegradability of oxo-biodegradable polyethylene were used also for nanocomposites.

Table 5-1 Composition of polyethylene nanocomposites

Sample name	PE (wt%)	PE-g-MA (wt%)	MMT (wt%)
LDPE (PE+F)	92	8	-
LDPE + 2% Clay (PE 2C)	90	8	2
LDPE + 3% Clay (PE 3C)	85	12	3
LDPE + 5% Clay (PE 5C)	75	20	5

5.2 Result and discussion

5.2.1 Morphology of polyethylene nanocomposites

5.2.1.1 Wide angle x-ray diffraction (WAX)

WAX patterns of polyethylene nanocomposites with different concentrations of clay (Cloisite® 15A) are shown in Figure 5-1. It can be seen that the characteristic peak of Cloisite® 15A is found at 2.78°. Using Bragg's law ($n\lambda = 2d \sin\theta$), d-spacing of Cloisite 15A was calculated to be 3.02 nm. A shift of peaks of the WAX curves to lower angles indicates the degree of dispersion and intercalation of clay particles into the polymer matrix while the absence of peaks indicates that polymer and clay particles exist in an exfoliated structure. It can be seen in Figure 5-1 that the characteristic peak of organoclay @ 2.78° has nearly disappeared in the case of PE 2C indicating that nanocomposite with 2% clay has nearly exfoliated structure. On the other hand, the presence of a shoulder in

the curves for PE 3C and PE 5C indicate an intercalated structure for these two nanocomposites.

To form an exfoliated structure, long polyethylene chain has to enter between clay layers, separate them apart and form a new structure with different properties compared to feed materials (Reddy *et al*. 2008). If the polymer engages with clay layers, increases the d-spacing but cannot separate the clay platelets, an intercalated structure is formed. In this structure, the stacked shape of the clay layer will be still maintained in the newly formed nanocomposite. In such case, the shoulder in the WAXS curve shifts toward the lower angle compare to that for pure Cloisite® 15A (Figure 5-1). As a result, these two nanocomposites possess different physical and chemical properties. The WAX results therefore suggest that, in the preparation of polyethylene nanocomposites, 2% clay is low but sufficient to achieve a nearly exfoliated structure while 3 and 5% clay lead to nanocomposites with intercalated structure. Therefore, it can be expected from these results, the nanocomposites with 2, 3 and 5% clay will exhibit different behaviour in their thermal oxidation and biodegradation.

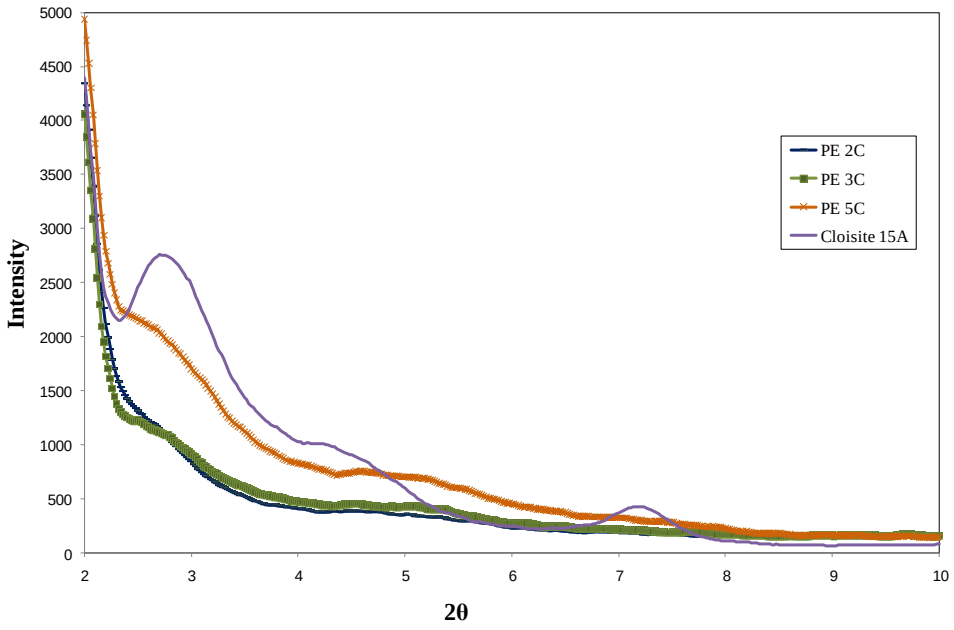

Figure 5-1 WAX patterns of PE nanocomposites with different loadings of Cloisite® 15A

5.2.2 Abiotic stage

5.2.2.1 Thermogravimetric Analysis (TGA)

The results of thermogravimetric analysis for polyethylene nanocomposites with 2, 3 and 5% clay are presented in Figure 5-2 and Table 5-2. As was expected, polyethylene nanocomposite with 2% clay shows different thermal degradation trend compared to nanocomposites with 3 and 5% clay as they have different morphological structure. PE 2C shows an enhancement of about 20˚C at onset temperature and at least 10˚C at all other temperatures and this could be attributed to the exfoliated structure of this nanocomposite. On the other hand, PE 3C and PE 5C nanocomposites exhibit different pattern. Their onset temperatures were significantly higher than that of pure PE and relatively close to those of

PE+F and PE 2C. However, they exhibit a faster decomposition than the other samples tested at about 475˚C and higher.

These results can be explained using the barrier effects brought in by the clay in nanocomposites. It has been observed by many researchers that introduction of clay to polymer matrix enhances the thermal stability of resulting nanocomposite due to the mass transfer barrier effects of clay which limits the amount of oxygen entering the matrix and hinders the discharge of volatile gases produced during degradation (Zhu *et al*. 2001, Ray & Okamoto 2003, Ray & Bousima 2005 and Becker *et al*. 2004). The thermal degradation results observed in nanocomposite with 2% clay can be attributed to the mechanism mentioned above.

Another mechanism for the thermal degradation in polyethylene nanocomposites was suggested by Jang & Wilkie (2005). They suggested that the presence of clay introduces two additional degradation pathways to normal pathway for polymers namely chain scission followed by β-scission. They suggested that radical recombination reaction and extensive random scission occur in the presence of clay readily, and the rate of these reactions increase with an increase in the clay loading. They explained their experimental results on thermal degradation by suggesting that the products of thermal degradation could get trapped in between the well-dispersed clay layers and get superheated during TGA testing. Their observations also agreed with the suggestions of Ray & Okamato (2003) which stated that clay layers keep the heat transferred to them between their stacks, thereby acting like an internal heat source to the nanocomposites and accelerating the rate of degradation.

The effect of the presence of quaternary alkylammonium on the organically modified montmorillonite and the catalytic effect of alkylammonium cations decomposition which leads to Hoffmann elimination reaction should be considered too in explaining the thermal degradation observed in this case. The products of Hoffmann elimination reaction are also considered to catalyse the degradation process (Cho & Paul, 2001). Xie *et al*. (2001) and Davis *et al*. (2003) proposed another theory for the faster degradation of nanocomposites as compared to pure polymers. They suggested that the complex crystallographic structure and the presence of weakly acidic SiOH and strongly acidic bridging hydroxyl groups at the edges clay minerals form catalytically active sites in the structure which lead to a higher rate of degradation in nanocomposites.

It can be concluded from results obtained from thermogravimetric analysis that nanocomposites with an exfoliated structure exhibit higher thermal stability because barrier effects of clay are dominant in this structure. On the other hand, in nanocomposites with intercalated structure, the clays platelets keep their stacked shape and raw properties which help them to trap heat and the products of degradation between their layers, making the nanocomposites with this structure less thermally stable. It is also worth noting that the midpoint temperature of clay itself is 70˚C lower than that of polyethylene.

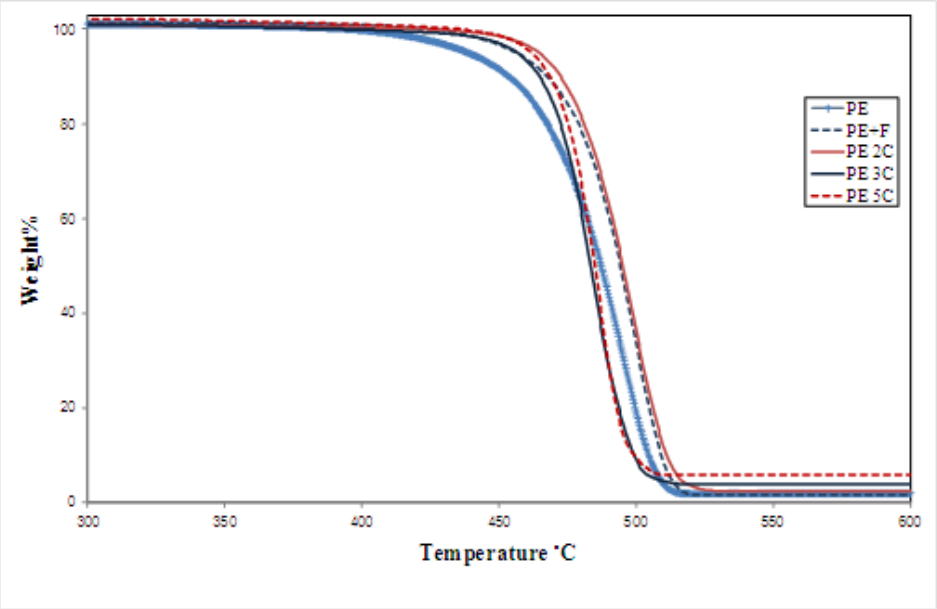

Figure 5-2 TGA curves of polyethylene, PE+F and polyethylene nanocomposites in nitrogen

Table 5-2 TGA data, in nitrogen, for polyethylene, PE+F and polyethylene nanocomposites

PE, wt%	Fusabond, wt%	Clay, wt%	$T_{0.1}$, ˚C	$T_{0.5}$, ˚C
100	-	-	453.8	487.3
92	8	-	467.5	494.4
90	8	2	472.6	495.2
85	12	3	464.9	483.5
75	20	5	468.7	485

5.2.2.2 Fourier Transform Infrared Spectroscopy (FTIR) analysis of thermally oxidised polyethylene nanocomposites

FTIR spectra of PE nanocomposites before and after 14 days of thermal degradation are shown in Figures 5-3 to 5-5. It is clear from the spectra that exposure of films of nanocomposites and PE+F (in the absence of pro-oxidant) to heat for 14 days does not lead to any significant degradation as no appreciable changes can be seen in the spectra. In other words, nanocomposites do not degrade much by heat in 14 days and their behaviour is similar to that polyethylene which was explained in Chapter 4. This result is a confirmation on what was explained before, that at lower temperatures the barrier effects of clay is dominant which helps to enhance the thermal stability of nanocomposites. Therefore, no traces of degradation can be observed in the spectra. It can be assumed that by increasing the temperature or exposure time, the catalytic effects of clay can start to influence the degradation process.

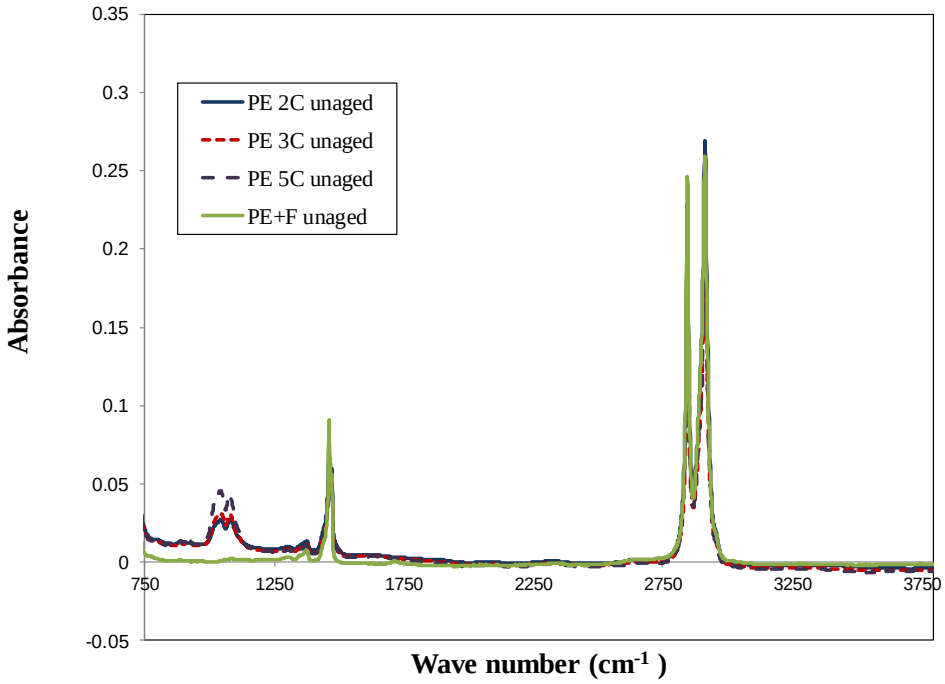

Figure 5-3 FTIR spectra of PE nanocomposites before exposure to heat

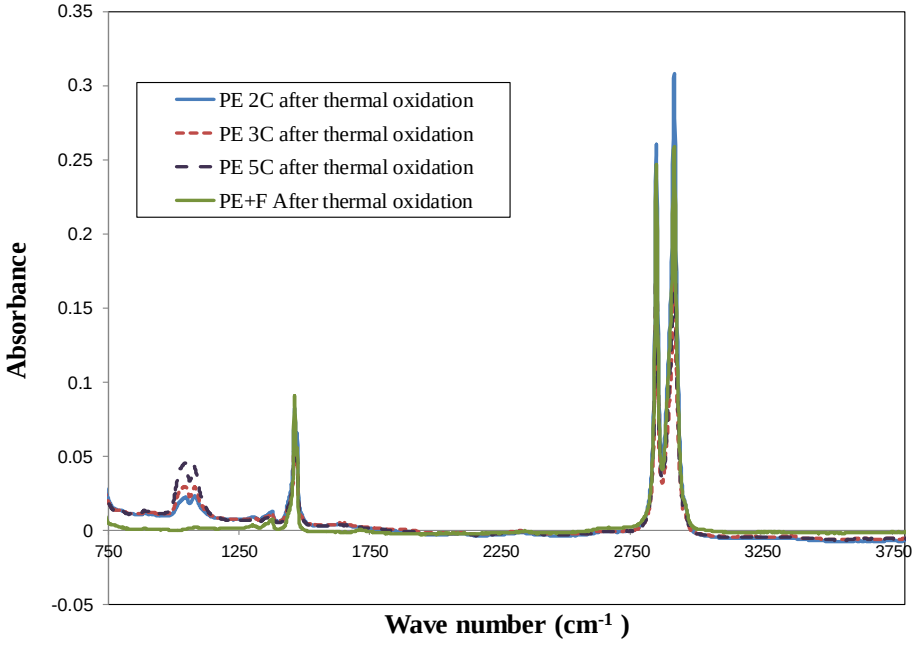

Figure 5-4 FTIR spectra of PE nanocomposites after 14 days of exposure to heat

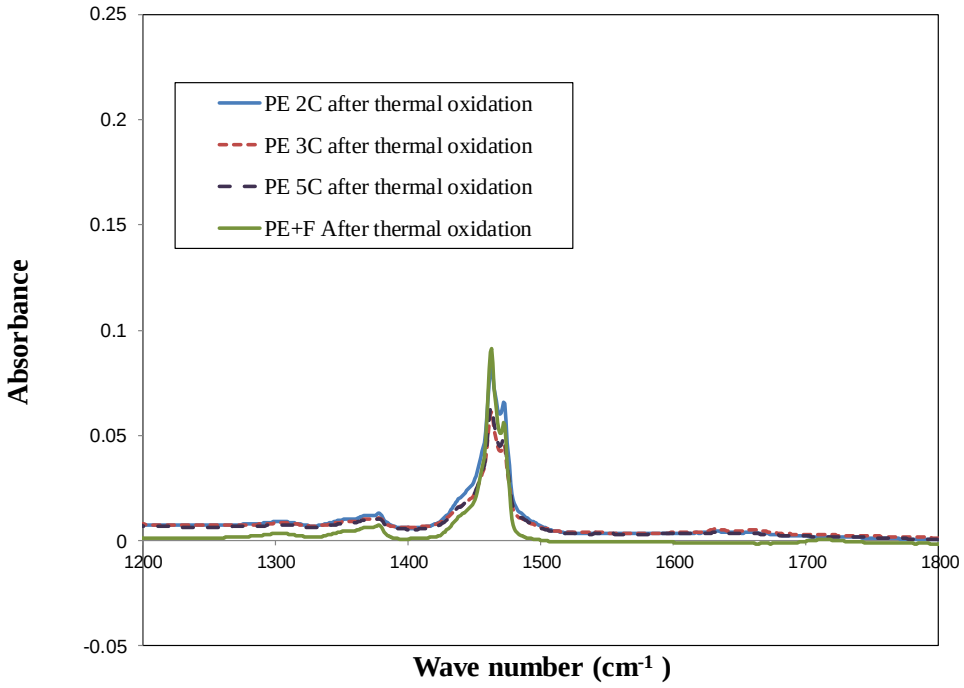

Figure 5-5 FTIR spectra of PE and PE+F before and after 14 days of exposure to heat

5.2.3 Biotic stage

5.2.3.1 Biodegradation analysis

Biodegradation analysis was carried out as explained in Chapter 4. Biodegradation results for polyethylene nanocomposites are shown in Figures 5-6 to 5-8. It is clear from Figure 5-6 that the degree of biodegradation decreases with an increase in clay loading in nanocomposites. Degree of biodegradation is considerably higher in nanocomposite with 2% clay and it decreases with increase in clay concentration in nanocomposites with 3 and 5% clay. This result can be attributed to the fact that the presence of clay in polymer matrix leads to torturous zigzag diffusion pathway for gases (Giannelis 1996, Burnside & Giannelis 1995, LeBaron 1999, Ray *et al.* 2003, Fredrickson & Bicerano 1999 and Lange & Wyser 2003). Oxygen, during its passage through the clay layers, has to change its

direction many times while diffusing through to the matrix. Figure 5-9 shows a simple scheme of the torturous zigzag diffusion pathway in an exfoliated polymer–clay nanocomposite (Yano *et al.* 1993). It has been reported by other researchers also that the presence of clay in nanocomposites reduces the molecular mobility in a polymer matrix and subsequently leads to a drop in diffusion and permeability (Pavildou & Papaspyrides 2008, Ray *et al*. 2003, Chang *et al.* 2003, Ke & Yongpring 2005 and Ogasawara *et al*. 2006). It can be also added that the mass transport mechanism in pure polymers follows mostly Fick's law while the mass transfer in nanocomposites is closer to transport of penetrant molecules. For example, when water molecules absorbed on the surface, they penetrate into the nanocomposite. Then these water molecules are absorbed by hydrophilic surface of clay, become immobilized, therefore, they cannot penetrate to the matrix easily (Drozdov *et al*. 2003).

Another interesting observation in biodegradation results shown in Figure 5-8 is that the degradation rate of PE 2C and PE 3C nanocomposites starts to decrease after around 35 days of incubation. The downward trend in degradation means slower degradation rate in these samples. On the other hand, the biodegradation rate in PE 5C still has a slightly upward trend at this stage. Another strange behaviour was observed for PE 3C. Not only its biodegradation rate slows down dramatically after 40 days, the quantity of cumulative CO_2 also starts to decrease (Figure 5-8). This observation may be explained using the theory suggested by Ogasawara *et al*. (2006). They mentioned that the permeability of polymer matrix and silicate layer is different in nanocomposite structure. In addition, pure polymer itself consists of crystalline-amorphous phases which have different characteristics in terms of permeability. They suggested that the coexistence of different phases in nanocomposites causes complex transport phenomena.

In spite of these explanations, it is to be noted here that the prediction of biodegradation rate behaviour of polymer nanocomposites after only 45 days in impossible. Forty five days does not seem to be a sufficient time to study the biodegradability of polyethylene nanocomposites. Moreover, the biodegradation mechanism of polyethylene nanocomposite is complex as it goes through different phases depending on the effect of clay concentration.

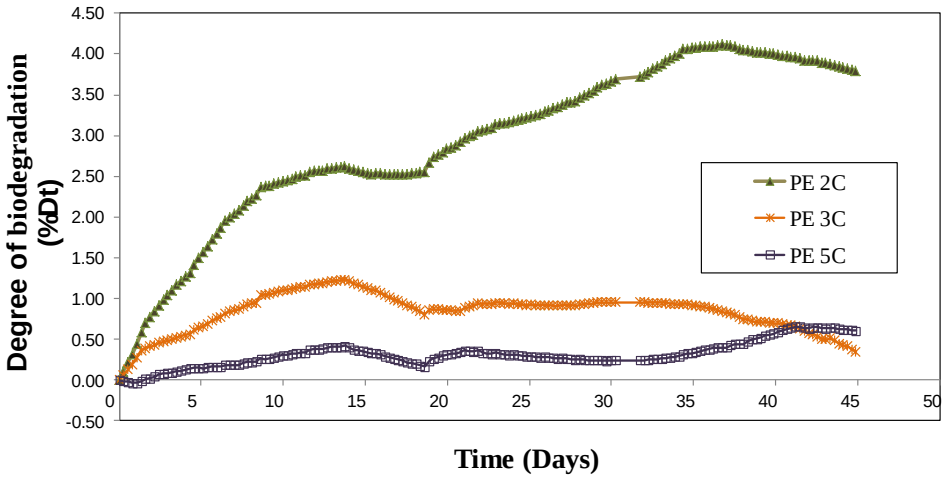

Figure 5-6 Biodegradation rate of polyethylene nanocomposites in 45 days of incubation

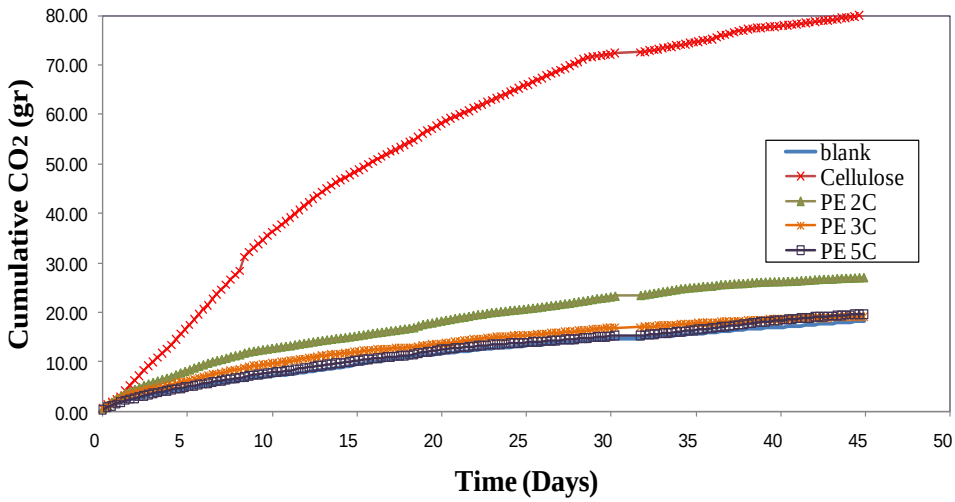

Figure 5-7 Cumulative CO_2 evolved from polyethylene nanocomposite during incubation period

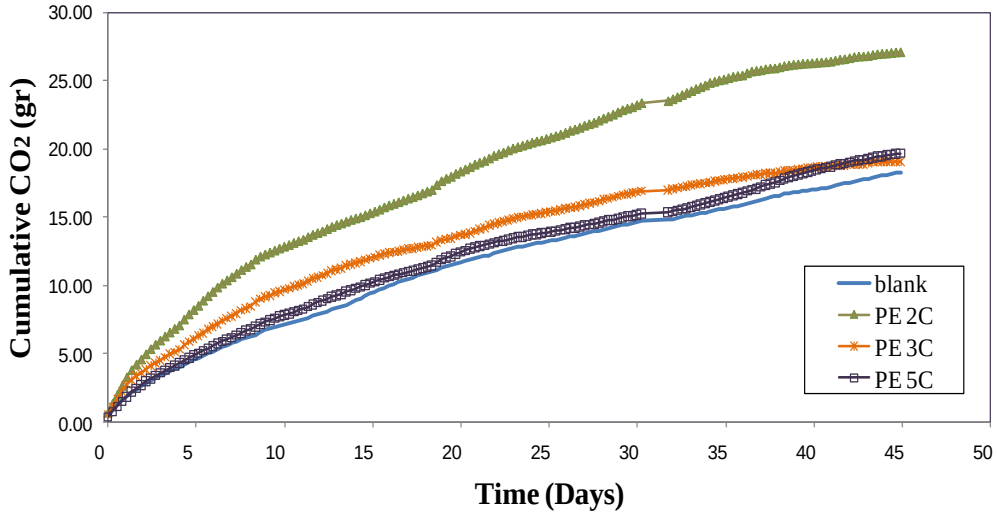

Figure 5-8 Cumulative CO_2 evolved from polyethylene nanocomposite during incubation period

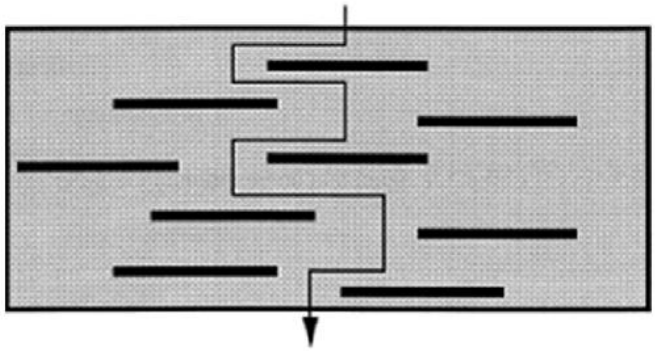

Figure 5-9 Proposed model for the torturous zigzag diffusion path in an exfoliated polymer–clay nanocomposite (Yano *et al*. 1993)

5.2.3.2 Fourier Transform Infrared Spectroscopy (FTIR) analysis after composting

PE nanocomposites films were subjected to Fourier Transform Infrared Spectroscopy after 45 days of incubation in compost. The changes in FTIR spectra due to the difference in clay loadings in nanocomposites are apparent in Figures 5-10 and 5-11. It is clear that the peak corresponding to the methylene band (1470 cm^{-1}) increases for all nanocomposites after composting. The appearance of two peaks between 1000 and 1120 cm^{-1} can be assigned to the Si-O stretching bands due to presence of silicate in MMT (Farmer & Russell 1964). It is evident that the intensity of band increases with increasing clay concentration in nanocomposites. Figures 5-17 shows a better comparison of FTIR spectra for nanocomposites before and after composting. It can be observed that, after composting, the intensity of absorbance at around 1540-1670 cm^{-1} increases which can be attributed to the formation of N-H (1-amide) II and N-H (2-amide) II, which is a carbonyl group (R-C=O) linked to a nitrogen atom (N). Also, an increase in absorbance can be seen in hydroxyl group region (3200-3600 cm^{-1}). In this region, the absorbance increases with clay loading in nanocomposites (i.e. from PE 2C to PE 5C).

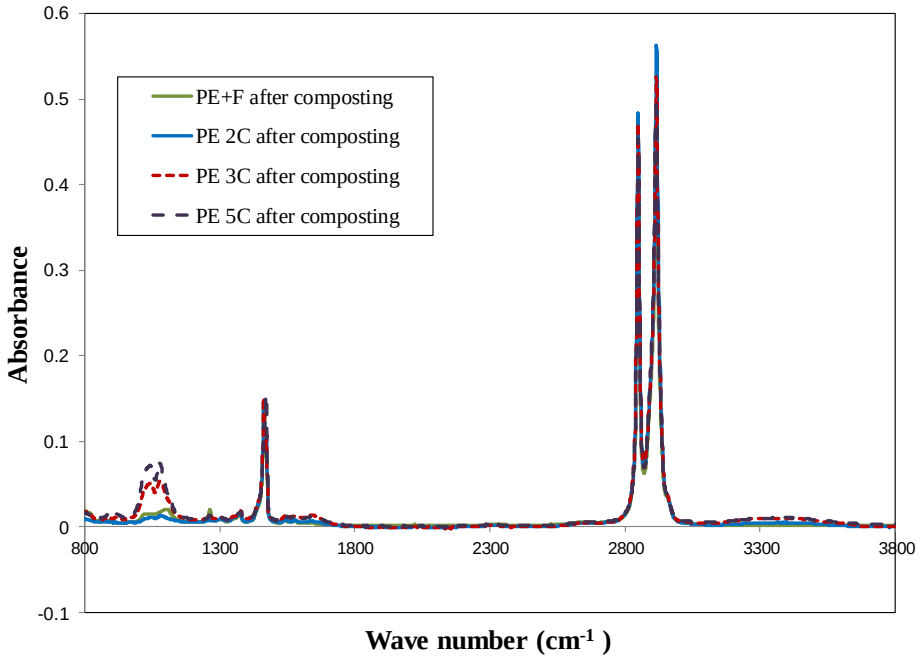

Figure 5-10 FTIR spectra of PE nanocomposite after 45 days of composting

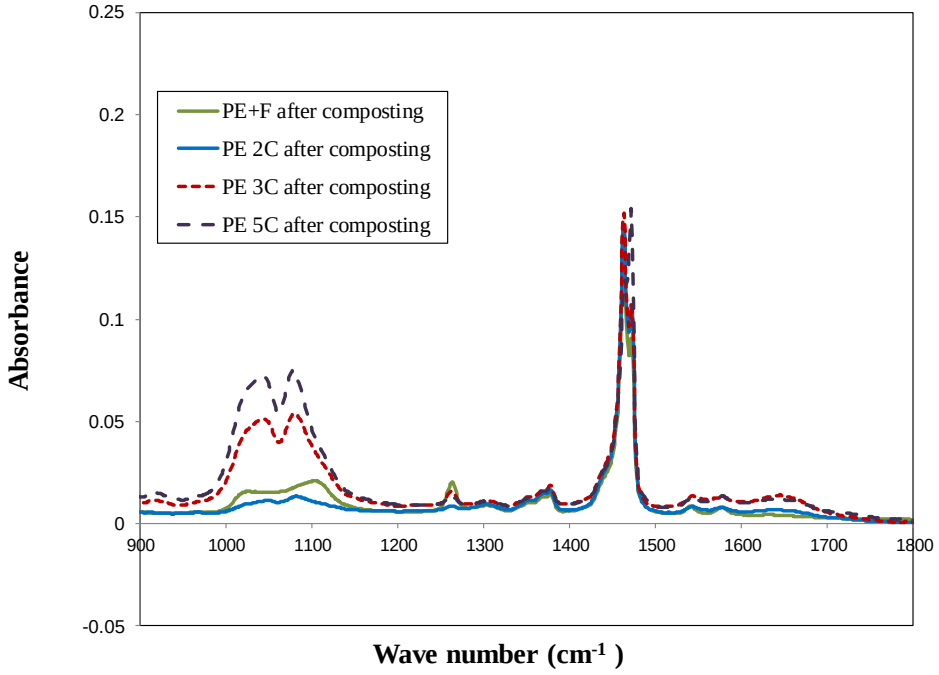

Figure 5-11 FTIR spectra of PE nanocomposite after 45 days of composting

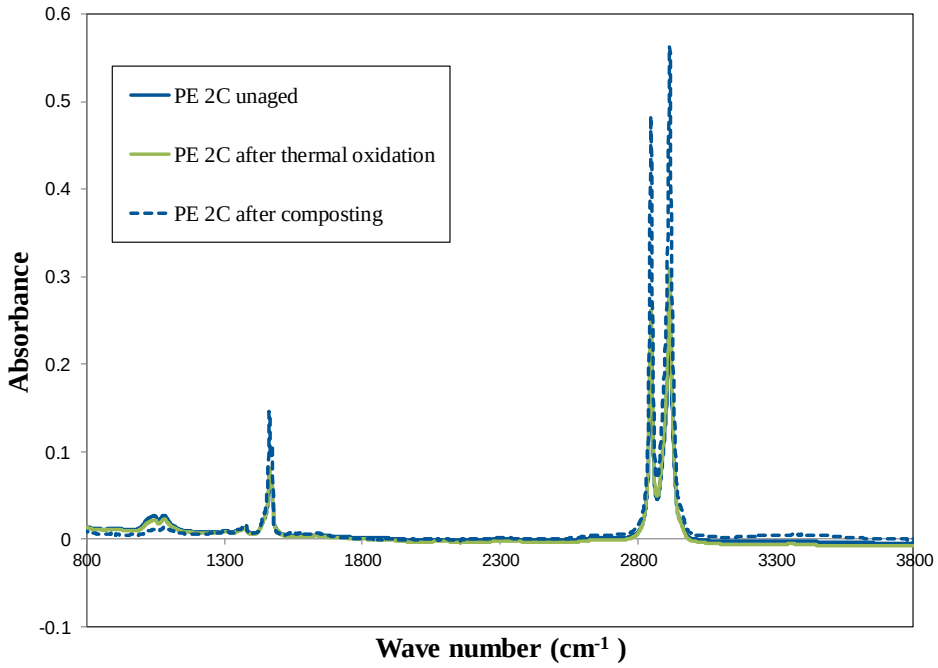

Figure 5-12 FTIR spectra of PE 2C after 45 days of composting

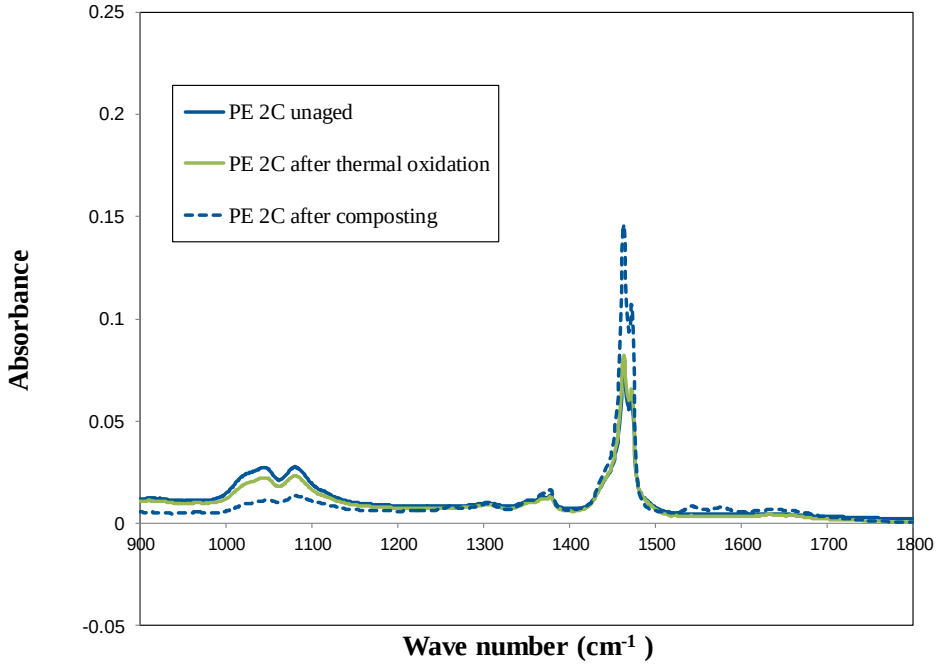

Figure 5-13 FTIR spectra of PE 2C after 45 days of composting

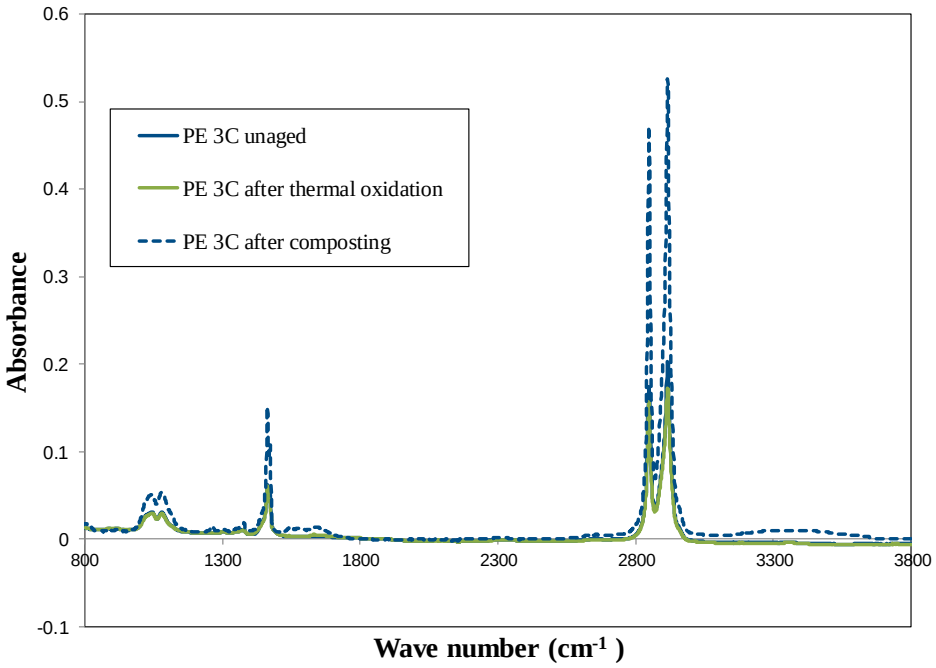

Figure 5-14 FTIR spectra of PE 3C after 45 days of composting

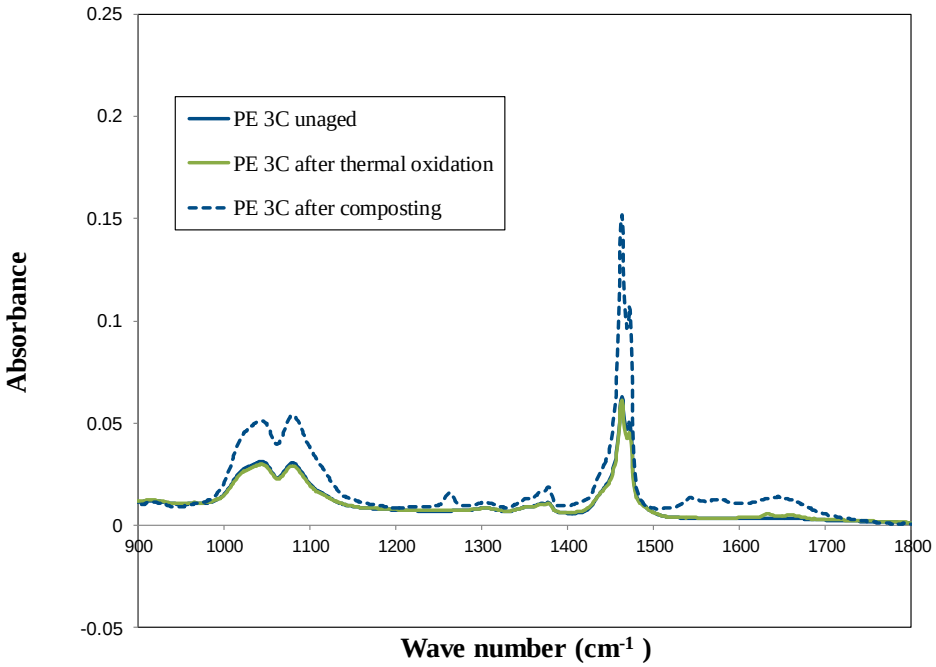

Figure 5-15 FTIR spectra of PE 3C after 45 days of composting

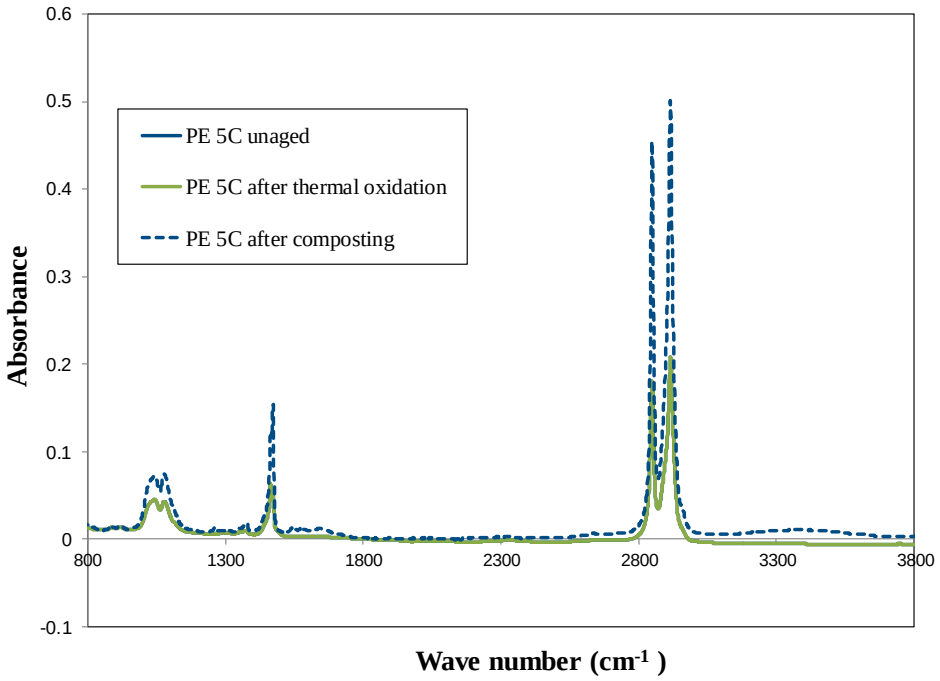

Figure 5-16 FTIR spectra of PE 5C after 45 days of composting

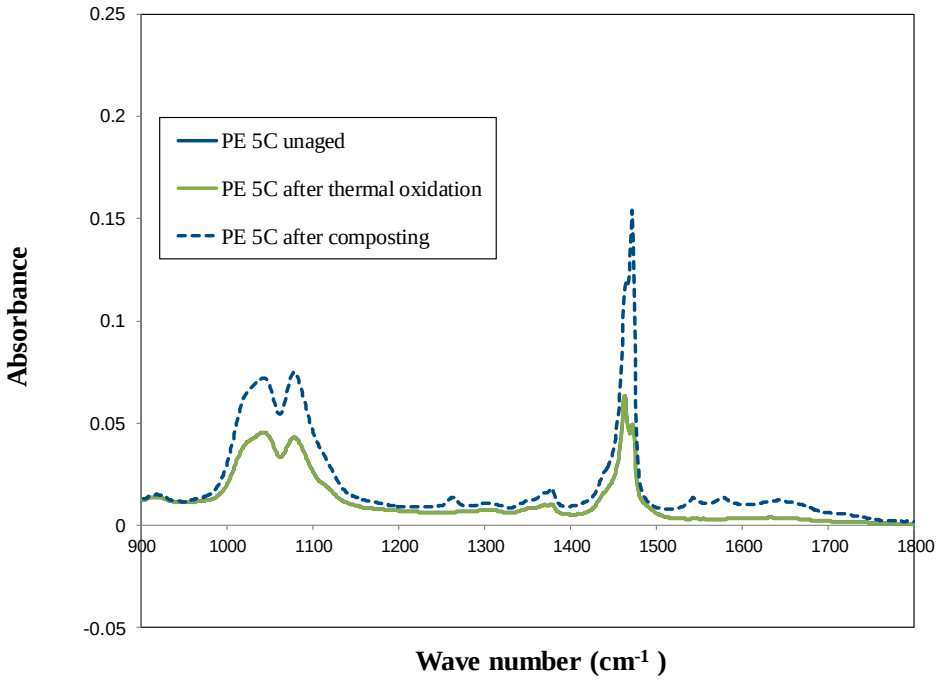

Figure 5-17 FTIR spectra of PE 5C after 45 days of composting

Changes in carbonyl index values after thermal degradation and composting are shown in Figure 5-18 for nanocomposites used in this study. By looking at the carbonyl index values in Y axis, it is clear that these values are relatively very small indicating that the level of carbonyl group formation in polyethylene nanocomposites is not high. However, an increasing trend can be observed in carbonyl index values of composted samples with the increase in clay loading. These results indicate that the presence of clay helps in breaking down the nanocomposite in biodegradation stage but to a smaller extent. Similar results will be discussed in detail in Chapter 6 to illustrate the effect of pro-oxidant on the biodegradation of OPE nanocomposite samples.

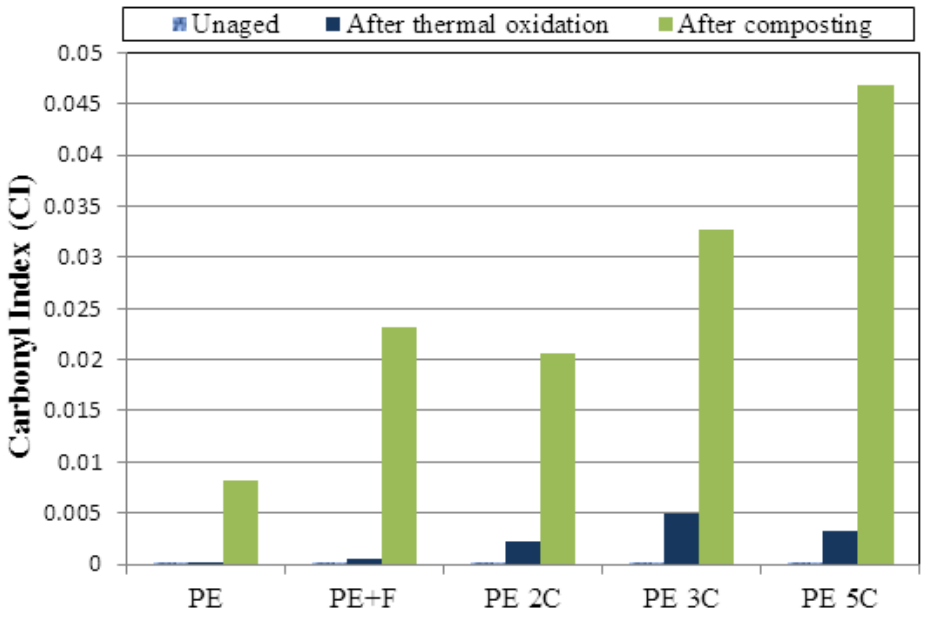

Figure 5-18 Changes of carbonyl index in two stages of oxo-biodegradation of PE nanocomposites

The above mentioned results from biodegradation rate, FTIR spectra and carbonyl index values suggest that the presence of clay helps to degrade nanocomposites in composting process. The carbonyl index and FTIR spectra results show that the number of functional

group increases (even in very small quantity) by increasing the clay loading during composting. On the other hand, the amount of CO_2 evolved decreases with increase in clay concentration. This implies that the rate of conversion of degradation products to CO_2 and H_2O (ultimate biodegradation products) is higher in nanocomposites with lower clay concentration because more functional groups can be observed in FTIR spectra for these samples. This can be attributed again to the barrier effect of clay which limits the diffusion of oxygen within nanocomposites and also slows down the escape of CO_2 produced in nanocomposites with higher clay loadings.

5.2.3.3 Biofilm

The presence of biofilm can be seen clearly in ESEM micrographs shown in Figures 5-19 to 5-21. The clear images of different type of bacteria and fungi can be seen on the surface of nanocomposite samples. It is also clear that more colonies of bacteria and fungi are formed during the composting period on nanocomposites with higher concentration of clay. This can be used as a qualitative measure to show that nanocomposite surface seems to be a suitable environment in terms of humidity, pH and nutrition for microbial growth and activity. Since clay is a natural hydrophilic mineral, it absorbs more water, and consequently attracts more microorganisms to the nanocomposite surface. Therefore it is clear from the micrograph images that the biodegradation, which is an assimilation of degradation products by microorganisms and conversion of them into CO_2 and H_2O, takes place in nanocomposite samples.

On the other hand, as explained in chapter 4, the presence of microorganisms in compost can also help in the degradation process. It has been shown by Yamada-Onodera *et al*. (2001) that polyethylene with high molecular weight can be degraded to lower molecular

weight fragments by hyphae of the fungus. The presence of hyphae, which look like a string, is evident in Figures 5-19 (a and b), 5-20 (b) and 5-21(b).

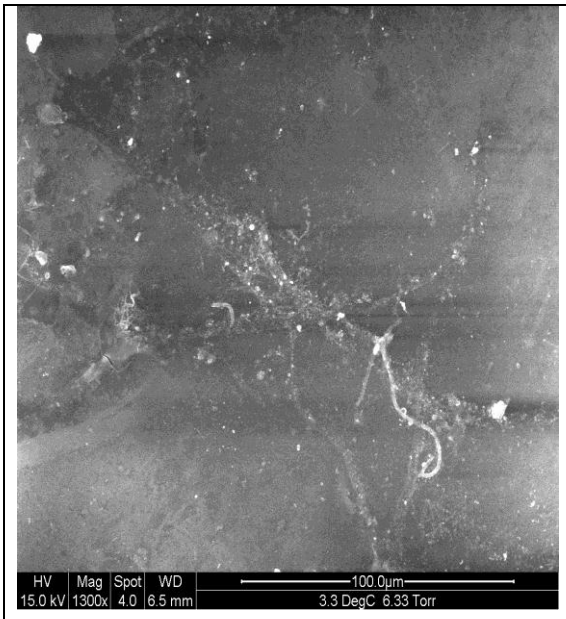

a

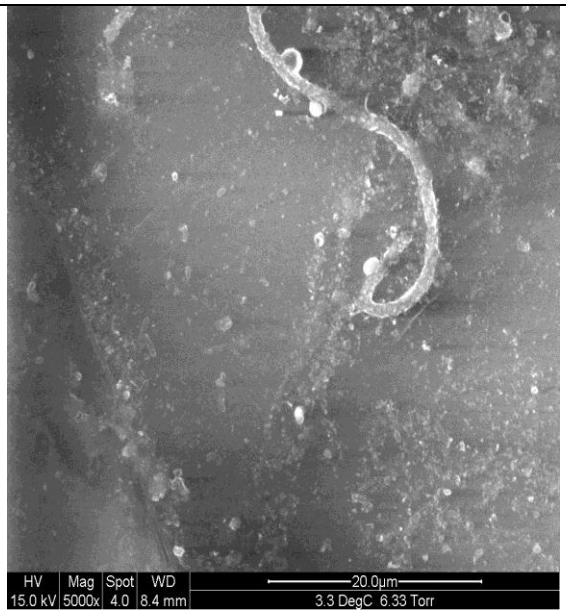

b

Figure 5-19 ESEM micrographs of biofilm on PE 2C surface after composting

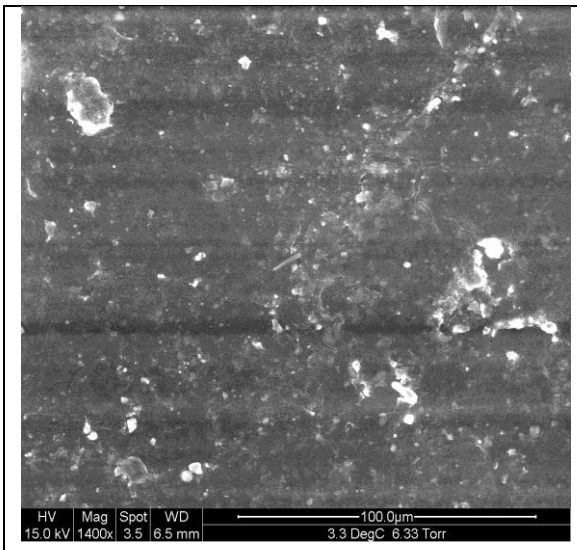

a

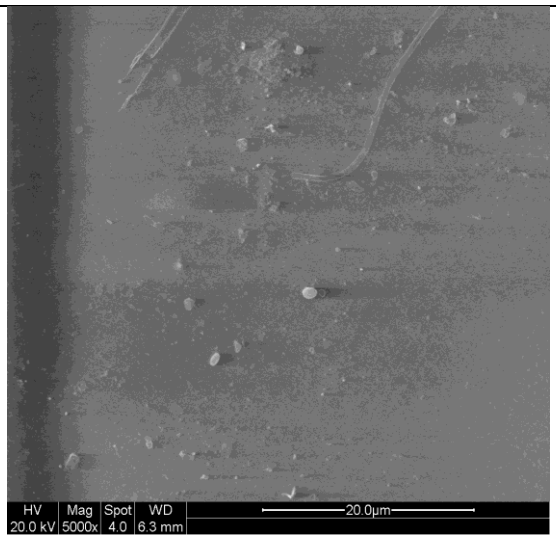

b

Figure 5-20 ESEM micrographs of biofilm on PE 3C surface after composting

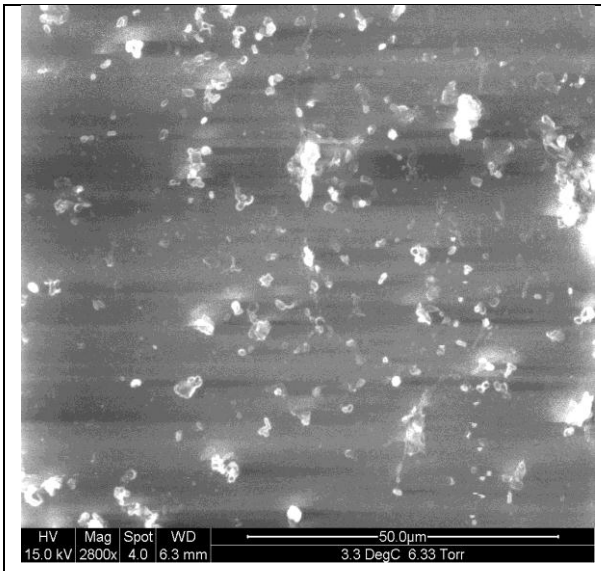

a

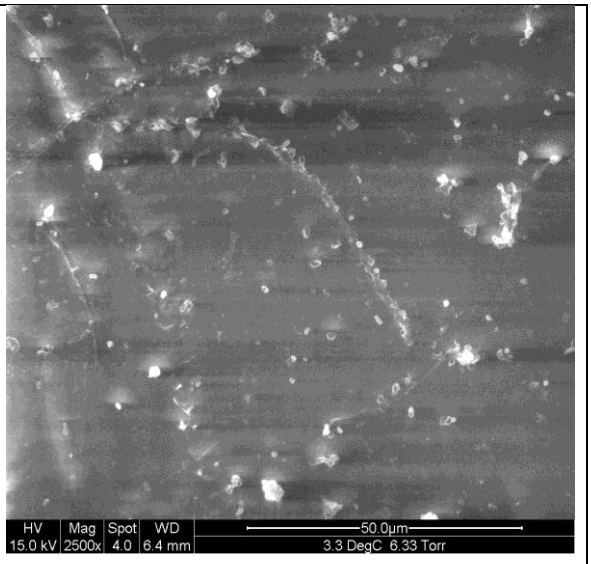

b

Figure 5-21 ESEM micrographs of biofilm on PE 5C surface after composting

5.3 Conclusion

Polyethylene nanocomposite samples with 2, 3 and 5% clay were tested by exposing them to heat for 14 days and then incubating them in compost for 45 days for biodegradation. The first conclusion is that 45 days is a relatively short period to study the biodegradation of poorly biodegradable polymer like polyethylene. The addition of clay led the biodegradation mechanism to become more complex and to have different phases. It can be concluded that, by increasing the incubation time, nanocomposite might go through another phases of biodegradation and show different behaviour. However, in general, it can be concluded that the presence of clay, enhances the biodegradability of polyethylene nanocomposite during composting. Clay also can help the microorganisms in breaking down the macromolecules into smaller fragments as it can be seen from FTIR and carbonyl index results. On the other hand, because of its hydrophilic nature, clay can attract more microorganisms to its surface. However, this influence decreases when clay loading in nanocomposite increases due to the barrier and insulator effects of clay in the nanocomposite structure.

6 Oxo-biodegradable polyethylene nanocomposite

6.1 Introduction

From Chapter 4, it was clear that the presence of pro-oxidant plays a vital role in biodegradation process, both in abiotic and biotic stages. Also it has been discussed in Chapter 5 that clay helps in the biodegradation process. It was also concluded that clay might also help in thermal oxidation over a longer period of time depending on its specific mineral structure and nature. In this chapter, the combined effect of pro-oxidant and clay on biodegradation of polyethylene will be discussed so as to develop a deeper understanding on the factors that are effective in polyethylene biodegradation mechanism. In this study, oxo-biodegradable polyethylene nanocomposites were prepared by blending clay (Cloisite® 15A), manganese stearate, and polyethylene with the aid of Fusabond as compatibiliser. Compositions of various nanocomposites used in this work are shown in Table 6-1. The procedure of preparing oxo-biodegradable nanocomposites was explained in Chapter 3. In this chapter, the results of thermal degradation and composting of oxo-biodegradable nanocomposites will be discussed.

Table 6-1 Compositions of oxo-biodegradable polyethylene nanocomposites

Sample name	PE (wt%)	PE-g-MA (wt%)	MMT (wt%)	Pro-oxidant (wt%)
LDPE (PE+F)	92	8	-	-
LDPE + Pro oxidant (OPE)	91	8	-	1
LDPE + 2% Clay + Pro oxidant (OPE 2C)	89	8	2	1
LDPE + 3% Clay + Pro oxidant (OPE 3C)	84	12	3	1
LDPE + 5% Clay + Pro oxidant (OPE 5C)	74	20	5	1

6.2 Result and discussions

6.2.1 Morphology of polyethylene nanocomposites

WAX patterns of OPE nanocomposites with 2, 3 and 5 wt% of clay (Cloisite® 15A) are shown in Figure 6-1. In general, it is clear from XRD patterns, those nanocomposites with pro-oxidant have a better miscibility with clay and polyethylene compared to nanocomposites without pro-oxidant. As can be seen from Figure 6-1, the characteristic peak of Cloisite® 15A at 2.78° has completely disappeared in the case of OPE 2C suggesting that polyethylene and clay particles exist in a nearly exfoliated structure. Disappearance of characteristic peak of clay in OPE 2C and the presence of a small shoulder in the XRD curves of OPE 3C and OPE 5C indicate that polyethylene chains have

successfully entered between clay platelets thereby forming well-intercalated structures. So, oxo-biodegradable nanocomposites is expected to possess different degradation behaviour compared to PE and PE nanocomposites. It has been shown by many researchers that increasing the clay loading changes the structure and morphology of nanocomposites and limits the extent of exfoliation (Gopakumar *et al*. 2002, Reddy *et al.* 2008, Kumanayaka *et al*. 2010). This change can be attributed to the reduction in the affinity between polymer matrix and clay particles.

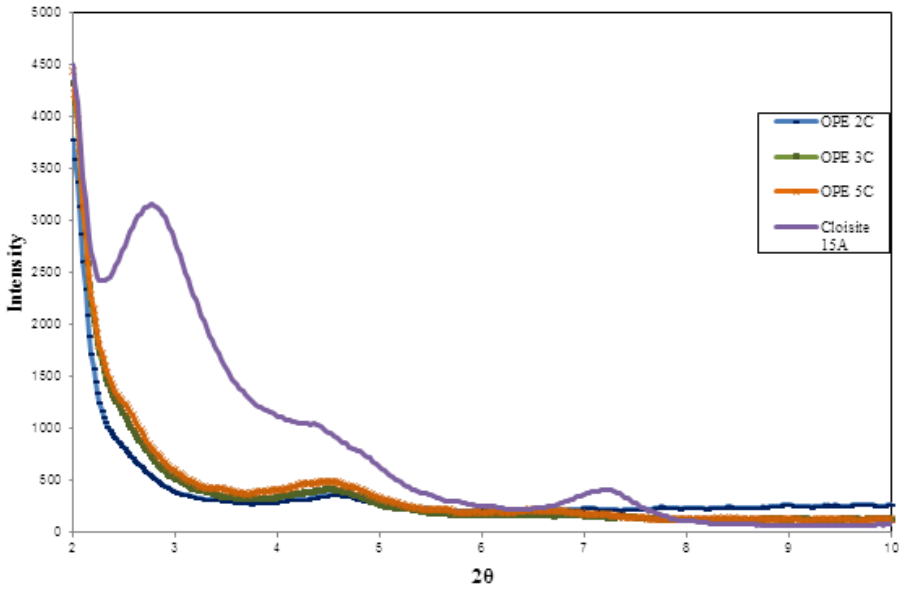

Figure 6-1 WAX patterns of OPE nanocomposites

6.2.2 Abiotic stage

6.2.2.1 Thermogravimetric Analysis (TGA)

TGA traces of oxo-biodegradable nanocomposites are depicted in Figure 6-2 and the corresponding data are presented in Table 6-2. It can be seen that, by adding clay to OPE structure, the onset temperature has shifted slightly towards higher temperatures indicating

that OPE nanocomposites have higher thermal stability than OPE. However, OPE with 5% clay exhibits lower thermal stability at higher temperatures. In general, all oxo-biodegradable polyethylene nanocomposites show similar behaviour. They decompose at relatively lower temperatures compared to polyethylene nanocomposites (discussed in Chapter 5). The onset temperature for OPE nanocomposite is significantly higher than that of PE and slightly higher than that of OPE. These results suggest that the presence of clay up to certain concentration enhances the thermal stability of OPE nanocomposites. The changes in the thermal stability of OPE 5C at higher temperatures are similar to those of PE 3C and 5C discussed in Chapter 5. It can be attributed to the alignment of clay platelets in intercalated structure which allows the storage of heat between the clay layers thereby leading to superheating of polymer and faster degradation. Details of this mechanism have been explained in Chapter 5.

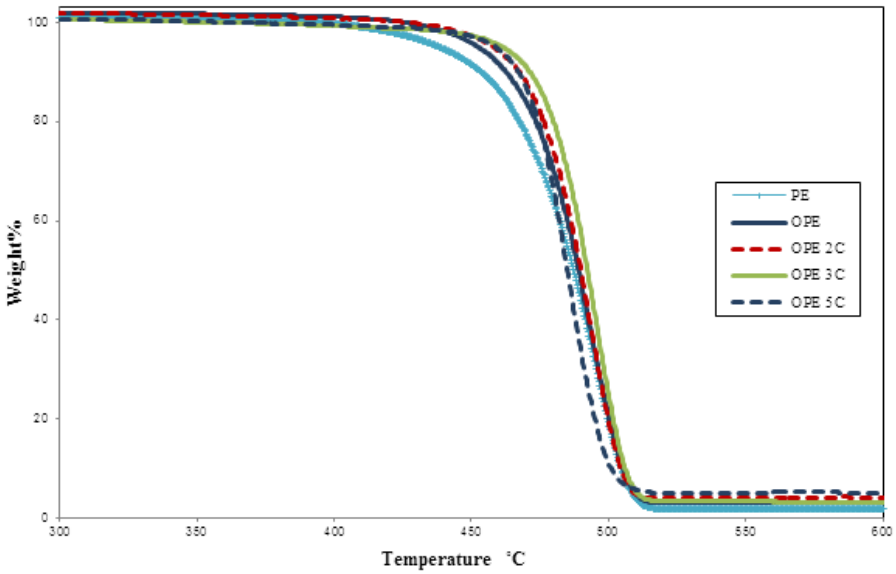

Figure 6-2 TGA curves of PE, OPE and OPE nanocomposites in nitrogen

Table 6-2 TGA data, in nitrogen, for polyethylene, PE+F, OPE and OPE nanocomposites

PE, wt%	Fusabond, wt%	Clay, wt%	Pro-oxidant, wt%	$T_{0.1}$, ˚C	$T_{0.5}$, ˚C
100	.	.	.	453.8	487.3
92	8	.	.	467.5	494.4
91	8	.	1	462.8	489.1
89	8	2	1	467.5	489.7
84	12	3	1	471.5	492.3
74	20	5	1	467.2	485.3

6.2.2.2 Fourier Transform Infrared Spectroscopy (FTIR) analysis of thermally oxidised OPE nanocomposites

FTIR spectra of oxo-biodegradable nanocomposite subjected to 14 days of thermal degradation in an oven at 70°C are shown in Figures 6-3 and 6-4. The spectra show similar patterns of changes of absorption for OPE and OPE nanocomposites. Qin *et al.* (2003) stated that the degradation mechanism in nanocomposites will be different if the shape and position of peaks in FTIR spectra for them are different compared to the blends without clay. They also stated that the degradation mechanism will be similar if the shape and position of peaks in FTIR spectra are similar. From the above discussion, it can be stated that mechanism of thermal oxidation in OPE and OPE nanocomposites is similar. Moreover, from Figures 6-3 and 6-4, it is clear that the extent of thermal degradation for OPE and OPE 2C after 14 days of exposure time is similar. However, the extent of thermal

degradation in nanocomposites with higher concentration of clay is found to be relatively lower. This result can be attributed to the barrier effect of clay explained in Chapters 4 and 5. All the above results, therefore, suggest that the presence of clay does not change the degradation mechanism in OPE nanocomposites but leads to limited thermal oxidation under higher clay loading. In addition to its barrier effect, clay influences the thermal degradation also by decreasing the number of radicals that are actively involved in initiation and propagation phases (Solomon 1968). Solomon attributed this finding to the presence of aluminium ions located at the crystal edge of silicate structure which act like Lewis acidic sites in clay minerals. Solomon proposed two possible mechanisms in which free radicals engage in thermal degradation (Figure 6-5). The first possible mechanism happens when electron is transferred from radical to Lewis acidic sites leading to the formation of carbonium ions. The second mechanism occurs when initiating or propagating free radicals are absorbed by weak Lewis acid sites in clay and then recombined. In either mechanism, less number of free radicals would be available for initiation or propagation reactions.

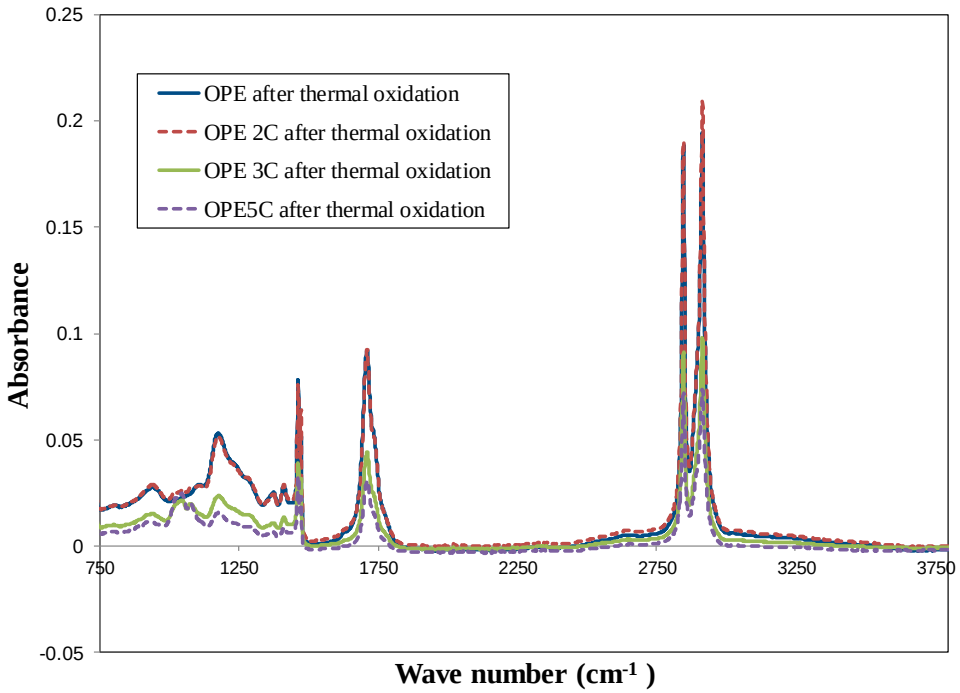

Figure 6-3 FTIR spectra of OPE nanocomposite after thermal degradation for 14 days

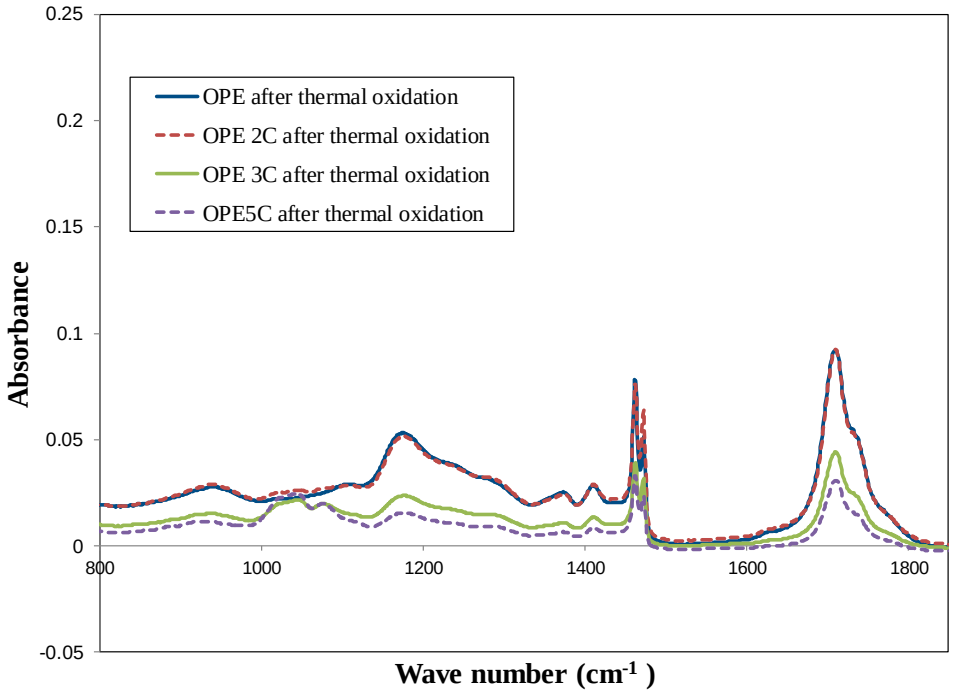

Figure 6-4 FTIR spectra of OPE nanocomposite after thermal degradation for 14 days

Because FTIR spectra of thermally degraded OPE and OPE 2C have an interesting behaviour and are very similar, it has been decided to monitor thermal degradation of OPE nanocomposites as a function of time and record the differences in spectra. Results for this test are shown in Figures 6-6 to 6-10.

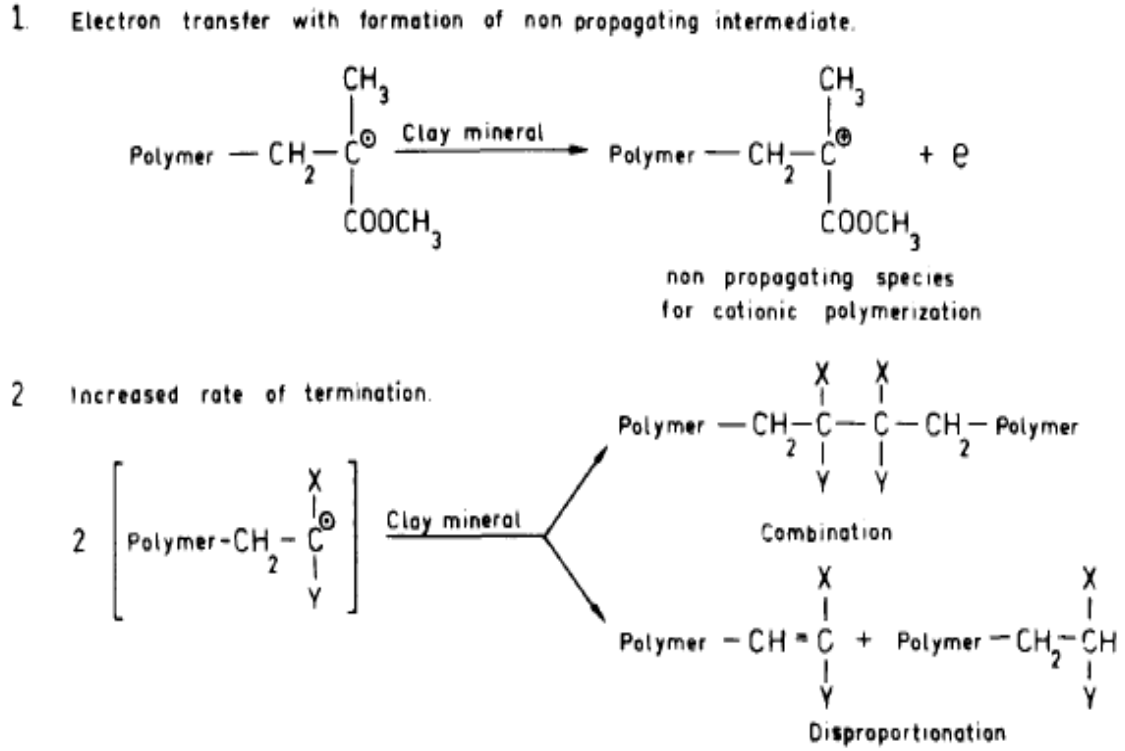

Figure 6-5 Possible mechanisms for free radical reactions by clay minerals

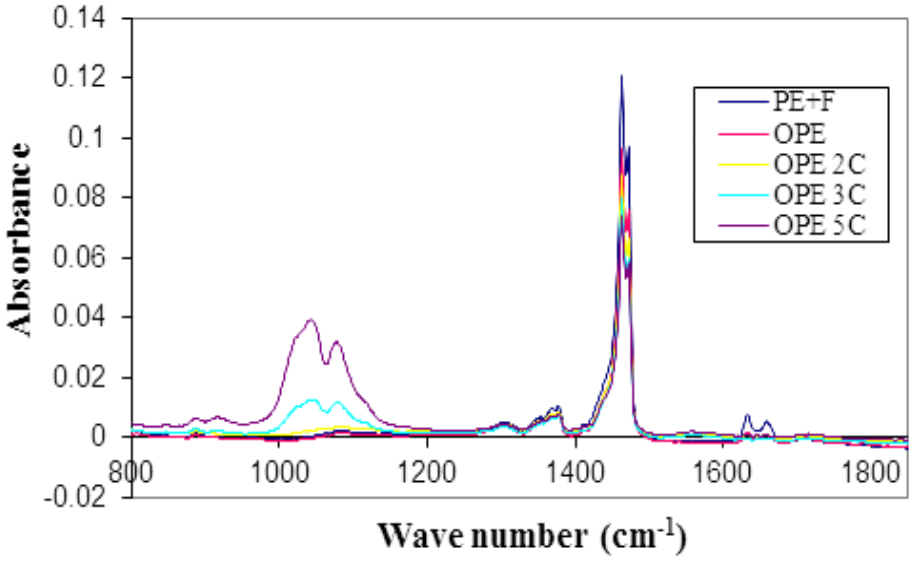

Figure 6-6 FTIR spectra of unaged samples

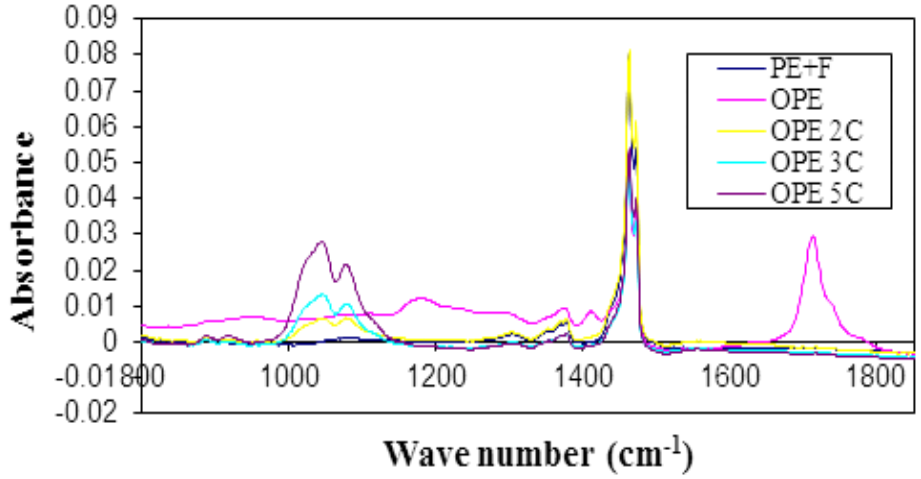

Figure 6-7 FTIR spectra of samples after 3 days in oven at 70°C

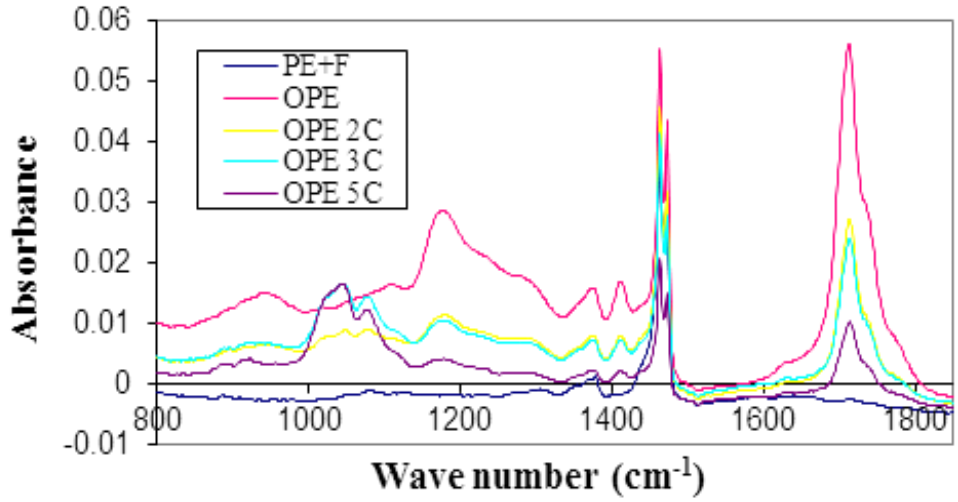

Figure 6-8 FTIR spectra of samples after 6 days in oven at 70°C

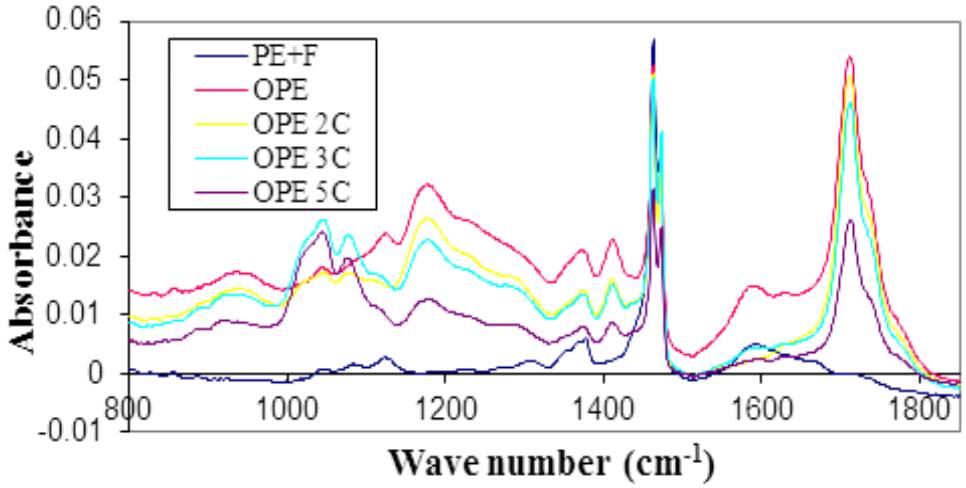

Figure 6-9 FTIR spectra of samples after 9 days in oven at 70°C

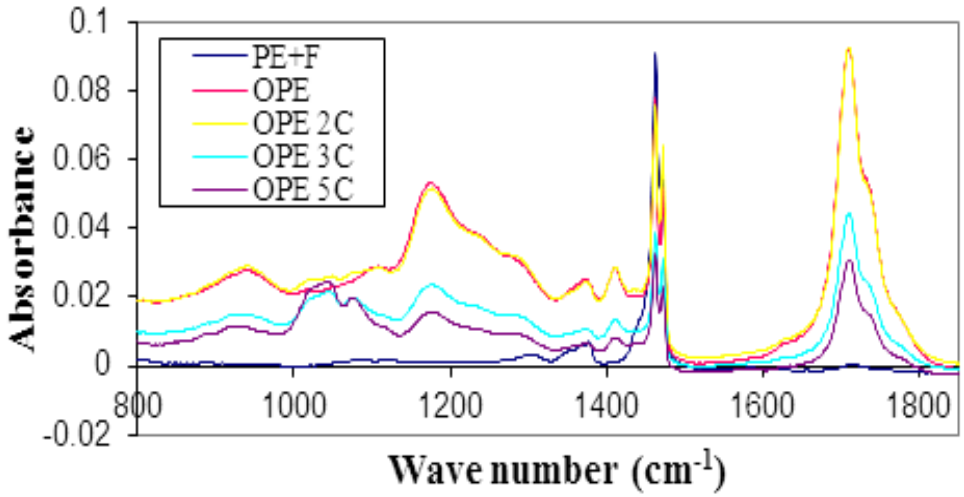

Figure 6-10 FTIR spectra of samples after 14 days in oven at 70°C

It is clear from Figures 6-6 to 6-10 that thermal oxidation in OPE and OPE nanocomposites follow a particular trend. Thermal oxidation in OPE starts relatively immediately after exposure to heat. The formation of carbonyl groups (1690-1870 cm^{-1}) after 3 days of heat exposure is evident in Figure 6-7. In addition, two weak peaks form around 1350-1470 cm^{-1} indicating the bending vibrations of alkanes. The appearance of band around 995-1350 cm^{-1} indicates the stretching vibrations of alcohols and phenols (1000-1300 cm^{-1}) and/or carboxylic acids and its derivatives (970-1250 cm^{-1}). From Figure 6-8, which represents the spectra after 6 days, it can be seen that all OPE nanocomposites start to degrade. However, the rate of degradation decreases with an increase in clay loading. This is probably because the diffusion path for oxygen within nanocomposites is becoming increasingly tortuous with increase in clay concentration, which subsequently leads to reduced rate of oxidation. Further studies with higher concentrations of clay are required to understand the mechanism behind the lower thermal oxidation rates at higher clay contents. It is also clear that the intensity of absorbance for peaks in OPE is higher. From day 9 to the end of thermal degradation period, the rate of degradation is slower in

OPE but remarkably higher for OPE nanocomposites, especially for OPE 2C (Figures 6-9 and 6-10). It can be seen that the extent of degradation for OPE and OPE 2C is very similar at the end of 14 days. The gradual increase in the degradation rate is possibly due to the presence of alkyl ammonium salts in clay structure as well as capacity to store heat by clay between its layers. The effect of alkyl ammonium on degradation will be explained later in biotic degradation section.

The rate of oxidation can also be monitored by measuring the amount of carbonyl groups accumulated and using carbonyl index (CI) values. Figure 6-11 shows the changes in CI values for PE+F, OPE and OPE nanocomposites as a function of thermal degradation time. The very small increase in CI value for PE+F after 14 days of oxidation indicates that the effect of thermal oxidation on PE+F is insignificant. In contrast, the CI value for OPE increases dramatically during the oxidation period indicating that the pro-oxidant accelerates the polymer degradation process rapidly in this case. The CI values for nanocomposite samples (OPE 2C, 3C & 5C) also increase with oxidation time and their trends are similar to that for OPE. It should be noted that, as was expected, the CI values for nanocomposites decrease with increase in clay content.

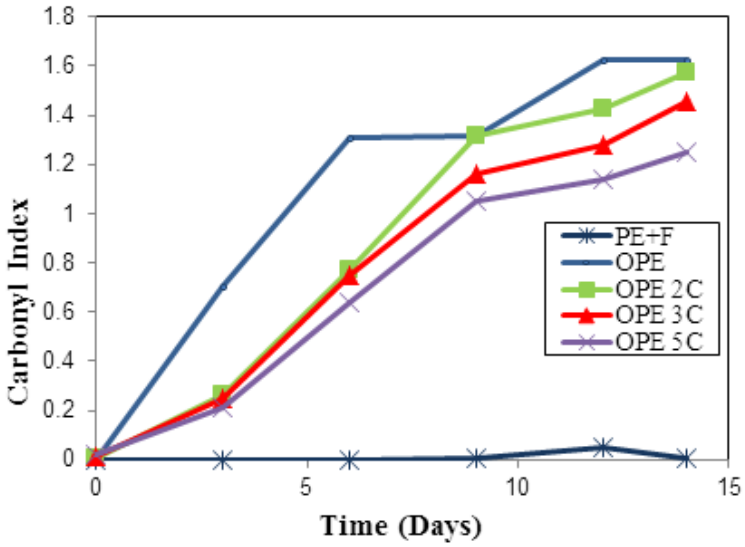

Figure 6-11 Changes of carbonyl index (CI) of PE+F, OPE and OPE nanocomposites exposed to heat for 14 days at 70°C

6.2.3 Biotic stage

6.2.3.1 Biodegradation analysis

Results representing biodegradation behaviour of oxo-biodegradable nanocomposites in composting system are shown in Figures 6-12 to 6-14.

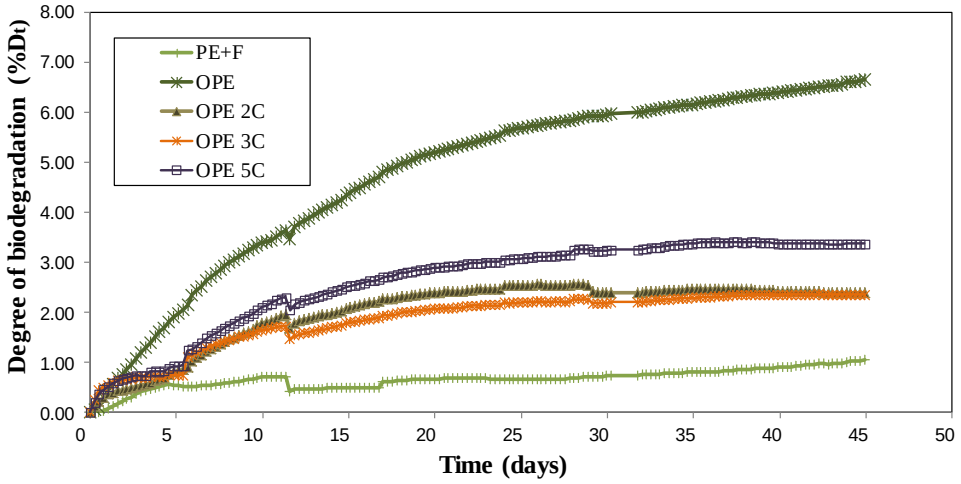

Figure 6-12 Degree of biodegradation for OPE nanocomposites in 45 days of incubation in composting system

From Figure 6-12, it is evident that the degree of biodegradation is remarkably higher in OPE compared to OPE nanocomposites. This result shows the undoubtable effect of manganese stearate in improving the biodegradation process. In OPE nanocomposites, however, biodegradation rate increases with an increase in clay loadings unlike the thermal degradation. For example, the degree of biodegradation in OPE 5C is significantly higher than that of OPE 2C and 3C at the end of incubation time. The other notable difference in the biodegradation behaviour of OPE and OPE nanocomposites is in the slope of the biodegradation curve. Biodegradation curves of all samples, except that of PE+F, have a relatively sharp upward trend in the beginning. However, the degradation rate slows down gradually after about 12 days. The rate of biodegradation of OPE nanocomposites can be considered to be constant towards the end of incubation time. On the other hand, the biodegradation rate of OPE has an upward trend during the whole of 45 days of incubation time although its degradation rate declines like those for other samples used in this work. This observation, therefore, confirms that the biodegradation rate in OPE increases with

time. PE+F exhibits a rather slow degradation rate during the composting period. After 45 days of incubation, its rate of degradation could only reach to 1%.

It is also clear from Figures 6-13 and 6-14 that the amount of CO_2 evolved for PE+F is close to the one obtained from the blank vessel. This observation shows that polyethylene has poor degradation behaviour especially when there is no degradation additive in the structure. On the other hand, it is clear from these figures that OPE without clay has the highest cumulative CO_2 value indicating that the addition of clay leads to slower biodegradation process and therefore slower CO_2 evolution.

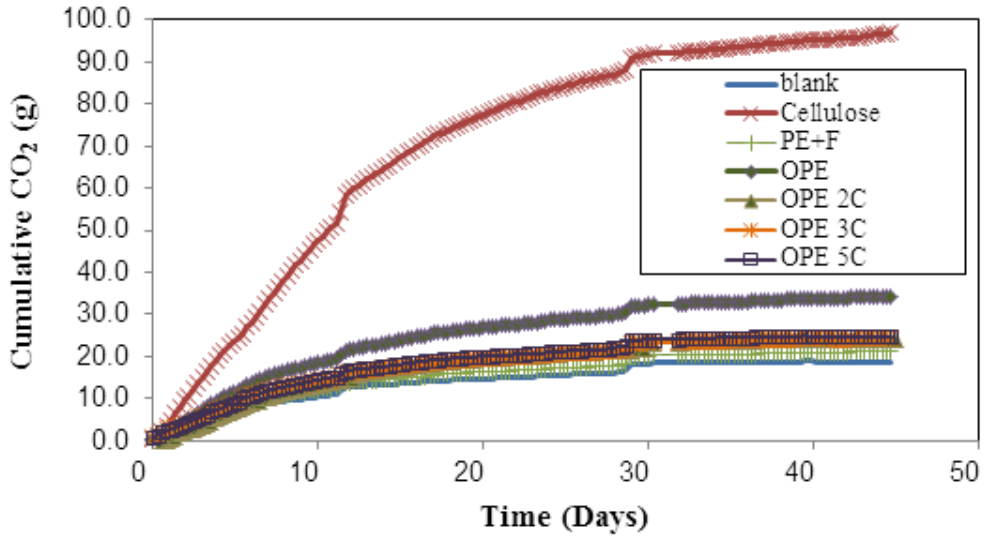

Figure 6-13 Cumulative CO_2 evolved from OPE nanocomposites and cellulose during incubation period

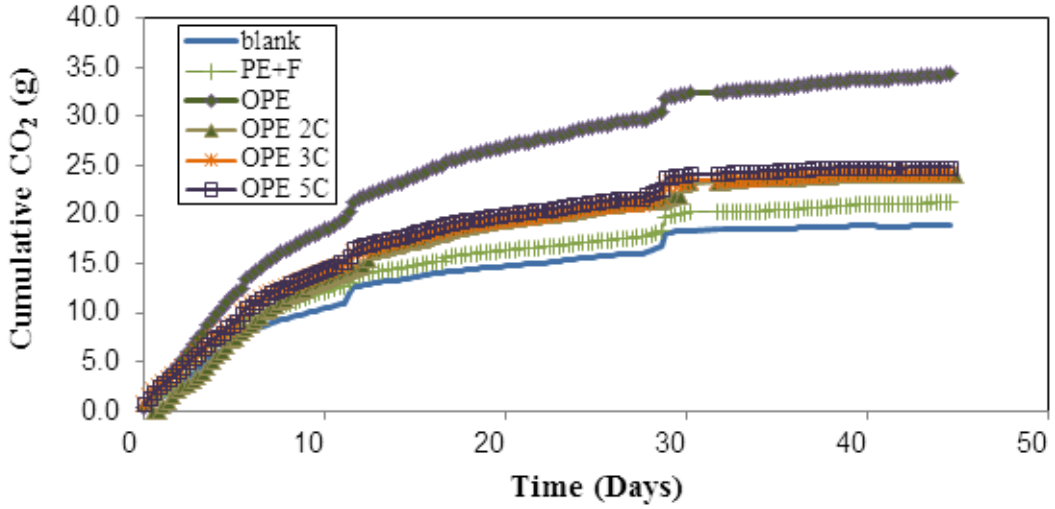

Figure 6-14 Cumulative CO_2 evolved from OPE nanocomposites during incubation period

6.2.3.2 Fourier Transform Infrared Spectroscopy (FTIR) analysis after composting

After the composting period, samples were examined by Fourier Transform Infrared Spectroscopy (FTIR) as explained before and the results are depicted in Figures 6-15 and 6-16. The first conclusion that can be drawn from FTIR results is that the degradation pathways for OPE and OPE nanocomposites are different. Qin *et al*. (2003) explained that degradation mechanisms are different when the shape and position of peaks in FTIR spectra differs. They also mentioned that different degradation mechanisms will lead to different degradation products which will consequently lead to different spectra due to different functional groups in the degradation products.

From Figures 6-15 and 6-16, it can be also seen that OPE leads to remarkably bigger and broader peak in carbonyl groups region (1690-1870 cm^{-1}) compared to OPE nanocomposites. On the other hand, OPE does not exhibit any absorption at 1500-1680

cm^{-1}, which can be assigned to the formation of N-H (1-amide) II and N-H (2-amide) II group (a carbonyl group (R-C=O) linked to a nitrogen atom (N)). Like nanocomposites discussed in Chapter 5, absorbance in hydroxyl group region (3000 - 3600 cm^{-1}) can be observed for OPE nanocomposites. Also, an increase in absorbance can be seen with an increasing clay loadings from OPE 2C to OPE 5C.

In addition to the above, it can be seen that the absorbance band at 1460 cm^{-1} is significantly higher for nanocomposites. This peak is assigned to methylene band and other olefins. On the other hand, peak at 1190 cm^{-1} disappears in the case of nanocomposites. This peak can be assigned to characteristic peaks of O-C functional groups which could be due to either stretching vibrations of alcohols and phenols (1000-1300 cm^{-1}) and/or carboxylic acids (970-1250 cm^{-1}). These changes will be discussed further below.

In order to investigate more about the biodegradation mechanisms and study how significant the pre-treatment (thermal oxidation) is for biodegradation, OPE nanocomposites were placed in composting system and their biodegradation behaviour was monitored during 45 days of incubation. FTIR spectra of the biodegraded samples are shown in Figures 6-17 and 6-18. It is clear from these figures that the only noticeable changes in spectra are in 1500-1680 cm^{-1} and 3000-3600 cm^{-1} bands. The former band is assigned to N-H (amide) II and the latter one indicates the formation of hydroxyl groups. There is no evidence of formation of any other functional groups after composting in OPE nanocomposite samples without pre-thermal degradation. These results clearly show the significant effect of pre-thermal treatment in the biodegradation process of OPE nanocomposites. It is also worth noticing that in the regions where spectra changes, stronger absorbance can be seen for OPE nanocomposites with higher clay loadings.

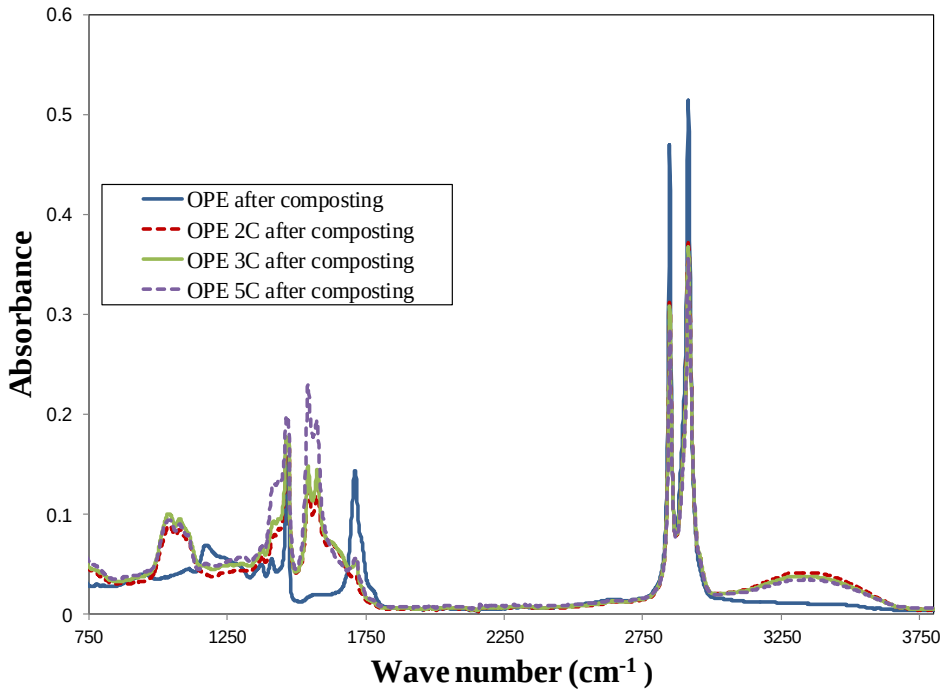

Figure 6-15 FTIR spectra of OPE and OPE nanocomposites after 45 days of composting

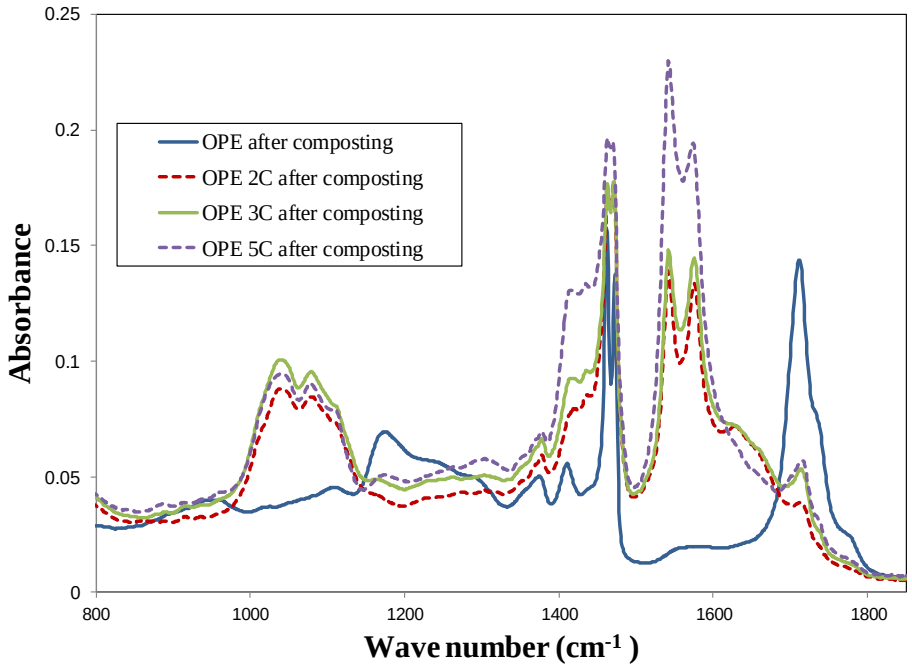

Figure 6-16 FTIR spectra of OPE and OPE nanocomposites after 45 days of composting

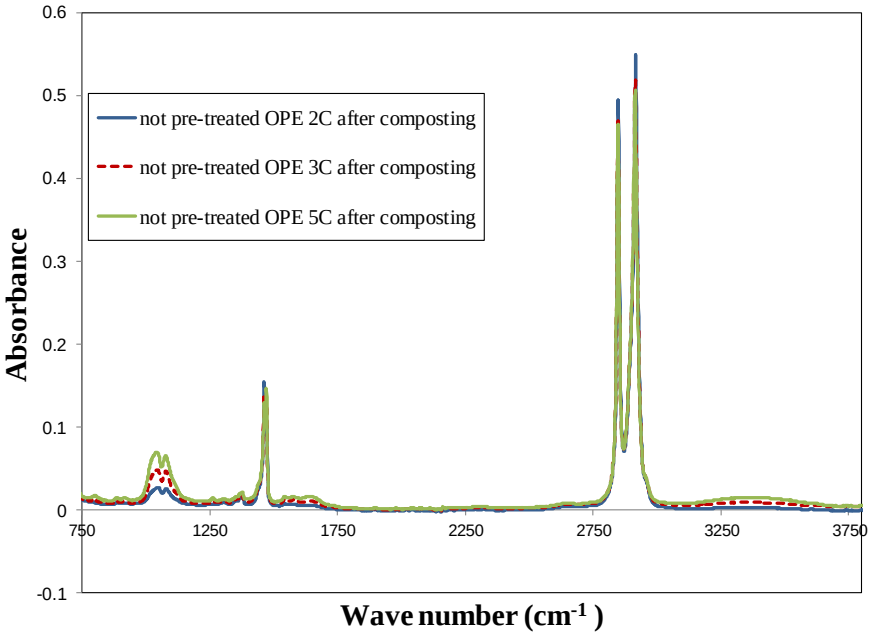

Figure 6-17 FTIR spectra of OPE nanocomposites (without pre-treatment) after 45 days of composting

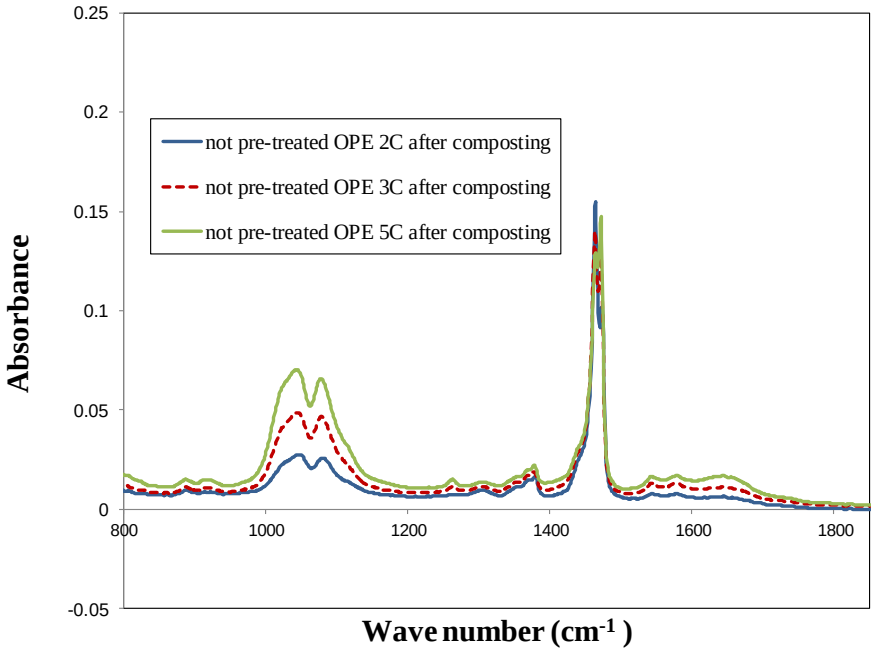

Figure 6-18 FTIR spectra of OPE nanocomposites (without pre-treatment) after 45 days of composting

The changes in FTIR spectra can be observed better when they are depicted as shown in Figures 6-19 to 6-24. These figures depict the changes experienced by the samples from the beginning to the final stage (after composting period). No significant changes can be seen in unaged OPE nanocomposites samples as well as in composted samples which were not pre-treated by heat, except for the two minor bands that was mentioned earlier. However, some changes in FTIR spectra are evident in OPE nanocomposites samples that were subjected to abiotic and biotic stages. Changes after abiotic stage have been discussed in the abiotic stage section in this chapter. Therefore, the discussion here will be on the changes experienced by the samples in the biotic stage. The appearance of the hydroxyl absorbance band (3000-3600 cm^{-1}) for all OPE nanocomposites samples after composting indicates the formation of this functional group during the composting. This result is similar to the results obtained for OPE and PE nanocomposites after composting (Chapters 4 and 5). However, the height of peaks is significantly higher for OPE nanocomposites which suggests a higher degree of degradation of these samples. On the other hand, the intensity of carbonyl group band (1690-1870 cm^{-1}) decreased remarkably for the composted samples compared to the spectra for thermally oxidised OPE 2C while it increases for OPE 3C and OPE 5C. It is also clear that the representative peaks of O-C functional group (alcohols and phenols (1000-1300 cm^{-1}) and/or carboxylic acids (970-1250 cm^{-1})) disappear for composted samples indicating complete assimilation of these products by microorganisms. So these results suggest that the presence of clay in lower concentration helps the microorganisms to utilise the products of thermal degradation while for higher clay loadings, more degradation products are observed in carbonyl region which indicates to further chain cleavage of OPE nanocomposites in composting period. In the case of OPE nanocomposites, a higher intensity absorbance peak at 1465 cm^{-1}

corresponding to methylene and olefins has been observed for composted samples regardless of their pre-treatment status. Furthermore, the formation of other products in olefin groups has been detected in OPE nanocomposites that have been pre-treated. This has been demonstrated by the strong peaks in the band 1350-1470 cm^{-1}, which can be assigned to the deformation bending vibrations of alkanes. The formation of these products was found to increase with increasing clay loadings in OPE nanocomposites. This phenomenon can be attributed to the decomposition of alkyl ammonium ions present in organically modified montmorillonite, which leads to the formation of tertiary amine, olefin, and acidic sites on the surface of nanocomposites according to the Hoffman reaction. It is also worth noting that olefin formation was found to increase with an increase in clay loading which confirms the above argument. These olefin and acidic sites, furthermore, catalyse the degradation process by enhancing the formation of free radicals. As was explained before, N-H (1-amide) II and N-H (2-amide) II (1540-1670 $cm^{-1)}$ were formed during the composting period, too.

It has been shown by Kumanayaka *et al.* (2010) that the molecular weight fraction of biodegraded nanocomposites shifted towards lower size fractions compared to polymer samples without clay. They concluded that the presence of clay allowed microorganisms to be able to perturb the whole of polymer volume while in the case of samples without clay, microorganisms could only consume the lower molecular weight products produced during abiotic stage which exist on the surface of polymer. This phenomenon can be seen clearly from the FTIR spectra of all OPE nanocomposites reported by them. It was shown that the extent of degradation is higher in OPE nanocomposites and the degradation products formed were in a much wider range compared to OPE. Kumanayaka *et al.* also concluded

that the presence of clay changes the degradation pathway by creating a different biotic environment thereby leading to a quicker degradation in nanocomposites.

The other reason for the higher intensity exhibited in FTIR peaks of all the composted samples was explained by Koutny *et al*. (2006). They stated that when the lower molecular fragments produced in the abiotic stage are degraded by microorganisms, water can diffuse easily into the whole material through the vacancies caused by consumption of smaller fragments. This would create a higher humidity level which would be suitable for the growth and activity of microorganisms. In addition, clay itself has the natural ability to absorb water because of its hydrophilic nature.

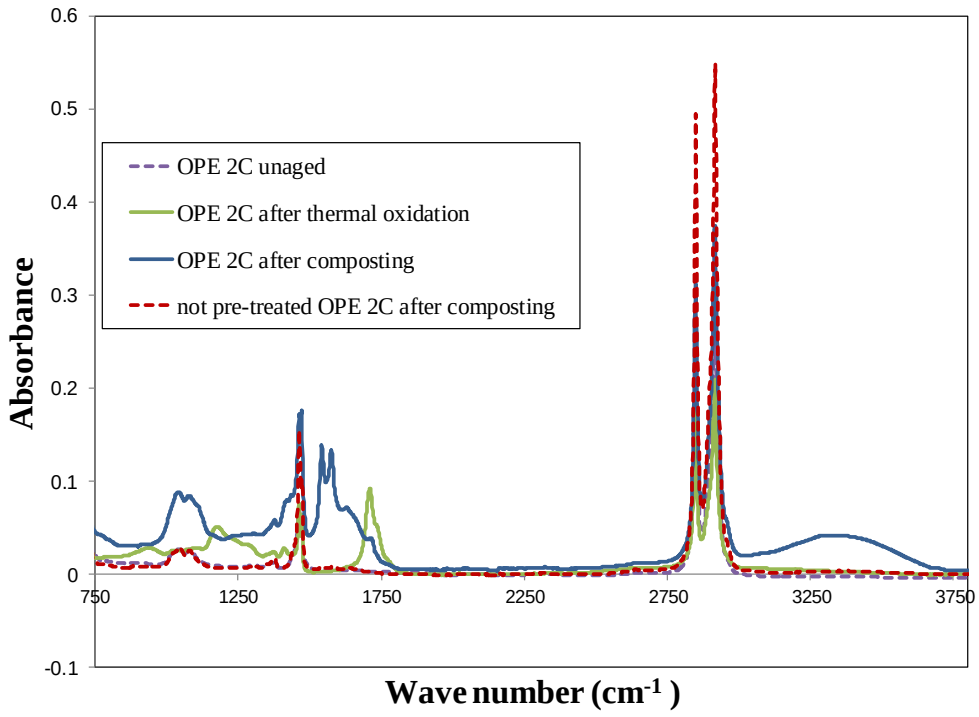

Figure 6-19 FTIR spectra for OPE 2C clay nanocomposite

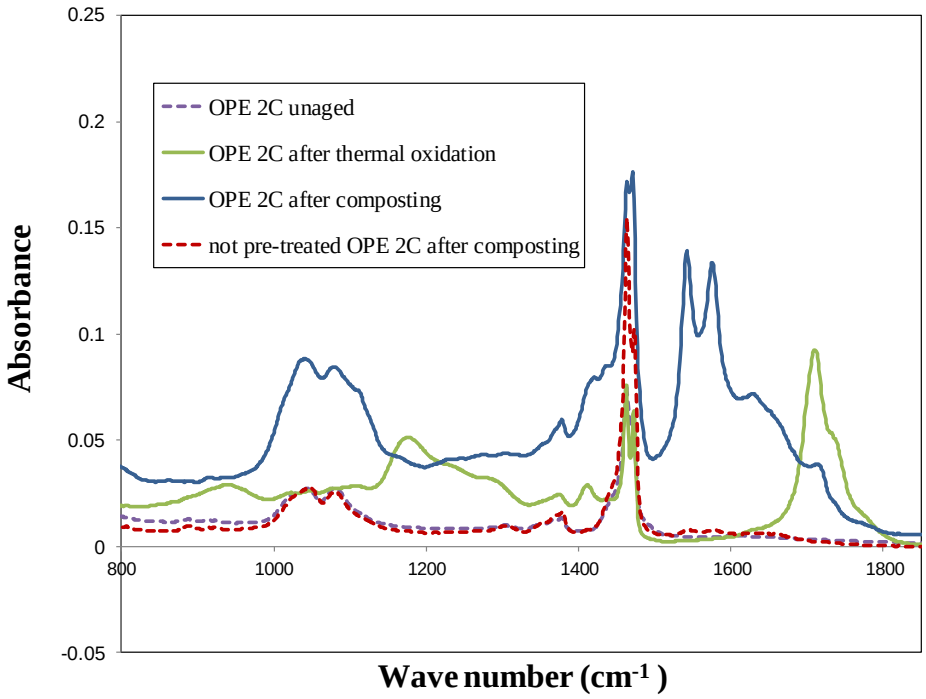

Figure 6-20 FTIR spectra for OPE 2C clay nanocomposites

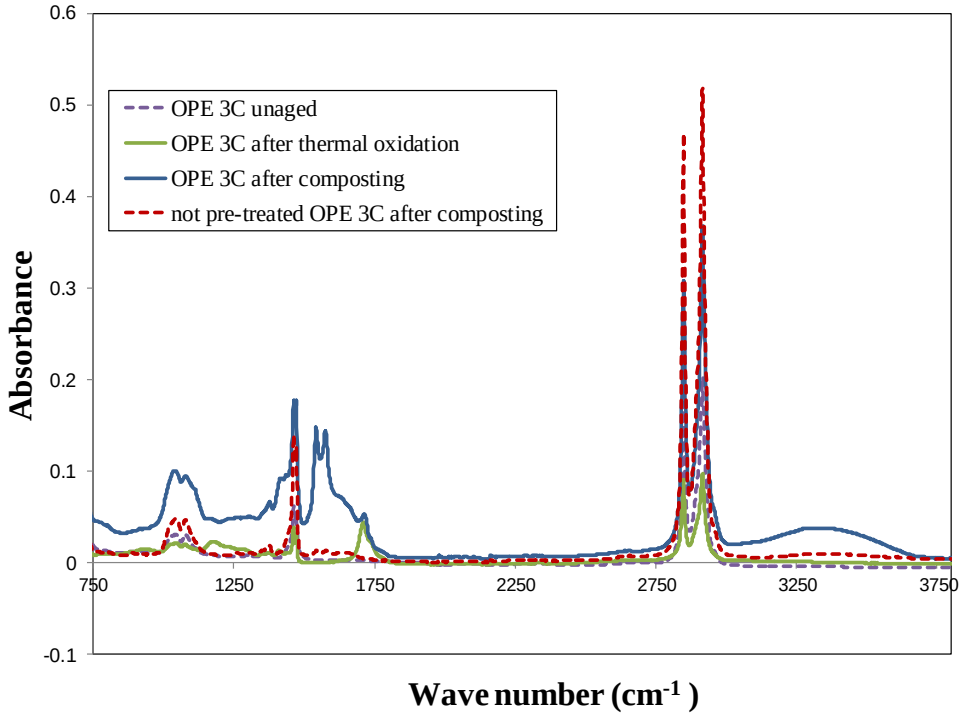

Figure 6-21 FTIR spectra for OPE 3C clay nanocomposites

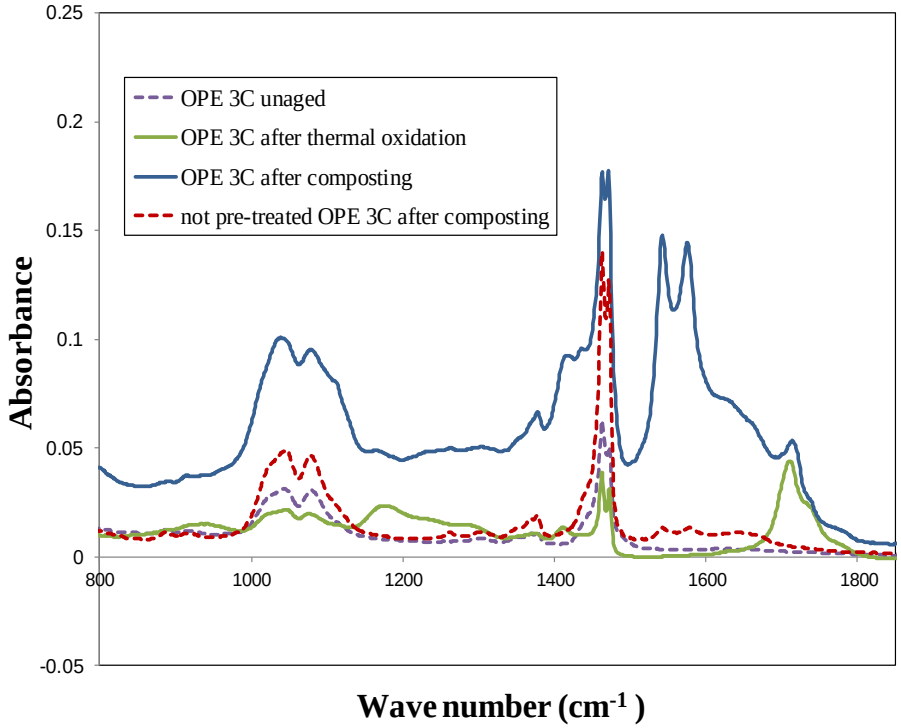

Figure 6-22 FTIR spectra for OPE 3C clay nanocomposites

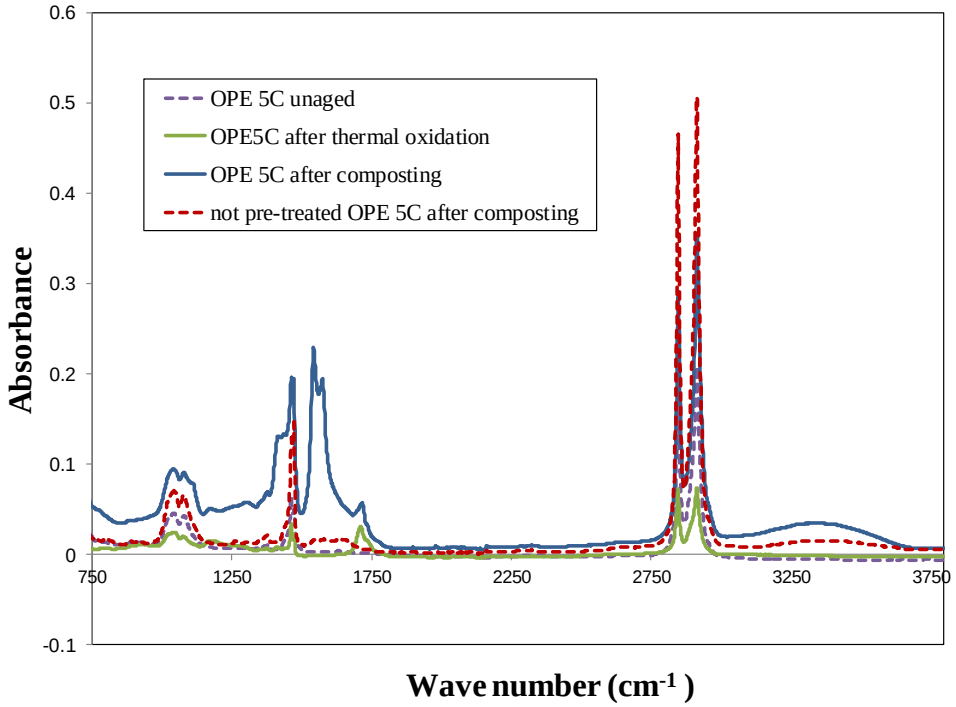

Figure 6-23 FTIR spectra for OPE 5C clay nanocomposites

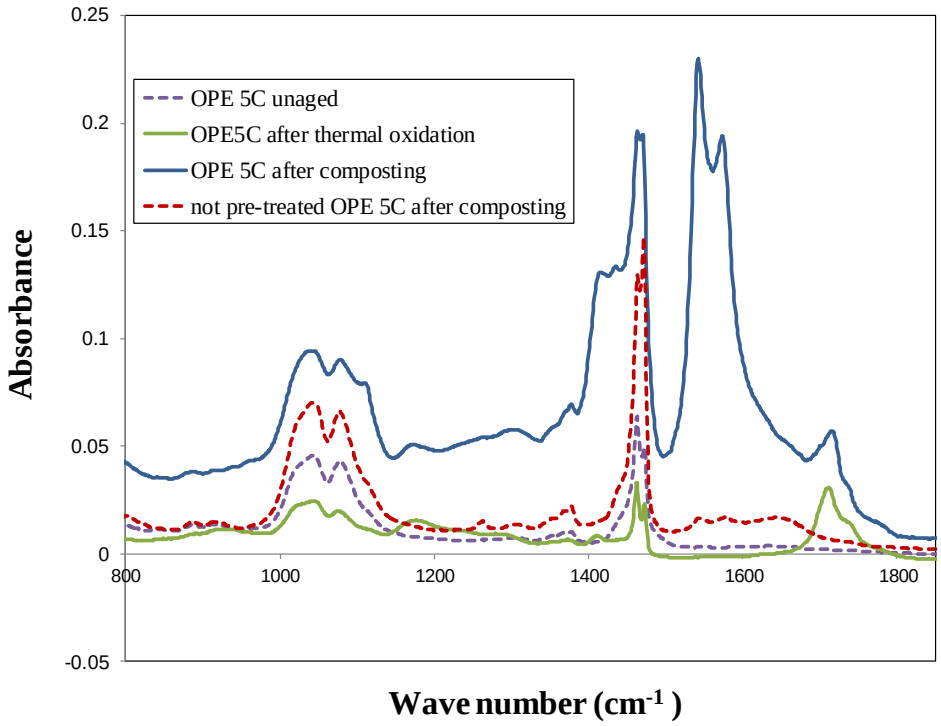

Figure 6-24 FTIR spectra for OPE 5C clay nanocomposites

The rate of carbonyl formation and consumption for PE+F, OPE and OPE nanocomposites are depicted in Figures 6-25 and 6-26, respectively. It is clear that, by incorporating clay into OPE structure, less products with carbonyl group were formed and the amount of products containing carbonyl groups decreased further with increasing clay loading in OPE nanocomposites. As explained before, this behaviour is a result of the barrier effects of clay in polymer matrix and also due to the reduction of mobility of molecules in the less permeable structure of nanocomposites. However, as was expected, the rate of carbonyl consumption in OPE is slower than that in OPE nanocomposites. This may be attributed to the more suitable environment that is available for microbial activities in OPE nanocomposites compared to OPE. The presence of clay balances the pH of the environment as it can act as an electron donor and neutralize the H+ formed after the microbial consumption of products. Unlike OPE nanocomposites, the surface of polymer

and environment in OPE tends to be acidic after a while which limits the microbial activity. On the other hand, it seems that the barrier effect of clay has a dominant role especially when clay concentration is greater than 2%. In such cases, the consumption rate is found to decrease gradually with increasing clay loading.

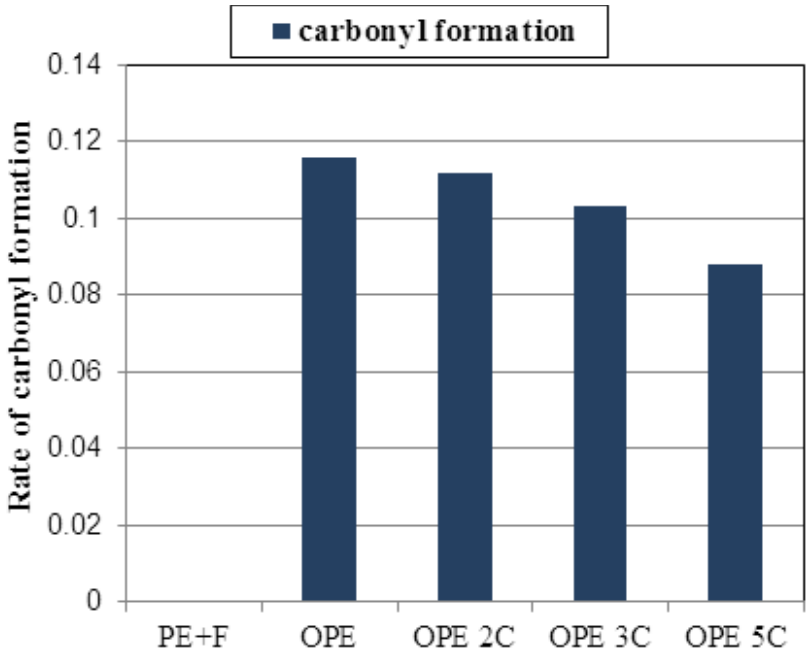

Figure 6-25 Rate of carbonyl formation for PE+F, OPE and OPE nanocomposites after composting

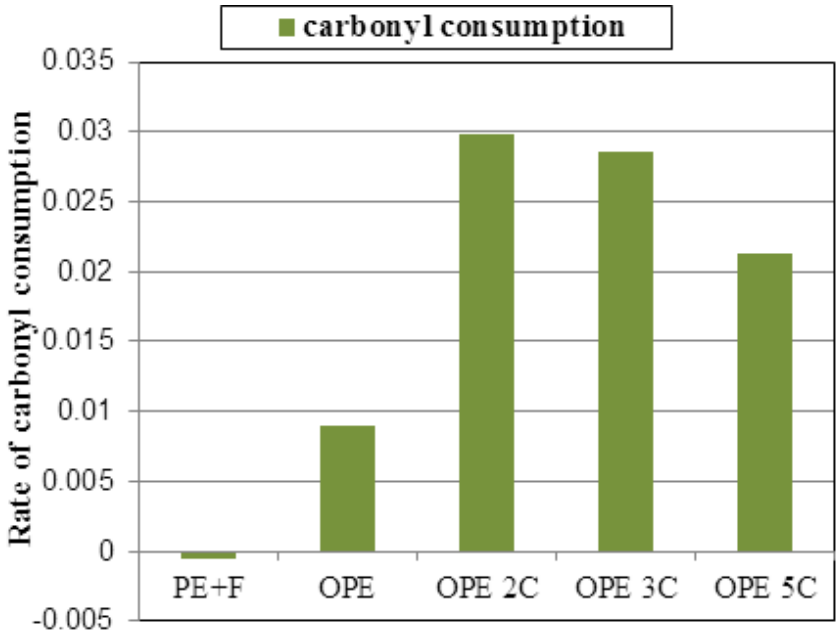

Figure 6-26 Rate of carbonyl consumption for PE+F, OPE and OPE nanocomposites after composting

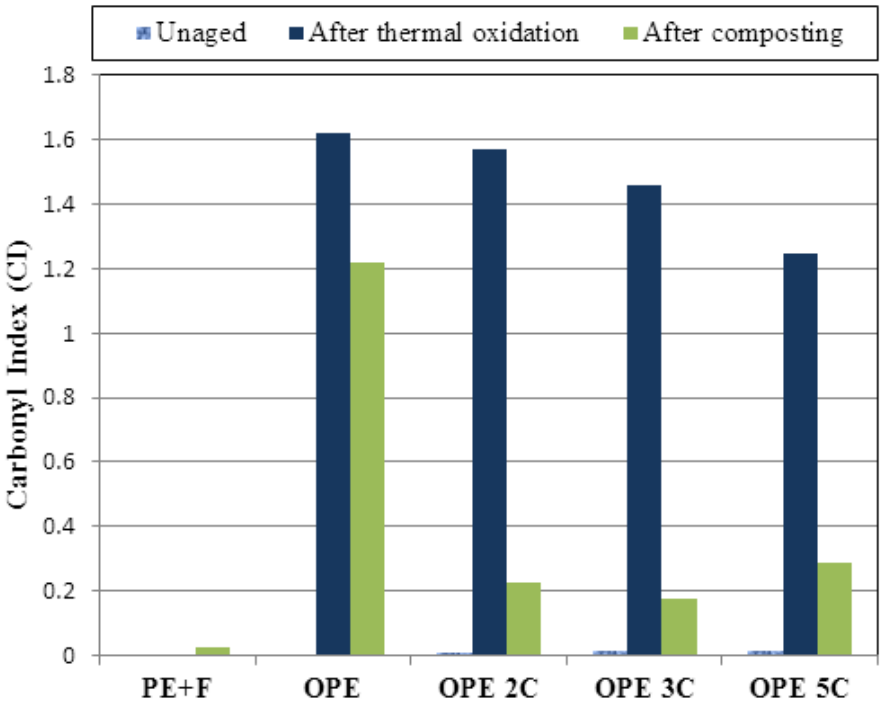

Figure 6-27 Changes of carbonyl index in two stages of oxo-biodegradation of PE+F, OPE and OPE nanocomposites

From Figure 6-27 and the rate of consumption of degradation products in test materials, it can be stated that the presence of clay in OPE nanocomposites plays a vital role in the biodegradation process of polymer. It is clear that microorganisms can utilise the products of degradation faster in the presence of clay. So, it can be assumed that in extended time, with the help of clay, the degree of degradation would be higher in OPE nanocomposites compared to OPE. It was also observed from FTIR spectra that, although the carbonyl group band had higher intensity, the formation of other functional groups occurred in OPE nanocomposites. It can be also predicted that the presence of these functional groups will lead to further chain cleavage and consequently higher degree of degradation over an extended periods under real composting condition.

The reason behind the contradictory effect of clay discussed above is because the clay mineral can act both as an electron donor and electron acceptor. The electron acceptor sites are aluminium ions and transition metal ions in the higher valency states in the silicate structure, and the electron donors are transition metal ions in the lower valency states in the silicate structure. The presence of aluminium with some other transition metal ions like Fe and Mn ions in silicate layers which have two oxidation states and can undergo redox reaction enables clay to act according to two different mechanisms. The redox reaction of Fe ions catalyses the peroxidation of hydrocarbon polymers and as a consequence the rate of hydroperoxide formation becomes remarkably higher in polymer nanocomposites (Scott & Wiles 2001). Kumanayaka *et al.* (2010) showed that MMT naturally contains Fe^{3+} ions in its octahedral sheets.

6.2.3.3 Biofilm

ESEM micrograph of composted OPE nanocomposites films are shown in Figures 6-28 to 6-34. Formation of different type of microorganisms (bacteria and fungi) is apparent from these micrographs.

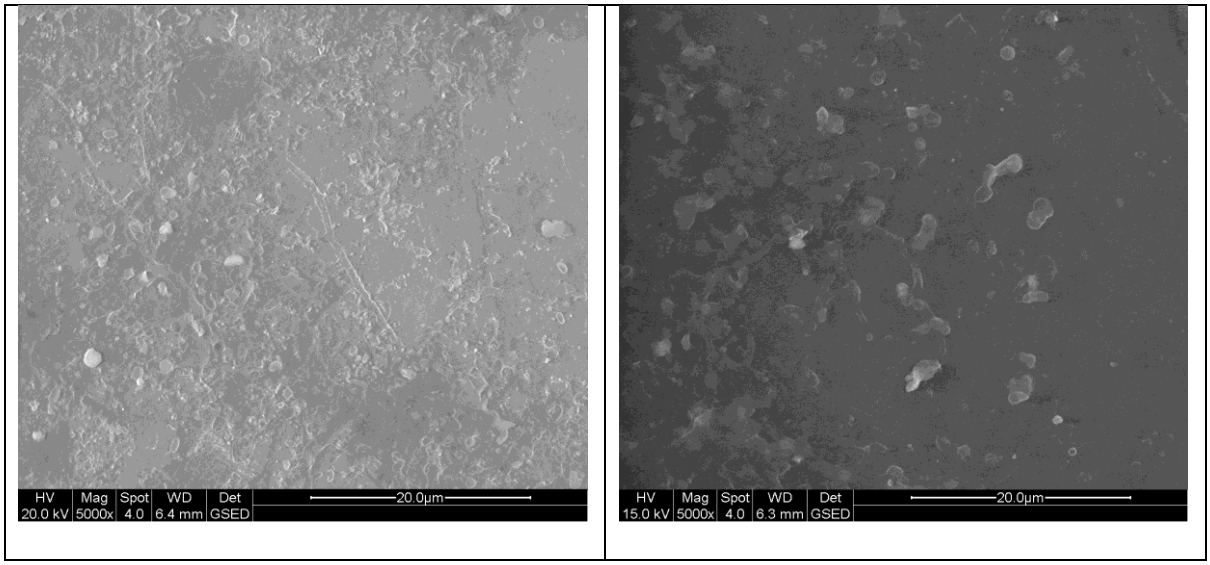

Figure 6-28 ESEM micrographs of biofilm on OPE 2C surface after composting

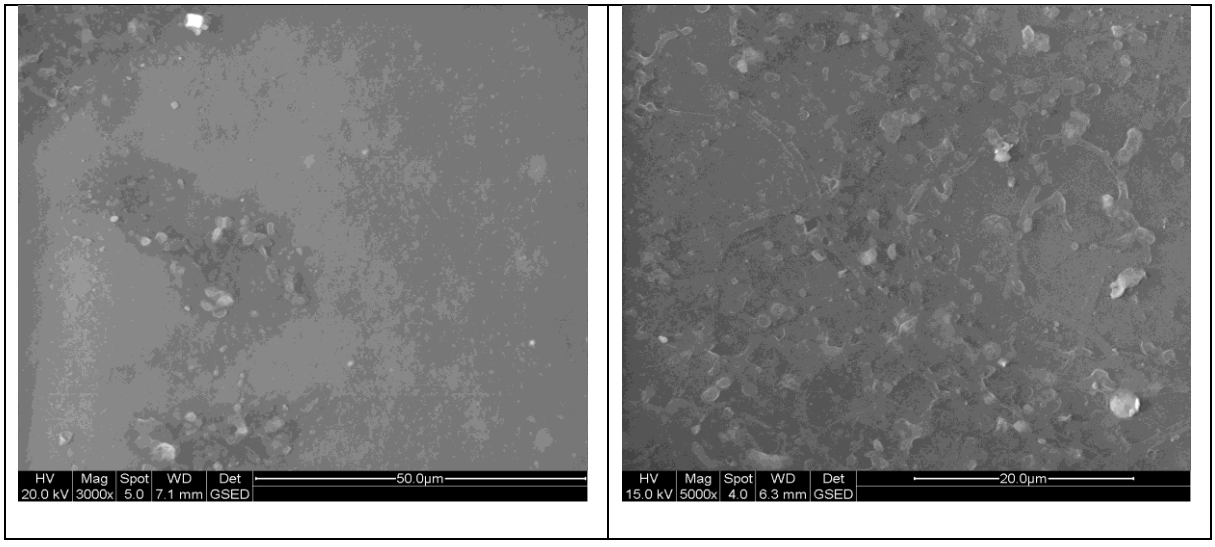

Figure 6-29 ESEM micrographs of biofilm on OPE 3C surface after composting

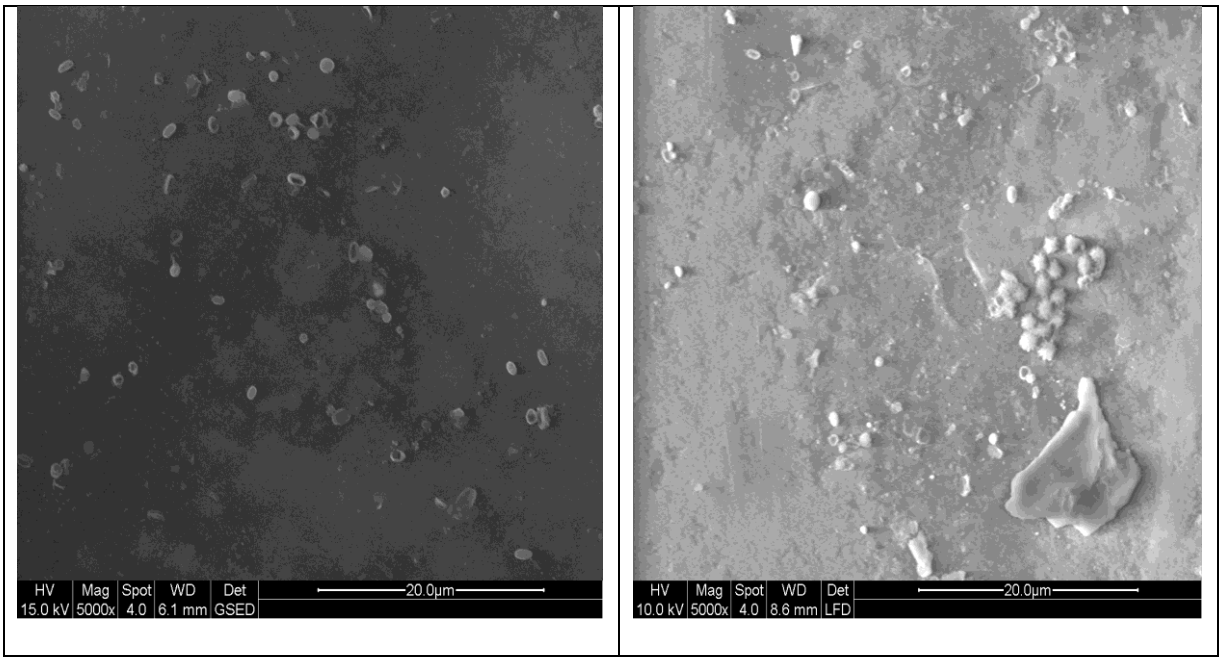

Figure 6-30 ESEM micrographs of biofilm on OPE 5C surface after composting

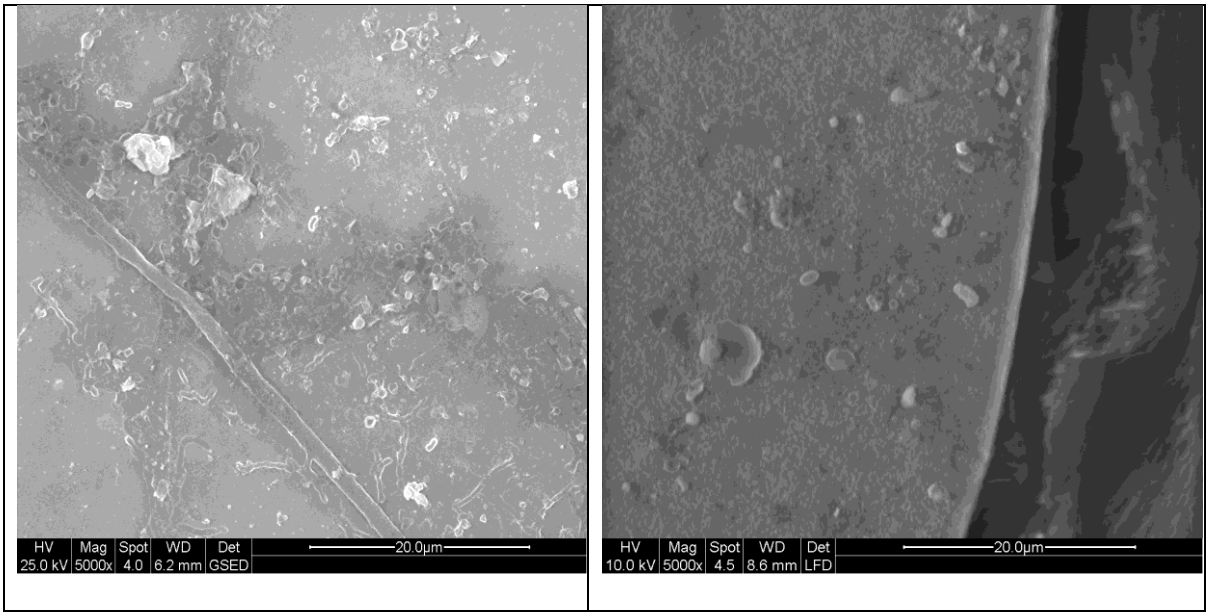

Figure 6-31 ESEM micrographs of biofilm on OPE 5C surface after composting

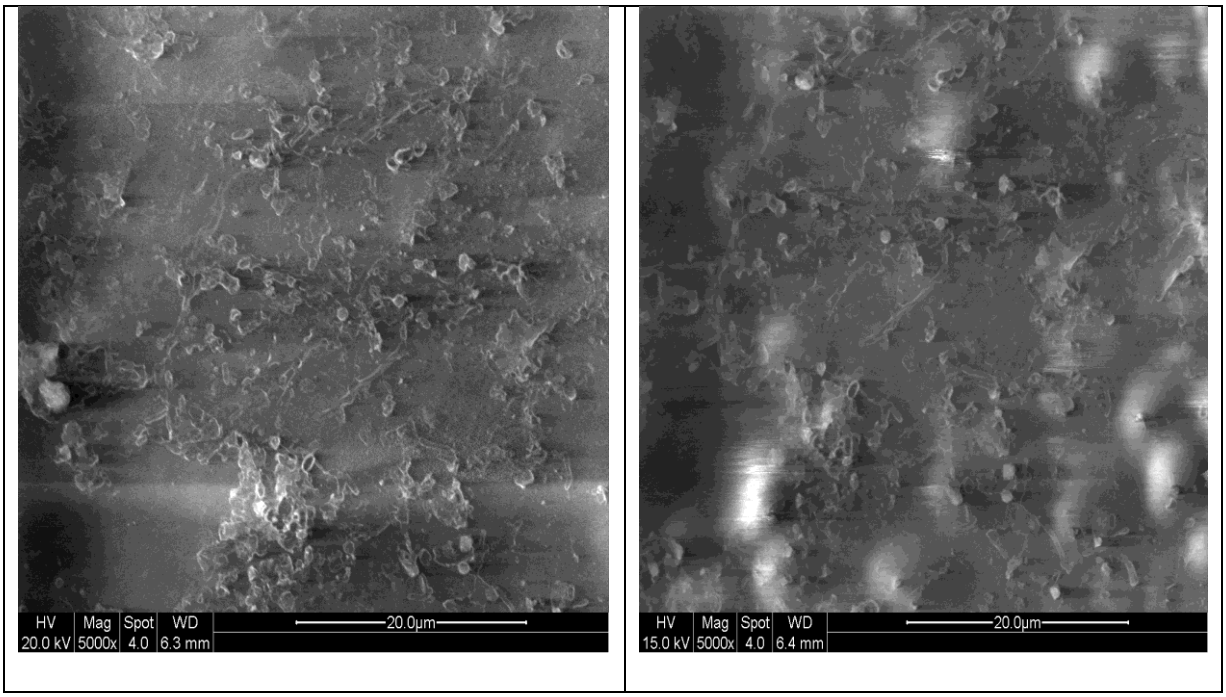

Figure 6-32 ESEM micrographs of biofilm on OPE 2C surface without pre thermal treatment after composting

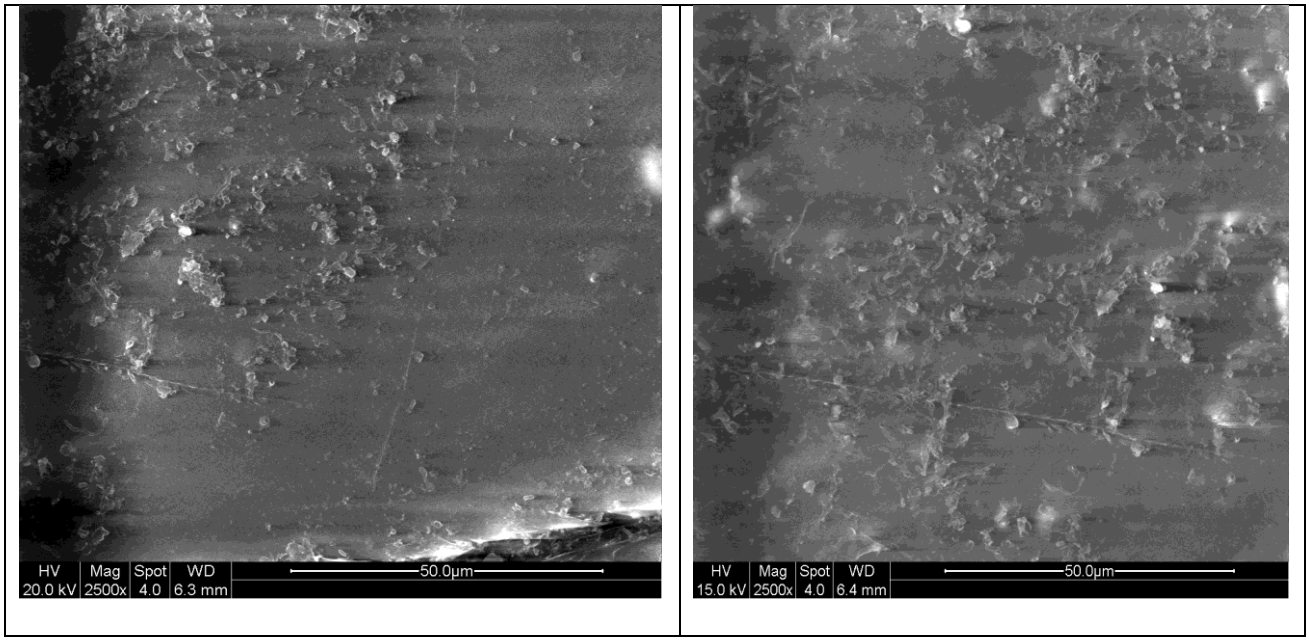

Figure 6-33 ESEM micrographs of biofilm on OPE 3C surface without pre thermal treatment after composting

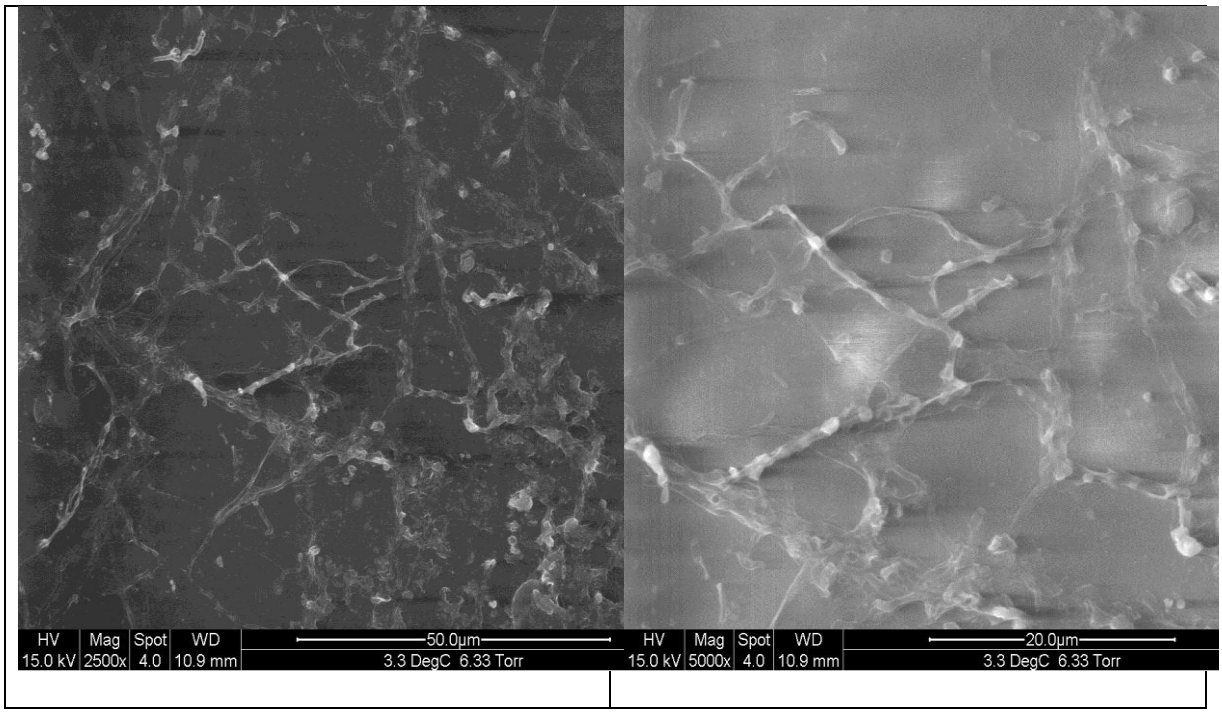

Figure 6-34 ESEM micrographs of biofilm on OPE 5C surface without pre thermal treatment after composting

Although biofilm is found on film samples without pre-thermal treatment, the bacterial variety is limited. On the other hand, formation of different species of bacteria has been observed on the surface of OPE nanocomposites samples which were pre-treated by heat before composting. This can be attributed to the presence of different degradation products in pre thermally treated OPE nanocomposites samples which attract different variety of microorganisms. It can be said that apparently each species of microorganism consume different range of products, depending on the functional groups.

6.3 Conclusions

Two stages involved in the biodegradability of OPE nanocomposites were studied. Abiotic stage (thermal oxidation) was carried out in an oven and biotic stage was carried out in a

composting system. The main objective of the study was to investigate the combined effects of manganese stearate and nanoclay on the biodegradation of polyethylene.

In general, thermal degradation results showed that the presence of clay has no significant effect on the degradation mechanism in OPE nanocomposites. However, the extent of thermal oxidation has been found to be limited by the presence of clay in the matrix especially under higher clay loading. It has been also found that the presence of manganese stearate as a pro-oxidant accelerates the thermal oxidation process significantly.

However, the effect of clay on composting period was remarkable. Although it has been shown that the presence of pro-oxidant is essential in degradation, especially in the early state of degradation when the free radicals are formed, it is clay that extensively develops the degradation process. Clay itself can not initiate the degradation easily and it may take long period of time for the polymer to degrade in the presence of clay without pro-oxidant. But as soon as the degradation process commences in macromolecule, clay contributes to the degradation process differently by either catalysing the reactions according to its particular nature or by making the environment suitable for the growth and activity of microorganisms. As a result, more and extensive degradation has been observed in samples which contains both pro-oxidant and nanoclay compared to the other samples tested. So, the co-existence of manganese stearate with nanoclay is vital in polyethylene structure to achieve an effective oxo-biodegradable polyethylene nanocomposite.

It can be also predicted from the results obtained that biodegradation in OPE nanocomposite samples will continue with time and final mineralisation of polyethylene nanocomposites can be achieved in extended period of time. However, it was not possible to test this statement in this work due to time constraints.

7 Modeling

7.1 Introduction

The knowledge on producing blends, nanocomposites, and biopolymers has improved significantly in the last decade due to the high demand for environmentally-friendly polymers. However, the knowledge on the polymer biodegradation process and the fate of polymers after their service life has not increased significantly yet. Without this knowledge, design of new generation of biodegradable polymers is not achievable. Although researchers have used different experimental methods for investigating and monitoring the biodegradation process of polymers, it is important to simulate the biodegradation process using mathematical models. Mathematical models are strong predictive tools and they help in predicting the biodegradation behaviour of tested materials under different conditions according to initial and boundary conditions of the proposed model. Time and cost constraints involved in running more experiments would not be preventative factors to further study of biodegradation process if mathematical models are used.

7.2 Fitting data to microbial growth models

It has been shown by Larson (1984) that polymer biodegradation process can be modeled using two different mathematical models: (1) the first-order rate model and (2) the logistic function model. Both models have been used by researchers to describe the microbial growth and degradation kinetics for batch systems (Larson *et al.* (1979), Rogers *et al.* (1997), Srinivasan & Viraraghavan (2000) and Reuschenbach *et al*. (2003)). When the rate of biodegradation is proportional to the concentration of the test chemical or produced

material, biodegradation is regarded as a first-order reaction and it can be expressed by a first-order rate equation:

$$v = -\frac{dS}{dt} = -k_1 S \qquad 7\text{-}1$$

where S is the concentration of test material or evolved CO_2, t is the time (days), k_1 is the first order rate constant (day^{-1}) and ν is the disappearance rate of material or the rate of biodegradation.

If the equation is rearranged in a useful form to calculate the total rate of consumption or production of materials rather than a specific rate, it can be expressed as follows:

$$S(t) = S_0 e^{-k_1 t} \qquad 7\text{-}2$$

where S is the remaining test material concentration or the amount of evolved CO_2 and S_0 is the initial concentration of test material or CO_2 at time t = 0.

In this study, the main objective is fitting the CO_2 evolution data to a mathematical model. Therefore, the definitions of kinetic parameters in the following equations are related to CO_2 evolution and biodegradation rate. If Equation 7-2 is solved analytically, its solution can be expressed as follows:

$$y = \begin{cases} 0 & for \quad x \le c \\ a(1 - e^{-k_1(t-c)}) & for \quad x \ge c \end{cases} \qquad 7\text{-}3$$

where y = degree of biodegradation (%), t = time (days), a = asymptote of CO_2 evolution curve (maximum biodegradation degree), k_1 = the rate constant (day^{-1}) and c = lag time

before CO_2 production occurs (days). In cases where the change in biodegradation rate with time is represented by S-shape curve, the following equation may be used to fit the experimental data:

$$y = a(1 - be^{-k_1 t})^{-1/n} \qquad 7\text{-}4$$

where y = degree of biodegradation (%), t = time (days), a = asymptote of curve (% degree of biodegradation), k_l = rate constant (day^{-1}), n = empirical constant and b = coordinate scaling factor (= 1 in single-dose batch systems). Larson *et al*. (1996) used both equations to determine the rate constant for biodegradation (k_1) and the extent of degradation for several test compounds. After analysing their results, Larson *et al.* have stated that the non-linear regression method, which they have used to fit their experimental data, can describe biodegradation patterns of different materials including materials with rapid and complete degradation without lag phases and materials with incomplete degradation with variable lag phases. Rogers *et al.* (1997) modified Equation 7-4 and fitted their experimental data to a modified logistic function (Equation 7-5) to quantify the kinetics of strychnine degradation in non-sterile Booleroo and Bute soils.

$$y = a + \frac{c}{1 + e^{-b(t-m)}} \qquad 7\text{-}5$$

where y = strychnine concentration, t = time (days), a = the lower asymptote (minimal strychnine concentration), c = the upper asymptote (maximum strychnine concentration), b = slope parameter, m = point of inflection of the curve. Another form of modified logistic model has been used by Reuschenbach *et al*. (2003) to fit their results of respirometric biodegradation tests to S-shape or sigmoidal curves (Equation 7-6):

$$y = \frac{L}{1 + Ae^{-kt}} - \frac{L}{1 + A} \qquad 7\text{-}6$$

where y = % theoretical COD or $ThCO_2$, t = time (days), and k = rate constant ($days^{-1}$), and L and A are curve fit parameters that are required to optimise the curve fitting to experimental data.

7.3 Validity of suggested models in predicting biodegradation pattern

CO_2 evolution data collected from each test vessel in 6-hour time intervals were used to calculate the degree of biodegradation (%) and the theoretical amount of CO_2 for each sample by taking that all the carbon (100%) in the test material will be converted to CO_2. These data were then used to plot the degree of biodegradation (%) graphs shown in previous chapters. The next step is to attempt to fit the experimental data to mathematical models used by other researchers to determine the best model that will estimate the trend observed in biodegradation curves for oxo-biodegradable polyethylene nanocomposites. It is worth noting that most of the biodegradation curves are biphasic. Therefore, it is appropriate to use two models to fit the biodegradation curves. However, the two phases are not very distinct in OPE biodegradation curve and therefore it has been decided to fit the biodegradation curve to just one model. The observed biphasic pattern suggests that there are two degradation phases in biodegradation process.

Similar to the curve fitting procedure mentioned above for CO_2 evolution data, attempts were made to fit data on biodegradation also to different mathematical models. The first phase of each biodegradation curve (time ≤ 3.5 days) was fitted to an exponential equation using non-linear regression method (Equation 7-7).

$$y = a(1 - e^{-k_1 t}) \qquad 7\text{-}7$$

where y = degree of biodegradation (%), t = time (days), a = asymptote of curve (maximum value of degree of biodegradation (%)), k_1 = rate constant (day^{-1}). The second phase (sigmoidal phase) of biodegradation curve was fitted by Equation 7-8.

$$y = \frac{L}{1 + Ae^{-k_2(t-b)}} + \frac{L}{1 + A} \qquad 7\text{-}8$$

where y = degree of biodegradation (%), t = time (days), L = asymptote of curve maximum value of degree of biodegradation (%)), k_2 = rate constant (day^{-1}), b = point of inflection of the curve (days) and A is a fitting parameter. Equation 7-7 is a first-order rate equation and Equation 7-8 is a modified form of logistic model. Several attempts have been made to modify the logistic model to a form which can fit the biodegradation curves with meaningful fitting parameters. The kinetic parameters for models were obtained by least squares analysis using MATLAB 7.10.0 (R2010a). The goodness of the fits is demonstrated by the correlation coefficients (r^2). All the fitted curves are shown in Figures 7-1 to 7-4. The kinetic parameters along with their associated 95% confidence intervals are shown in Table 7-1.

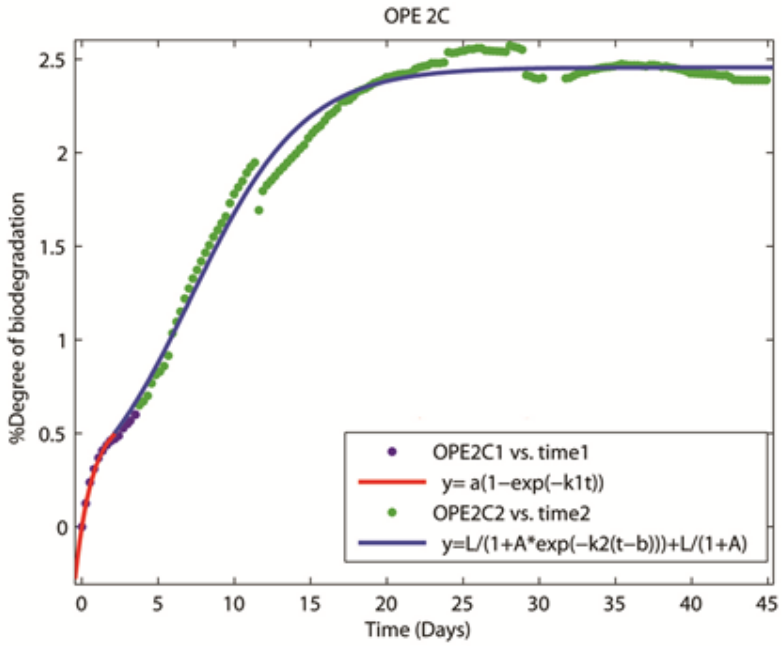

Figure 7-1 Kinetics of biodegradation of OPE 2C. The data were analysed with first-order rate (OPE 2C1 vs. time1) and a modified logistic model (OPE 2C2 vs. time2).

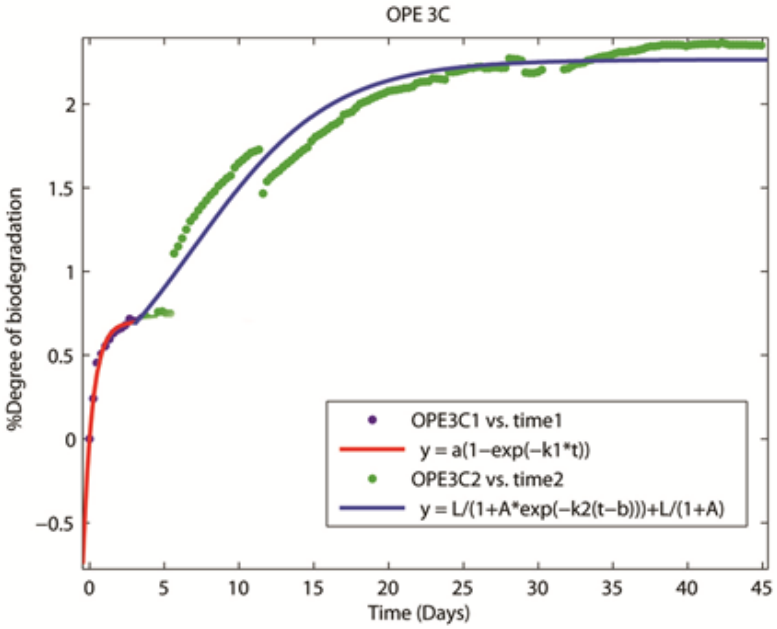

Figure 7-2 Kinetics of biodegradation of OPE 3C. The data were analysed with first-order rate (OPE 3C1 vs. time1) and a modified logistic model (OPE 3C2 vs. time2).

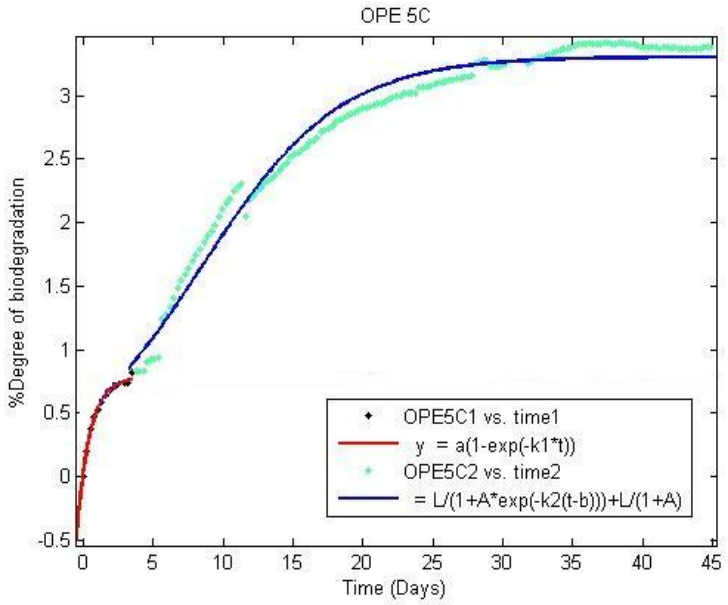

Figure 7-3 Kinetics of biodegradation of OPE 5C. The data were analysed with first-order rate (OPE 5C1 vs. time1) and a modified logistic model (OPE 5C2 vs. time2).

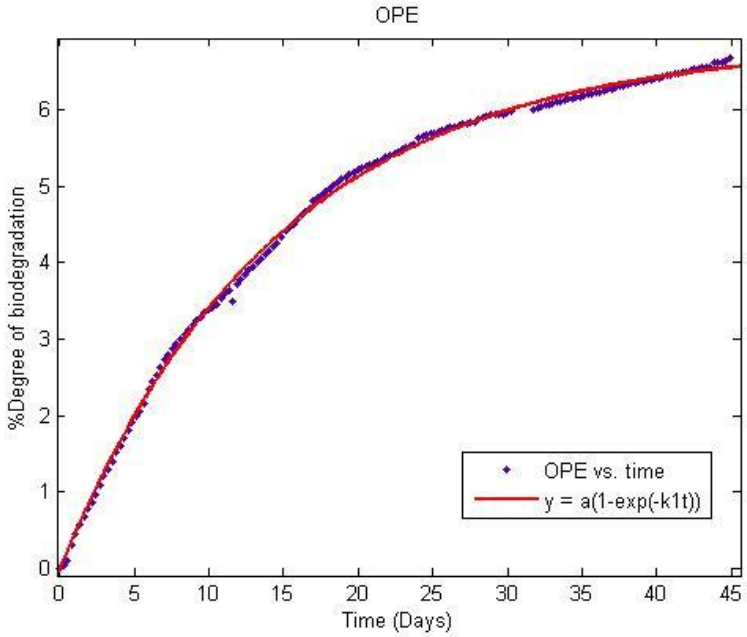

Figure 7-4 Kinetics of biodegradation of OPE. The data were analysed with first-order rate model (OPE vs. time).

As it can be seen from Table 7-1 and Figures 7-1 to 7-4, the asymptote of the curve (L) in Equation 7-8 represents the final biodegradation degree of OPE nanocomposites after 45 days, approximately. However, in real experimental data, the end points of curves are still showing an upward trend. This trend is slight for OPE nanocomposites and noticeable for OPE samples. Despite this difference, it can be concluded that, like other biodegradation model equations mentioned in the literature, the biodegradation of polyethylene nanocomposites can be represented by microbial growth equations, too.

Table 7-1 Kinetic parameters for the biodegradation model for oxo-biodegradable polyethylene nanocomposites

General Equation	$y = a(1-e^{-k_1 t})$			
Test compound	k_1 (day^{-1})	a	r^2	validity
OPE	0.0686 (0.0678,0.0695)	6.862 (6.83,6.894)	0.9987	$0 \leq t \leq 45$
OPE 2C	0.8567 (0.719,0.994)	0.593 (0.558,0.629)	0.9887	$t \leq 3.5$
OPE 3C	1.614 (1.411,1.817)	0.700 (0.679,0.721)	0.9898	$t \leq 3.5$
OPE 5C	1.111 (0.9858, 1.235)	0.779 (0.752,0.807)	0.993	$t \leq 3.5$

Table 7-1 Continued

General Equation	$y = \frac{L}{1+Ae^{-k_2(t-b)}} + \frac{L}{1+A}$						
Test compound	k_2 (day^{-1})	L	A	b (days)		r^2	Validity
OPE 2C	0.271 (0.236, 0.306)	2.456 (2.052, 2.86)	5.095e+4 (-4.204e+8, 4.205e+8)	-32.77	(-3045e+4, 3.038e+4)	0.9779	t > 3.5
OPE 3C	0.217 (0.17, 0.264)	2.264 (1.555,2.973)	- 3.405e+5 (-3.555e+10, 3.556e+10)	-51.83	(-4.814e+5, 4.813e+5)	0.9425	t > 3.5
OPE 5C	0.203 (0.175,0.230)	3.305 (2.759, 3.85)	2.517e+5 (-1.017e+10, 1.017e+10)	-52.91	(-1.995e+5, 1.994e+5)	0.9763	t >3.5

7.4 Discussion

The biodegradation patterns of OPE and OPE nanocomposites were studied to determine the biodegradation rate and the extent of biodegradation in polymer samples tested in this work. To quantify the kinetics of biodegradation process, biodegradation data were fitted to an exponential model and a modified logistic model. The change in biodegradation rate with time is an indication of the speed at which biodegradation occurs in the polymer. Therefore, fitting experimental data to a mathematical model is a useful exercise which enables us to analyse and compare the experimental degradation data for different polymer samples. Using the model equations considered in this work, the effect of clay concentration on the biodegradation rate of polyethylene nanocomposite was investigated.

The presence of biphasic curves for the biodegradation of OPE nanocomposites indicates the existence of two different phase in 45 days of incubation. It is also obvious from the kinetics data obtained that the degradation rate in the first phase is slower than the second phase. By studying the FTIR results shown in Chapter 6, an exponential increase in biodegradation can be detected in the first few days of incubation which indicates a rapid biodegradation of products of thermal degradation stage. The faster degradation rate observed in second phase can be attributed to the degradation of polymer macromolecules into smaller fragments with different functional groups and the biodegradation of functional groups to CO_2 and H_2O.

In this study, the pro-oxidant concentration was kept constant in all nanocomposites to study the effect of clay content on biodegradation exclusively. The results confirm the important role of clay on biodegradation behaviour of nanocomposites. It is clear that the biodegradation rate is slower at higher clay loadings (0.271 $days^{-1}$ for OPE 2C to 0.203 $days^{-1}$ for OPE 5C). This can be attributed to the barrier effect of clay as was explained in

previous chapters. Therefore, the clay is limiting the biodegradability of nanocomposites. OPE showed entirely different behaviour compared to OPE nanocomposites as was expected and its biodegradation data were fitted by an exponential model.

This ability to accurately determine biodegradation parameters from mathematical models can be used for comparison purposes especially for polyethylene nanocomposites with different clay loadings. Mathematical model, being a tool to analyse the kinetics of biodegradation, can also help to estimate the biodegradation potential of polymer compounds.

Finally, it should be noted that all the experimental results and mathematical models obtained in this study are only for a period of 45 days of incubation and it cannot be used to extrapolate for the full life of nanocomposites without further study. It is recommended to extend the biodegradation study beyond 45 days as it may show other phases of biodegradation.

8 Conclusions and recommendations

8.1 Conclusions

The rising global issue of “plastic pollution”, especially plastic bags pollution, is increasing the public awareness of importance of producing environmentally friendly plastic bags which can be biodegraded completely after their service life and transformed into the carbon cycle harmlessly. Attempts to solve this problem have led to the production of so-called “biodegradable plastic bags”. These plastic bags disintegrate into smaller fragments in the presence of light, heat and oxygen after they are discarded into environment. These small and mostly toxic fragments remain in the environment for prolonged period and pollute the underground water and soil. It can be said that the attempts to address the plastic bags pollution problem correctly are not successful yet.

The major focus of this work was to develop a fundamental understanding on the polyethylene biodegradation mechanism and investigate the roles of main factors that affect the biodegradation process. The main objective was to determine the optimum conditions under which the biodegradation of polyethylene can be improved. Another objective of this work was to develop a mathematical model for the biodegradation of oxo-biodegradable polyethylene nanocomposites so as to predict the kinetics of biodegradation and therefore, study the biodegradation behaviour without the constraints of time and money. This work will be beneficial to industry as it can provide a better knowledge on the role of pro-oxidant and clay on the biodegradation process. It will also be useful in designing more environmentally-friendly polyethylene nanocomposites that will biodegrade in the environment.

The following conclusions can be drawn from this study:

- WAXS studies reveal that morphology of polyethylene nanocomposites changes from nearly exfoliated structure to intercalated structure with increasing clay loading in nanocomposites and this structural change could be a possible reason for the different biodegradation behaviours exhibited by polyethylene nanocomposites with different clay loadings.
- Thermal degradation of polyethylene and polyethylene nanocomposites containing pro-oxidant leads to the formation of low molecular weight compounds with various functional groups; however, in nanocomposite samples without pro-oxidant, the same heat exposure does not lead to significant degradation. Heat does not degrade pure polyethylene during 14 days of testing period.
- The products of oxidation stage contain functional groups. These functional groups make the polymer film hydrophilic and make it more attractive to microorganisms. Therefore, the biodegradation takes place at a faster rate on the polymer film.
- The addition of manganese stearate as a pro-oxidant helps in different aspects of both abiotic and biotic stages of biodegradation process. The presence of manganese stearate in polymer helps to initiate and propagate the radical formation leading to the production of more oxidation products in a shorter oxidation period. According to FTIR results, manganese also helps in continuing the polymer degradation process leading to the generation of oxidation products during the incubation period.
- Thermal degradation results showed that the presence of clay has no significant effect on the thermal degradation mechanism in OPE nanocomposites. However, oxidation process is slower for nanocomposites with higher clay loadings.

- It is clear that 45 days is a relatively short period to study the biodegradation of polyethylene nanocomposites. Moreover, the addition of clay made the biodegradation mechanism more complex. It seems that biodegradation in the presence of clay consists of different phases. It is possible that nanocomposites can go through another phase of biodegradation and show different behaviour if incubation time is increased.
- The presence of clay enhances the biodegradability of polyethylene nanocomposites remarkably during the composting period. Clay can help the microorganisms in breaking down the macromolecules into smaller fragments by providing a better environment for the activity and growth of microorganisms. This can be seen from FTIR and carbonyl index results. Hydrophilic nature of clay can attract more microorganisms to its surface. However, this influence decreases when clay loading in nanocomposites increases due to the barrier and insulator effects of clay in the nanocomposite structure.
- The presence of pro-oxidant is essential in degradation, especially in the early stages of degradation. But according to results from this work it can be claimed that it is clay that extensively improves the degradation process. Clay itself cannot initiate the degradation easily and it may take long time for the polymer to degrade in the presence of clay without pro-oxidant. But as soon as the degradation process commences in macromolecule, clay contributes to the degradation process differently either by catalysing the reactions according to its particular nature or by making the environment suitable for the growth and activity of microorganisms. More and extensive degradation has been observed in samples containing both pro-oxidant and nanoclay compared to the other samples tested. It can be said

confidently that the co-existence of manganese stearate and nanoclay in polyethylene structure is vital in achieving an effective oxo-biodegradable polyethylene nanocomposites.

- Mathematical modeling is a useful tool in analysing the kinetics of biodegradation. Therefore, it can give an estimate of the biodegradation potential of polyethylene compounds.
- All the results and conclusions obtained in this work were obtained from studying the biodegradation behaviour of tested samples in a short incubation period of 45 days and therefore they cannot be expected to reveal the full details of biodegradation of nanocomposites. It is recommended to extend the biodegradation time period beyond 45 days as it may reveal more phases of biodegradation during longer incubation time.
- It is possible to say that materials which have slow rates of biodegradation under testing conditions may still biodegrade at reasonable rates in natural environment. The high test material concentration within limited defined space, low microorganisms concentration, relatively shorter exposure time under testing condition are some of the factors involved in this study which could have probably led to a lower degree of degradation under testing conditions compared to that under natural environment.
- Considering the fact that degree of biodegradation curves for OPE nanocomposites samples show an upward trend even at the end of 45 days of incubation, it is reasonable to claim that biodegradation in these samples will continue with time and final mineralisation of them can be achieved over an extended period of time.

However, it was not possible to test this statement in this work due to time limitation.

8.2 Recommendation

The following are the recommendations for possible further work:

- The biodegradation stage can be carried out using more advanced and accurate techniques whereby the process can be monitored atomically. In such case, some errors in measuring the CO_2 evolution rate can be avoided.
- More investigations can be carried out using different concentrations of pro-oxidant in OPE and OPE nanocomposites to find the optimum concentration.
- It is recommended to extend the biodegradation test to a longer period and investigate the possibility of other phase changes in biodegradation as a function of time. This is highly recommended especially for polyethylene which has very low biodegradation rate in natural environment.
- Thermal degradation can be carried out under lower temperatures to simulate the conditions in colder environment.
- Studying the changes in molecular weight distribution with time in both abiotic and biotic stages can be beneficial to develop a better understanding of the whole process of biodegradation.

References

1. Albertsson, AC, Andersson, SO & Karlsson, S 1987, 'The mechanism of biodegradation of polyethylene', *Polymer Degradation and Stability*, vol. 18, no. 1, pp. 73-87.
2. Albertsson, AC & Banhidi ZG 1980, 'Microbial and oxidative effects in degradation of polyethene', *Journal of Applied Polymer Science*, vol. 25, no. 8, pp. 1655–1671.
3. Albertsson, AC & Karlsson, S 1988, 'The 3 Stages in Degradation of Polymers - Polyethylene as a Model Substance', *Journal of Applied Polymer Science*, vol. 35, no.5, pp. 1289–1302.
4. Albertsson, AC & Karlsson, S 1990, 'The influence of biotic and abiotic environments on the degradation of polyethylene', *Progress in Polymer Science*, vol. 15, no. 2, pp. 177-92.
5. Albertsson, AC, Barenstedt, C & Karlsson, S 1992, 'Susceptibility of enhanced environmentally degradable polyethylene to thermal and photo-oxidation', *Polymer Degradation and Stability*, vol. 37, no. 2, pp. 163-71.
6. Albertsson, AC & Karlsson, S 1993, 'Aspects of biodeterioration of inert and degradable polymers', *International Biodeterioration & Biodegradation*, vol. 31, no. 3, pp. 161-70.
7. Albertsson, AC & Karlsson, S 1995, 'Degradable polymers for the future', *Acta Polymerica*, vol. 46, no. 2, pp. 114-123.
8. Albertsson, AC, Erlandsson, B, Hakkarainen, M & Karlsson, S 1998, 'Molecular weight changes and polymeric matrix changes correlated with the formation of

degradation products in biodegraded polyethylene', *Journal of polymers and the Environment*, vol. 6, pp. 187-195.

9. Alexandre, M & Dubois P 2000, 'Polymer–layered silicate nanocomposites: preparation, properties and uses of a new class of materials', *Material Science Engineering*, vol. 28, pp.1–63.
10. Aguado, J, Serrano, DP & Miguel, GS 2007, 'European trends in the feedstock recycling of plastic wastes', *Global NEST J*, vol.9, no.1, pp.12-19.
11. Arnaud, R, Dabin, PJL, Al-Malaika, S, Chohan, S, Coker, M & Scott, G 1994, 'Photooxidation and biodegradation of commercial photodegradable polyethylene', *Polymer Degradation and Stability*, vol. 46, no. 2, pp. 211-224.
12. AS-ISO 14855- 2005 Plastic materials—Determination of the ultimate aerobic biodegradability and disintegration under controlled composting conditions—Method by analysis of evolved carbon dioxide
13. Bandyopadhyay, S, Chen, R & Giannelis, EP 1999, 'Biodegradable organic–inorganic hybrids based on poly(l-lactide)', *Journal of Macromolecule Science*, vol. 81, pp. 159–160.
14. Becker, O, Varley, RJ & Simon, GP 2004,'Thermal stability and water uptake of high performance epoxy layered silicate nanocomposites', *Eur Polym J*, vol. 40, pp. 187–195.
15. Beyer, G 2002, 'Nanocomposites: a new class of flame retardants for polymers', *Plastic Additives Compound*, vol. 4, no.10, pp. 22–27.
16. Bahattacharya, SN, Gupta, RK & Musa R 2007, *Polymeric nanocomposites, theory and practice*, Hanser Gardner, Ohio, USA.

17. Bonhomme, S, Cuer, A, Delort, AM, Lemaire, J, Sancelme, M & Scott, G 2003, 'Environmental biodegradation of polyethylene', *Polymer Degradation and Stability*, vol. 81, no. 3, pp. 441-452.
18. Burman, L& Albertsson AC. 2005, 'Chromatographic fingerprint e a tool for classification and for predicting the degradation state of degradable polyethylene', *Polymer Degradation and Stability*, vol.89, pp.50-63.
19. Burnside, SD & Giannelis, EK 1995, 'Synthesis and properties of new poly (dimethylSiloxane) nanocomposites', *Chem. Mater*, vol.7, pp. 1597-1600.
20. Chiellini, E, Corti, A & Swift, G 2003, 'Biodegradation of thermally-oxidized, fragmented low-density polyethylene', *Polymer Degradation and Stability*, vol. 81, no. 2, pp. 341-351.
21. Chiellini, E, Corti, A, D'Antone, S & Baciu, R 2006, 'Oxo-biodegradable carbon backbone polymers - Oxidative degradation of polyethylene under accelerated test conditions', *Polymer Degradation and Stability*, vol. 91, no. 11, pp. 2739-2747.
22. Chiellini, E, Corti, A & D'Antone, S 2007, 'Oxo-biodegradable full carbon backbone polymers - biodegradation behaviour of thermally oxidized polyethylene in an aqueous medium', *Polymer Degradation Stability*, vol. 92, no. 7, pp. 1378–1383.
23. Chin, IJ, Thurn-Albrecht, T, Kim, HC, Russell, TP & Wang, J 2001, 'On exfoliation of montmorillonite in epoxy', *Polymer*, vol. 42, pp. 5947–5952.
24. Cho, JW & Paul, DR 2001, 'Nylon 6 nanocomposites by melt compounding', *Polymer*, vol. 42, pp. 1083–1094.
25. Dabrowski, F, Bourbigot, S, Delobel, R & LeBras, M 2000, 'Kinetic modeling of the thermal degradation of polyamide 6 nanocomposite', *Eur Polym J*, vol. 36, pp. 273–284.

26. Davis, RD, Gilman, JW & VanderHart, DL 2003, 'Processing degradation of polyamide 6/montmorillonite clay nanocomposites and clay organic modifier', *Polymer Degradation and Stability*, vol. 79, no. 1, pp. 111-121.
27. Denault, TJ & Labrecque, EB 2004, Technology Group on Polymer Nanocomposites – PNC-Tech. Industrial Materials Institute. National Research Council Canada, 75 de Mortagne Blvd. Boucherville, Québec, J4B 6Y4.
28. Dennis, HR, Hunter, DL, Chang, D, Kim, S, White, JL & Cho JW 2001, 'Effect of melt processing conditions on the extent of exfoliation in organoclay-based nanocomposites', *Polymer*, vol.42, pp. 9513– 9522.
29. De vlieger, JJ 2003, Green plastics for food packaging. In: R. Advenainen, Editor, Novel food packaging techniques, Woodhead Publishing Limited and CRC Press LLC, England/USA , pp. 519–534
30. Dintcheva, NT, Al-Malaika, S & La Mantia, FP 2009, 'Effect of extrusion and photooxidation on polyethylene/clay nanocomposites', *Polymer Degradation and Stability*, vol. 94, no. 9, pp. 1571-1588.
31. Durmus, A, Kasgoza, A & Macoskob, CW 2007, 'Linear low density polyethylene (LLDPE)/clay nanocomposites. Part I: Structural characterization and quantifying clay dispersion by melt rheology', *Polymer*, vol.48, no. 15, pp. 4492–4502.
32. Ehrlich, LH 1990, 'Geomicrobiology', Marcel Dekker Inc., pp. 347-419.
33. EPA (The Environmental Protection Agency 2010, *Municipal Solid Waste in The United States: 2009 Facts and Figures*, United States Environmental Protection Agency, Office of Solid Waste (5306P), <www. Epa.gov>
34. Erlandsson, B, Karlsson, S & Albertsson, AC 1997, 'The mode of action of corn starch and a pro-oxidant system in LDPE: influence of thermo-oxidation and UV-

irradiation on the molecular weight changes', *Polymer Degradation and Stability*, vol. 55, no. 2, pp. 237-245.

35. Esma YC & Ulku Y 2010, 'Characteristics of Impact Modified Polystyrene/ Organoclay Nanocomposites', *Polymer Composites*, vol. 31, no. 11, pp. 1853-1861.
36. Farmer, VC & Russell JD 1964, 'The infra-red spectra of layer silicates', *Spectrochimica Acta*, vol. 20, pp. 1149–1173.
37. Feuilloley, P, Cesar, G, Benguigiu, L, Grohens, Y, Pillin, I, Bewa, H, Lefaux, S & Jamal, M 2005, 'Degradation of polyethylene designed for agricultural purposes', *Journal of polymers and the environment*, vol. 13, no. 4, pp. 349-355.
38. Fischer, H 2003, 'Polymer nanocomposites: from fundamental research to specific applications', *Mater Science Engineering*, vol. 23, pp. 763–772.
39. Fornes, TD, Yoon, PJ, Keskkula, H & Paul, DR 2001, 'Nylon 6 nanocomposites: the effect of matrix molecular weight', *Polymer*, vol.42, pp. 9929– 9940.
40. Fredrickson, GH & Bicerano J 19999, 'Barrier properties of oriented disk composites', *J Chem Phys*, vol.110, pp. 2181‑2188.
41. Giannelis, PE 1996, 'Polymer Layered Silicate Nanocomposites', *Advanced Materials*, vol. 8, no. 1, pp. 120-126.
42. Griffin GJL, United States Patent: 4016117 (1977); 4021388 (1977); 4218350 (1980); 4983651 (1991).
43. Gopakumar, TG, Lee, JA, Kontopoulou, M & Parent, JS 2002, 'Influence of clay exfoliation on the physical properties of montmorillonite/polyethylene composites', *Polymer*, vol. 43, no. 20, pp. 5483-5491.
44. Gowarikar, VR, Viswanathan, NV & Sreedhar, J 2000, 'Copolymerization. In: Polymer Science', New Age International, India, pp. 205–206.

45. Hakkarainen, M, Albertsson, AC & Karlsson, S 1997, 'Susceptibility of Starch-Filled and Starch-Based LDPE to Oxygen in Water and Air', *Journal of Applied polymer science*, vol. 66, pp. 959-967.
46. Hamid, HS, Amin, MB & Maadhah, AG (eds) 1992, Handbook of polymer degradation, Maecel dekker Inc., New York.
47. Harnden R.M., 1990, United States Patent: 5096941
48. Hinksen, H, Moss, S, Pauquet J-R & Zweifel, H 1991, 'Degradation of Polyolefins During Melt Processing', *Polymer Degradation and Stability*, vol. 34, no.1, pp. 279-293.
49. Hotta, S & Paul, DR 2004, 'Nanocomposites formed from linear low density polyethylene and organoclays', *Polymer*, vol. 45, pp. 7639–7654.
50. Hudson, 1995, United States Patent: 5393831
51. Jakubowicz, I 2003, 'Evaluation of degradability of biodegradable polyethylene (PE)', *Polymer Degradation and Stability*, vol. 80, no. 1, pp. 39-43.
52. Jakubowicz, I, Yarahmadi, N & Petersen, H 2006, 'Evaluation of the rate of abiotic degradation of biodegradable polyethylene in various environments', *Polymer Degradation and Stability*, vol. 91, no. 7, pp. 1556-1562.
53. Jang BN & Wilkie CA 2005, 'The thermal degradation of polystyrene nanocomposite', *Polymer*, vol. 46, no. 9, pp. 2933–2942.
54. Karlsson, S & Albertson AC 1998, 'Biodegradable polymers and environmental interaction', *Polymer Engineering Sci*ence, vol. 38, no. 8, pp. 1251–1253.
55. Kawai, F, Watanabe, M, Shibata, M, Yokoyama, S & Sudate, Y 2002, 'Experimental analysis and numerical simulation for biodegradability of polyethylene', *Polymer Degradation and Stability*, vol. 76, pp. 129-135.

56. Kawai, F, Watanabe, M, Shibata, M, Yokoyama, S, Sudate, Y & Hayashi, S 2004, 'Comparative study on biodegradability of polyethylene wax by bacteria and fungi', *Polymer Degradation and Stability*, vol. 86, pp.105-114.
57. Khabbaz, F, Albertsson, AC & Karlsson, S 1999, 'Chemical and morphological changes of environmentally degradable polyethylene films exposed to thermo-oxidation', *Polymer Degradation and Stability*, vol. 63, no. 1, pp. 127-138.
58. Khabbaz F & Albertsson AC 2000, 'Great advantages in using a natural rubber instead of a synthetic SBR in a pro-oxidant system for degradable LDPE', *Biomacromolecules*, vol. 1, pp. 665-673.
59. Ke, Z & Yongping B 2005, 'Improve gas barrier property of PET film with montmorillonite by in situ interlayer polymerization', *Mater Lett*, vol.59, pp. 3348‑3351.
60. Kim, CM, Lee, DH, Hoffmann, B, Kressler, J & Stoppelmann, G 2001, 'Influence of nanofillers on the deformation process in layered silicate/polyamide 12 nanocomposites', *Polymer*, vol. 42, pp. 1095–1100.
61. Kirk, TK, Tien, M & Faison, BD 1984, 'Biochemistry of the oxidation of lignin by Phanerochaete', *chrysosporium Biotechnol. Adv*., vol. 2, pp. 183–199.
62. Kornmann, X, Lindberg, H & Berglund, LA 2001, 'Synthesis of epoxy–clay nanocomposites: influence of the nature of the clay on structure', *Polymer*, vol.42, pp. 1303–1310.
63. Koutny, M, Lemaire, J & Delort, A-M 2006, 'Biodegradation of polyethylene films with prooxidant additives', *Chemosphere*, vol. 64, no. 8, pp. 1243-1252.

64. Koutny, M, Sancelme, M, Dabin, C, Pichon, N, Delort, A-M & Lemaire, J 2006, 'Acquired biodegradability of polyethylenes containing pro-oxidant additives', *Polymer Degradation and Stability*, vol. 91, no. 7, pp. 1495-1503.

65. Kumanayaka, TO, Parthasarathy, R & Jollands, M 2010, 'Accelerating effect of montmorillonite on oxidative degradation of polyethylene nanocomposites', *Polymer Degradation and Stability*, vol.95, no. 4, pp. 672–676.

66. Lange, J & Wyser, Y 2003, 'Recent innovations in barrier technologies for plastic packaging−a review', *Packag Technol Sci*, vol.16, pp.149‑158.

67. Larson, RJ 1984, 'Kinetic and ecological approaches for predicting biodegradation rates of xenobiotic organic chemicals in natural ecosystems', In: M.K. Klug and CA. Reddy (eds.), Current Perspectives in Microbial Ecology, American Society for Microbiology, Washington, D.C., pp. 677-686.

68. Larson, R J, Hansmann, MA & Bookland EA 1996, 'Carbon dioxide recovery in ready biodegradation tests: mass transfer and kinetic considerations', *Chemosphere*, Vol. 33, No. 6, pp. 1195-1210.

69. LeBaron, PC, Wang, Z & Pinnavaia TJ 1999, 'Polymer–layered silicate nanocomposites: an overview', *Applied Clay Science*, vol. 15, pp. 11–29.

70. Lee, J-H, Daeseung, J, Chang-Eui, H, Rhee, KY & Advani, SG 2005, 'Properties of polyethylene layered silicate nanocomposites prepared by melt intercalation with a PP-g-MA compatibilizer', *Composites Science and Technology*, vol. 65, no. 16, pp. 1996-2002.

71. Lepoittevin M, Devalckenaere N, Alexandre PM, Kubies D, Calberg C, Jérômeb, R & Duboisa, P 2002, 'Poly(ε-caprolactone)/clay nanocomposites prepared by melt

intercalation: mechanical, thermal and rheological properties', *Polymer*, vol. 43, pp. 4017-4023.

72. Linos, A, Reichelt, R, Keller, U & Steinbuchel, A 2000, 'A gram-negative bacterium, identified as Pseudomonas aeruginosa AL98, is a potent degrader of natural rubber and synthetic cis-1,4-polyisoprene', *FEMS Microbiology Letters*, vol. 182, no. 1, p. 155-161.
73. Liu, LM, Qi, ZN & Zhu, XG 1999, 'Studies on nylon-6 clay nanocomposites by melt intercalation process', *J Appl Polym Sci*, vol. 71, pp. 1133–1138.
74. Liu, X & Wu, Q 2002, 'Polyamide 66/clay nanocomposites via melt intercalation', *Macromol Mater Eng*, vol. 287, pp. 180–186.
75. Lu, H, Hu, Y, Xiao, J, Kong, Q, Chen, Z & Fan, W 2005, 'The influence of irradiation on morphology evolution and flammability properties of maleated polyethylene/clay nanocomposite', *Mater Lett*, vol. 59, no. 6, pp. 648–651.
76. Maquelin, K, Kirschner, C, Choo-Smith, LP, Van de Braak, N, Endtz, HP, Naumann, D & Puppels, JGJ 2002, ' Identification of medically relevant microorganisms by vibrational spectroscopy', *Microbiol. Methods*, vol.51, pp.255-271.
77. Manias, E, Touny, L.A, Strawhecker, L.W, K., Lu, B & Chung, TC 2001, 'Polypropylene/montmorillonite nanocomposites. Review of the synthetic routes and materials properties.' *Chem. Mater*, vol. 13, no. 10, pp. 3516-3523.
78. Mohee, R, Unmar, GD, Mudhoo, A & Khadoo, P 2008, 'Biodegradability of biodegradable/degradable plastic materials under aerobic and anaerobic conditions', *Waste Manage*, vol. 28, no. 9, pp. 1624–1629.

79. Morawiec, J, Pawlak, A, Slouf, M, Galeski, A, Piorkowska, E & Kransnikowa N 2005, 'Preparation and properties of compatibilized LDPE/organo-modified montmorillonite nanocomposites', *Eur Polym J*, vol.41, pp. 1115‑1122.

80. Morgan, AB & Gilman JW 2003, 'Characterization of polymer–layered silicate (clay) nanocomposites by transmission electron microscopy and X-ray diffraction: a comparative study', *Journal of Applied Polymer Science*, vol. 87, pp. 1329–1338.

81. Murata, K, Hirano, Y, Sakata, Y & Uddin, MA 2002, 'Basic study on a continuous flow reactor for thermal degradation of polymers', *J Anal Appl Pyrolysis*, vol.65, no.1, pp.71-90.

82. Ogasawara, T, Ishida, Y, Ishikawa, T, Aoki, T & Ogura, T 2006, 'Helium gas permeability of montmorillonite/epoxy nanocomposites', *Composites: Part A*, vol. 37, pp. 2236–2240.

83. Ojeda, TFM, Dalmolin, E, Forte, MMC, Jacques, RJS, Bento, FM & Camargo, FAO 2009, 'Abiotic and biotic degradation of oxo-biodegradable polyethylenes', *Polymer Degradation and Stability*, vol. 94, no. 6, pp. 965-970.

84. Okada, M 2002, 'Chemical syntheses of biodegradable polymers', *Progress in Polymer Sci*., vol. 27, pp. 87-133

85. Orhan, Y & Buyukgungor, H 2000, 'Enhancement of biodegradability of disposable polyethylene in controlled biological soil', Int. *Biodeterior. Biodegrad*., vol. 45, pp. 49–55.

86. Orhan, Y, Hrenovic, J & Buyukgungor, H 2004,' Biodegradation of plastic compost bags under controlled soil conditions', *Acta Chim Slov*, vol. 51, pp. 579-588.

87. Pandey, JK, Raghunatha Reddy, K, Pratheep Kumar, A & Singh, RP 2005, 'An overview on the degradability of polymer nanocomposites', *Polymer Degradation and Stability*, vol. 88, no. 2, pp. 234-250.
88. Pavlidoua, S & Papaspyrides, CD 2008, 'A review on polymer–layered silicate nanocomposites', *Progress in Polymer Science*, vol. 33, pp. 1119–1198
89. Pinnavaia, TJ & Beall, GW (eds) 2000, Polymer-Clay nanocomposites, *John Wiley & Sons Inc*., New York.
90. *Plastic bag facts; The scoop on plastic* 2010, viewed 12 December 2010, <http://www.gogreenstreet.com/plastic-bag-facts-the-scoop-on-plastic/.>
91. Pometto, AL, Lee, BT & Johnson KE 1992, 'Production of an extracellular polyethylene-degrading enzyme(s) by Streptomycesspecies', *Appl. Environ. Microb*., vol. 58, pp. 731–733.
92. Porter, D, Metcalfe, E & Thomas, MJK 2000, 'Nanocomposite fire retardants—a review', *Fire Mater*, vol. 24, pp. 45–52.
93. Pospisil, M, Hofer, M, Znojil, V, Netikova, J, Vacha, J, Hola, J & Vacek 1998, 'A: Granulocyte colony stimulating factor and drugs elevating extracellular adenosine synergize to enhance hematopoietic reconstitution in irradiated mice', *Eur J Haematol*, vol.60, pp. 172-180.
94. Preston, CML, Amarasinghe, G, Hopewell, JL, Shanks, RA & Mathys, Z 2004, 'Evaluation of polar ethylene copolymers as fire retardant nanocomposite matrices', *Polymer Degradation and Stability*, vol. 84, pp. 533–44.
95. Qin, H, Zhao, C, Zhang, S, Chen, G & Yang, M 2003, 'Photo-oxidative degradation of polyethylene/montmorillonite nanocomposite', *Polymer Degradation and Stability*, vol. 81, no. 3, pp. 497-500.

96. Qin, H, Zang, Z, Feng, M, Gong, F, Zhang, S & Yang, M 2004, 'The influnece of interlayer cations on the photo-oxidative degradation of polyethylene/montmorillonite composites', *Journal of Polymer Science*: Part B: Polymer Physics, vol. 42, pp. 3006-12.

97. Ray, SS & Bousima, M 2005, 'Biodegradable polymers and their layered silicate nanocomposites: in greening the 21st century materials world', *Prog Mater Sci,* vol. 50, pp. 962–1079.

98. Ray, SS & Okamoto, M 2003, 'Polymer/layered silicate nanocomposites: a review from 'Degradation of abiotically aged LDPE films containing pro-oxidant by bacterial consortium', *Polymer Degradation and Stability*, vol. 93, no. 10, pp. 1917-22.

99. Ray, SS & Okamoto, M 2003, 'Polymer/layered silicate nanocomposites: a review from preparation to processing', *Progress in Polymer Science*, vol. 28, no. 11pp. 1539-641.

100. Reddy, M.M, Gupta, R.K, Bhattacharya S. N. & Parthasarathy, R 2007 'Structure property relationship of melt intercalated maleated polyethylene nanocomposites', *Korea-Australia Rheology Journal*, vol. 19, no. 3, pp. 133-39.

101. Reddy, MM, Gupta, RK, Bhattacharya, SN & Parthasarathy, R 2008, 'abiotic oxidation studies of oxo-biodegradable polyethylene', *Journal of polymers and environment,*Vol.16, pp.27-35

102. Reddy, MM, Deighton, M, Gupta, RK, Bhattacharya, SN & Parthasarathy, R 2009, 'Biodegradation of Oxo-Biodegradable Polyethylene', *Journal of Applied Polymer Science,* vol. 111, no.3, pp. 1426–1432.

103. Reuschenbach, P, Pagga, U & Strotmann, U 2003, A critical comparison of respirometric biodegradation tests based on OECD 301 and related test methods', *Water research*, vol. 37, pp. 1571-1582

104. Rodriguez-Vazquez, M, Liauw, CM, Allen, NS, Edge, M & Fontan, E 2006, 'Degradation and stabilisation of poly(ethylene-stat-vinyl acetate): 1 – Spectroscopic and rheological examination of thermal and thermo-oxidative degradation mechanisms', *Polymer Degradation and Stability*, vol. 91, no. 1, pp. 154-164.

105. Rogers, SL, Kookana, RS, Oliver, DP & Richards, AR 1997, 'Microbial degradation of strychnine rodenticide in south Australian agricultural soils: laboratory studies', *Soil Biol. Biochem*, Vol. 30, No. 2, pp. 129-134.

106. Roy, PK, Titus, S, Surekha, P, Tulsi, E, Deshmukh, C & Rajagopal, C 2008, 'Degradation of abiotically aged LDPE films containing pro-oxidant by bacterial consortium', Polymer Degradation Stability, vol. 93, no.10, pp. 1917–1922.

107. Roy PK, Hakkarainen, M, Varma, IK & Albertsson AC 2011, 'Degradable Polyethylene: Fantasy or Reality', *Environmental Science & Technology*, vol. 45, pp. 4217–4227

108. Schmidt, D, Shah, D & Giannelis, EP 2002, 'New advances in polymer/layered silicate nanocomposites', Curr Opin Solid State Mater, vol.6, pp. 205‑212.

109. Scott G 1997, 'Abiotic control of polymer biodegradation', *TRIP*, vol.5, pp. 361-368.

110. Scott, G & Wiles, DM 2001, 'Programmed-life plastics from polyolefins: A new look at sustainability ', *Biomacromolecules*, vol. 2, no. 3, pp. 615-22.

111. Scott, G., Standards for environmentally biodegradable polymers. 1st ed. Biodegradable polymers for industrial applications, ed. R. Smith. 2005, Cambridge: CRC Press. 531.

112. Singh, B & Sharma N 2007, 'Optimized synthesis and characterization of polystyrene graft copolymers and preliminary assessment of their biodegradability and application in water pollution alleviation technologies', *Polymer Degradation and Stability*, vol. 92, pp. 876-85.

113. Singh, B & Sharma, N 2008, 'Mechanistic implications of plastic degradation', *Polymer Degradation and Stability*, vol. 93, no. 3, pp. 561-84.

114. Sipinen, AJ, & Rutherford, DR 1993, 'A Study of the Oxidative Degradation of Polyolefins', *Journal of Environmental Polymer Degradation*, vol. 1, no. 3, pp. 193-202

115. Shah RK & Paul DR 2006, 'Organoclay degradation in melt processed polyethylene nanocomposites', *Polymer*, vol. 47, no. 11, pp. 4075–4084.

116. Shelley, JS, Mather, PT & DeVries, KL 2002, 'Reinforcement and environmental degradation of nylon 6/clay nanocomposites', Polymer, vol. 42, pp. 5849–58.

117. Solomon, DH 1968, 'Clay minerals as electron acceptors and/or electron donors in organic reactions ', Clay and Clay Minerals, vol. 16, pp. 31-9.

118. Soto-Oviedo, MA, Lehrle, RS, Parsons, IW & Paoli, MAD 2003, 'Thermal degradation mechanism and rate constants of the thermal degradation of poly (epichlorohydrin-co-ethylene oxide), deduced from pyrolysis-GCeMS studies', Polymer Degradation and Stability, vol.81, no.3, pp.463-472.

119. Srinivasan, PT, Viraraghavan, T 2000, 'An analysis of the `Modified Sturm Test' data', Chemosphere, vol. 40, pp. 99-102.

120. Tayler, DR 2004, ‘Mechanistic aspects of the effect of stress on the rate of photochemical degradation reactions in polymers’, J Macromol Sci Part C Polym Rev, vol.44, no. 4, pp. 351-388.

121. Thellen, C, Orroth, C, Froio, D, Ziegler, D, Lucciarini, J & Farrell, R, 2005, ‘Influence of montmorillonite layered silicate on plasticized poly (lactide) blown films’, Polymer, vol. 46, pp. 11716–27.

122. Treece, MA & Oberhauser, JP 2007, ‘Ubiquity of soft glassy dynamics in polypropyleneeclay nanocomposites’, Polymer, vol. 48, no. 4, pp. 1083-1095.

123. Vaia, RA, Jandt, KD, Kramer, EJ & Giannelis EP 1996, ‘Microstructural Evolution of Melt Intercalated Polymer-organically Modified Layered Silicates Nanocomposites’, Chem. Mater, Vol., pp. 2628-2635.

124. Vaia, RA, Sauer, BB, Tse, OK & Giannelis, EP 1997, 'Relaxations of confined chains in polymer nanocomposites: Glass transition properties of poly (ethylene oxide) intercalated in montmorillonite.' Journal of Polymer Science Part B: Polymer Physics, vol. 35, no. 1, pp. 59-67.

125. Vyazovkin, S, Dranka, I, Fan, X & Advincula R 2004, ‘Kinetics of the thermal and thermo-oxidative degradation of a polystyrene‐clay nanocomposite’, Macromol Rapid Commun, vol. 25, pp. 498‐503.

126. Wang, KH, Choi, MH, Koo, CM, Cho,i CM & Chung IJ 2001, ‘Synthesis and characterization of maleated polyethylene/clay nanocomposites’, Polymer, vol. 42, pp. 9819–26.

127. Wiles, DM & Scott, G 2006, 'Polyolefins with controlled environmental degradability', Polymer Degradation and Stability, vol. 91, no. 7, pp. 1581-92.

128. Worldwatch Institute, 2009

129. Xie,W, Gao, Z, Liu, K, Pan,WP, Vaia, R & Hunter, D 2001, 'Thermal characterization of organically modified montmorillonite', Thermochim Acta, vol.367/368, pp. 339–50.

130. Yabannavar, AV. & Bartha, R 1994, 'Methods for Assessment of Biodegradability of Plastic Films in Soil', Appl. Environ. Microbiol, vol. 60, no.10, pp. 3608–3614.

131. Yang, HS, Yoon, JS & Kim, MN 2005, 'Dependence of biodegradability of plastics in compost on the shape of specimens', Polymer Degradation and Stability, vol. 87, pp.131-135.

132. Yano, K, Usuki, A, Okada, A, Kurauchi, T & Kamigaito, O 1993, 'Synthesis and properties of polyimide/clay hybrid', J Polym Sci Polym Chem, vol.31, pp.2493‑8.

133. Zanetti, M, Lomakin, S & Camino, G 2000, 'Polymer layered silicate nanocomposites', Macromolecule Material Engineering, vol. 279, pp. 1–9.

134. Zanetti, M & Costa, L 2004, 'Preparation and combustion behavior of polymer/layered silicate nanocomposites based upon PE and EVA', Polymer, vol. 45, pp. 4367–73.

135. Zanetti, M, Bracco, P & Costa, L 2004, 'Thermal degradation behavior of PE/clay nanocomposites', Polymer Degradation Stability, vol. 85, pp. 657–65.

136. Zhai, H, Xu, W, Guo, H, Zhou, Z, Shen, S & Song, Q 2004, 'Preparation and characterization of PE and PE-g-MAH/montmorillonite nanocomposites', Eur Polym J, vol.40, pp. 2539–45.

137. Zhao, C, Qin, H, Gong, F, Feng, M, Zhang, S & Yang, M 2005, 'Mechanical, thermal and flammability properties of polyethylene/clay nanocomposites', Polymer Degradation Stability, vol. 87, pp. 183–9.

138. Zhang, J & Wilkie, CA 2003, 'Preparation and flammability properties of polyethylene–clay nanocomposites', Polymer Degradation Stability, vol.80, pp.163–9.

139. Zheng, QH, Yu, AB, Lu, GQ & Paul, DR 2005, 'Clay-based polymer nanocomposites: research and commercial development', J Nanosci Nanotechnol, vol.5, pp. 1574‑92.

140. Zhu, J, Uhl, FM, Morgan, AB & Wilkie CA 2001, 'Studies on the mechanism by which the formation of nanocomposites enhances thermal stability', Chem Mater, vol.13, pp. 4649–54.